Oförutsedd dioxinbildning vid avfallsförbränning

Dioxiner bildas snabbare, vid lägre temperaturer och under andra förhållanden än man tidigare sett. Detta kan påverka hur man i framtiden utformar provtagningsutrustning, rökgasfilter i avfallsförbränningsanläggningar samt behandlar flygaska från avfallsförbränning. Det visar Eva Weidemann i sin avhandling.

Dioxiner är ett samlingsnamn för en grupp klorerade organiska molekyler där vissa uppvisar hormonstörande och cancerframkallande egenskaper. Att dioxiner bildas vid avfallsförbränning, när rökgaserna svalnar är känt sedan 70-talet. Med dagens moderna anläggningar är dock utsläpp via skorstenen minimala eftersom dioxinerna filtreras bort från rökgasen och fastnar i flygaskan.
I sitt avhandlingsarbete visar dock Eva Weidemann hur de miljöstörande dioxinerna kan bildas under specifika förhållanden som man inte tidigare känt till. Bland annat beskriver hon att dioxiner kan bildas inuti filtren i en storskalig anläggning för sopförbränning.

– Anläggningens utsläpp ligger fortfarande under de lagstadgade utsläppsgränserna, men det är ju inte bra överhuvudtaget att dioxiner bildas. Vi har kunnat identifiera nyckelparametrar för bildningen och vet i stora drag hur det sker. Våra iakttagelser kan bidra till att man designar bättre filter i framtiden, säger Eva Weidemann.

Ett annat problem är att dioxiner kan bildas i provtagningsutrustningen då prover tas vid höga temperaturer och Eva Weidemann har undersökt hur man kan utföra provtagningar av dioxiner på ett bättre sätt vid höga temperaturer för att undvika att detta sker. Lösningen är effektivare kylning i ett kritiskt steg, som då hindrar dioxinbildningen och leder till en mer korrekt provtagning.

Eva Weidemann har också tittat på hur dioxiner i avfallsförbränningsaska påverkas av olika behandlingar för att hitta möjliga metoder att rena askorna. Resultaten är inte helt entydiga, men hon har identifierat pusselbitar som kan vara en hjälp på vägen.

– Om man kunde ta fram en bra reningsmetod för flygaskorna skulle det vara en miljövinst med avseende på dioxinproblematiken, men även ur andra perspektiv som exempelvis materialåtervinning, säger Eva Weidemann.

Avfallsförbränning är trots dioxinbildning ett bra alternativ för att tillvarata energi ut de sopor som inte kan sorteras och återvinnas. Avfallet minskar i vikt och volym och bakterier och lukt försvinner. Dessutom är förbränning en mer klimatsmart hanteringsmetod i jämförelse med att lägga avfallet på en soptipp, eftersom metangasen som bildas vid förmultning är en mer potent växthusgas än koldioxiden som bildas vid förbränning. Den utsläppsproblematik som tillskrevs metoden under 80-talet är i dag närapå eliminerad med hjälp av avancerade filter och reningssystem, samt regelbundna utsläppskontroller.

Eva Weidemann har utfört sin forskarutbildning inom Företagsforskarsskolan vid Umeå universitet i samarbete med Umeå Energi.

Waste Incineration Residue

Persistent organic pollutants in flue gas and fly ash from waste incineration

Eva Weidemann

Department of Chemistry
Industrial Doctoral School
Umeå 2014

Waste Incineration Residues

Persistent organic pollutants in flue gas and fly ash from waste incineration

Eva Weidemann

Akademisk avhandling

som med vederbörligt tillstånd av Rektor vid Umeå universitet för avläggande av teknologie doktorsexamen framläggs till offentligt försvar i:
KB3B1, KBC-huset, fredagen den 26 september, kl. 10:00.
Avhandlingen kommer att försvaras på engelska.

Fakultetsopponent: Dr Kees Olie,
University of Amsterdam, Amsterdam, Nederländerna

Kemiska Institutionen/Department of Chemistry
Industrial Doctorate School
Doktorsavhandling/Doctoral thesis
Umeå 2014

Organization
Umeå University
Department of Chemistry

Document type
Doctoral thesis

Date of publication
5 September 2014

Author
Eva Weidemann

Title
Waste incineration residues – Persistent organic pollutants in flue gas and fly ash from waste incineration

Abstract

Modern societies produce large quantities of municipal solid waste (MSW), which is commonly disposed of by incineration. This has several advantages: it reduces the waste's volume and sterilizes it while also enabling energy recovery. However, MSW incineration has some notable disadvantages, the most widely debated of which is probably the production and release of persistent organic pollutants (POP) such as polychlorinated dibenzofurans (PCDF), dibenzo-p-dioxins (PCDD), biphenyls (PCB) and naphthalenes (PCN). Of the 210 PCDF and PCDD congeners, 17 are toxic, with hormone-disrupting and carcinogenic properties. Twelve of the 209 PCB congeners and at least 2 of the 75 PCN also exhibit such properties. These POP form in the post-combustion zones of MSW incineration plants and are removed from the flue gas using filtering devices that trap them in the fly ash

This thesis concerns the formation and degradation of POP in processes related to MSW incineration. The first paper describes a case study in which PCDD were forming in filters designed to remove them from flue gases, causing emission-related issues in a full-scale MSW incineration plant. It was shown that the PCDD formation was probably due to chlorophenol condensation on the filters' surfaces.

The second paper describes the validation of a cooling probe designed to prevent POP formation during high temperature (>450 °C) flue gas sampling. The results obtained also confirmed that PCDF and PCDD formation takes place at temperatures below 600 °C.

In the third paper, three different fly ashes were subjected to thermal treatment under an inert atmosphere in a rotary kiln and in sealed ampoules at 400 °C. The concentrations, degrees of chlorination and congener profiles of the POP in the treated ashes and emitted gases were compared to those for the untreated ashes. The trends observed for PCDF mirrored those for PCN, while the trends for PCDD closely resembled those for PCB. The PCDF congener profiles of the kiln ash were similar regardless of the initial ash composition, suggesting that the mechanisms of PCDF formation were similar in all cases.

The fourth paper describes the surface characterization of the three fly ashes studied in paper three by SEM, EDX, XPS and XRD. In addition, the thermal desorption and subsequent degradation of POP from the ashes was studied at temperatures of 300-900 °C. The composition of the gases released as the temperature increased differed between the ashes and depended on their composition. Doping experiments using isotopically labelled PCDF and PCDD suggests that PCDD desorbed at lower temperatures than PCDF.

This thesis examines several problems relating to POP formation during MSW incineration, from sampling to the ultimate fate of incineration residues. The results obtained illustrate the wide range of processes that contribute to thermal POP formation and degradation during and after MSW incineration.

Keywords
MSW, PCDD, PCDF, PCN, PCB, POP, formation, degradation, case study, flue gas sampling thermal treatment, fly ash, surface characterization

Language
English

ISBN
978-91-7601-113-3

Number of pages
75 + 4 papers

WASTE INCINERATION RESIDUES

Persistent organic pollutants in flue gas and fly ash from waste incineration

Eva Weidemann

Department of Chemistry
Industrial Doctorate School
Doctoral Thesis
Umeå 2014

ISBN: 978-91-7601-113-3
Cover picture: Popov Nikolay, www.shutterstock.com
Electronic version available at http://umu.diva-portal.org/
Printed at the KCB Service Centre, Umeå University, August 2014
Umeå, Sweden 2014

One must still have chaos in oneself to be able to give birth to a dancing star.
*– **Nietzsche***

To Zelda and Stephan

TABLE OF CONTENTS

ABSTRACT

Modern societies produce large quantities of municipal solid waste (MSW), which is commonly disposed of by incineration. This has several advantages: it reduces the waste's volume and sterilizes it while also enabling energy recovery. However, MSW incineration has some notable disadvantages, the most widely debated of which is probably the unintentional formation and release of persistent organic pollutants (POPs) such as polychlorinated dibenzofurans (PCDF), dibenzo-*p*-dioxins (PCDD), biphenyls (PCB) and naphthalenes (PCN). Of the 210 PCDF and PCDD congeners, 17 are toxic, with hormone-disrupting and carcinogenic properties. Twelve of the 209 PCB congeners and at least 2 of the 75 PCN also exhibit such properties. These POPs form in the post-combustion zones of MSW incineration plants and are removed from the flue gas using filtering devices that trap them in the fly ash

This thesis concerns the formation and degradation of POPs in processes related to MSW incineration. The first paper describes a case study in which PCDD formed in the filters designed to remove them from flue gases, causing emission-related issues in a full-scale MSW incineration plant. It was shown that the PCDD formation was probably due to chlorophenol condensation on the filters' surfaces.

The second paper describes the validation of a cooling probe designed to prevent POPs formation during high temperature (> 450 °C) flue gas sampling. The results obtained also confirmed that most PCDF and PCDD formation takes place at temperatures below 600 °C.

In the third paper, three different fly ashes were subjected to thermal treatment under an inert atmosphere in a rotary kiln and in sealed ampoules at 400 °C. The concentrations, degrees of chlorination and congener profiles of the POPs in the treated ashes and emitted gases were compared to those for the untreated ashes. The trends observed for PCDF mirrored those for PCN, while the trends for PCDD closely resembled those for PCB. The PCDF congener profiles of the kiln ash were similar regardless of the initial ash composition, suggesting that the mechanisms of PCDF formation were similar in all cases.

The fourth paper describes the surface characterization of the three fly ashes studied in paper three by SEM, EDX, XPS and XRD. In addition, the thermal desorption and subsequent degradation of POPs from the ashes was studied at

temperatures of 300-900 °C. The composition of the gases released as the temperature increased differed between the ashes and depended on their composition. Doping experiments using isotopically labelled PCDF and PCDD suggested that PCDD desorbed at lower temperatures than PCDF.

This thesis examines several problems relating to POPs formation during MSW incineration, from sampling to the ultimate fate of incineration residues. The results obtained illustrate the wide range of processes that contribute to thermal POPs formation and degradation during and after MSW incineration.

SAMMANFATTNING PÅ SVENSKA

Förbränning av hushållssopor är en vanlig metod för att hantera ett växande avfallsproblem. Metoden har flera fördelar, såsom minskning av volym och vikt, sterilisering och energiåtervinning. Sopförbränning har dock vissa nackdelar och det mest debatterade är sannolikt utsläpp av persistenta organiska föroreningar (POPs) som polyklorerad dibensofuran (PCDF), dibenso-p-dioxin (PCDD), bifenyl (PCB) och naftalen (PCN). Det finns totalt 210 PCDF- och PCDD- kongener, med mellan ett till åtta klor på kolskelettet, varav 17 är giftiga med hormonstörande och cancerframkallande egenskaper. Även tolv av totalt 209 PCB-kongener samt minst två av totalt 75 PCN-kongener uppvisar liknande egenskaper. Dessa klorerade organiska föroreningar bildas då rökgaserna kyls ner i sopförbränningsanläggningarna och avlägsnas från rökgaserna med hjälp av filter och hamnar i flygaskan. Denna avhandling handlar om bildning och nedbrytning av POPs i sopförbränningsrelaterade processer.

Den första artikeln är en fallstudie där PCDD bildas i filtren i en fullskalig sopförbränningsanläggning. Bildningen ledde till förhöjda halter organiska föroreningar i rökgaserna, vilket ledde till ökade utsläpp. Den funna bildningsvägen för PCDD i filtren befanns sannolikt bero på kondensation av klorfenoler på filterytorna.

Den andra artikeln är en valideringsstudie av en kylprob avsedd att användas vid rökgasprovtagning vid hög temperatur (> 450 °C) för att undvika bildning av POPs under provtagningen. Studien bekräftade att majoriteten av PCDF- och PCDD- bildning i rökgaser från sopförbränning sker vid temperaturer under 600 °C.

I den tredje artikeln berättas om behandling av tre olika flygaskor från olika sopförbränningsanläggningar. Askorna behandlades vid 400 °C i inert atmosfär i både en roterugn och i förseglade ampuller. De resulterande koncentrationerna, kloreringsgraderna och kongenprofilerna av de organiska föroreningarna jämfördes. Likheter hittades mellan PCDF och PCN, medan PCDD och PCB betedde sig på ett annat sätt. Studien fann också att PCDF kongenprofiler i aska som behandlats i roterugnen liknade varandra, oberoende av askornas sammansättning, vilket tyder på en liknande bildningsväg.

För den fjärde artikeln, genomfördes ytkarakterisering (SEM, EDX, XPS och XRD) på de tre flygaskorna från artikel tre som sedan hettades upp från 30 °C till 900 °C i vacuum. Det som frigjordes på grund av uppvärmningen samt nedbrytningsprodukter från askorna studerades med hjälp av masspektrometri och infraröd spektroskopi. Studien fann att de gaser som frigjordes när temperaturen ökade skilde mellan askorna, beroende på deras sammansättning. Studien fann också att när aska dopad med isotopmärkt PCDF och PCDD utsattes för samma behandling, frigjordes PCDD vid lägre temperatur än PCDF.

Denna avhandling berör flera aspekter av problematiken kring klorerade organiska föroreningar som bildas vid sopförbränning, från provtagning till hur man ska hantera flygaskan. Avhandlingen belyser även olika typer av bildning och nedbrytning av POPs i varma processer kopplade till sopförbränning.

LIST OF PAPERS

I

In-filter PCDF and PCDD formation at low temperature during MSWI combustion

Eva Weidemann, Stellan Marklund, Henrik Bristav and Lisa Lundin
Chemosphere (2014) Vol. 102, pp 12–17

II

Accurate sampling of PCDD/F in high temperature flue-gas using cooled sampling probes.

Duong Ngoc Chau Phan, **Eva Weidemann**, Lisa Lundin, Stellan Marklund and Stina Jansson
Chemosphere (2012) Vol. 88, pp 832-836

III

Behaviour of PCDF, PCDD, PCN and PCB during thermal treatment of MSW incineration fly ash.

Eva Weidemann and Lisa Lundin.
Submitted to Journal of Hazardous Materials in August 2014

IV

Thermal desorption and degradation of municipal solid waste incineration fly ash.

Eva Weidemann, Lisa Lundin and Jean-Francois Boily
(Manuscript)

Extent of the authors contribution to the papers

I

The author contributed significantly to planning the case study and preforming the on-site sampling. The author also performed all laboratory work, quantification and evaluation of the data as well as writing the manuscript.

II

The author contributed significantly to the planning and evaluation of the experiments, and also contributed in execution of experiments, quantification of data and writing the manuscript.

III

The author planned and preformed the experimental work. The author did all laboratory work, quantification and evaluation of the data, and wrote the article.

IV

The author participated in planning the experiments and did the experimental work. The author also did the majority of data evaluation and writing of the manuscript.

ABBREVIATIONS

AhR	aryl hydrocarbon receptor
APCD	air pollution cleaning device
EDX	energy-dispersive X-ray spectroscopy
GC-HRMS	gas chromatography with high resolution mass spectrometry
IUPAC	International union of pure and applied chemistry
IW	industrial waste
MSW	municipal solid waste
Nm^3	cubic meter (of gas) normalized to 0 °C, 1 atm. and 11 % O_2
PCB	polychlorinated biphenyls
PCBz	polychlorinated benzenes
PCDD	polychlorinated dibenzo-*p*-dioxins
PCDF	polychlorinated dibenzofurans
PCPh	polychlorinated phenols
PCN	polychlorinated naphthalenes
PIC	products of incomplete combustion
POPs	persistent organic pollutants
PUFP	polyurethane foam plug
SEM	scanning electron microscope
SPE	Solid phase extraction
SWEDAC	Swedish board for accreditation and conformity assessment
TEF	toxic equivalency factor
TEQ	toxic equivalents
w:w	weight to weight
wt %	weight percent
XPS	X-ray photoelectron spectroscopy
XRD	X-ray diffraction

DEFINITIONS

Congener	An individual molecule within a compound group.
Isomers	Molecules with the same molecular formula but different chemical structures.
Homologue	A member of a series of structurally-related compounds. Among persistent organic pollutants, members of homologous series have identical carbon skeletons and numbers of chlorine substituents but differ in their positions of substitution.
Profile	The concentrations and/or relative abundances of homologue groups.
Pattern	The distribution and/or relative abundance of individual isomers within a homologue group.
Homologue fraction	Sum of the concentrations of all members of a homologous series normalized against the total summed concentrations of all compounds within the corresponding fraction ($\Sigma_{HOMOLOGUE}/\Sigma_{TOTAL}$).
Isomer fraction	Isomer concentration normalized against the summed concentrations of each member of the homologous series to which the isomer in question belongs.

SUBSTITUTION PREFIXES

Mo	(Mono-)	one
Di-	(Di-)	two
Tri-	(Tri-)	three
Te-	(Tetra-)	four
Pe-	(Penta-)	five
Hx-	(Hexa-)	six
Hp-	(Hepta-)	seven
O-	(Octa-)	eight
N-	(Nona)	nine
D-	(Deca)	ten

WASTE INCINERATION

The society we live in creates waste, and we have an obligation to take care of this waste in the best way possible to ensure that resources remain for the next generation. Some wastes such as paper, cardboard, glass and metals are easily recycled, allowing the corresponding resources to be retrieved readily. However, others pose a bigger challenge. One such challenging waste fraction is municipal solid waste.

Municipal solid waste (MSW) originates from our homes and consists of either un-sorted waste or wastes that are not yet sortable, e.g. used diapers. Food may be part of the MSW waste fraction but it is increasingly common for food waste to be separated from general waste and used for biogas production. MSW accounts for around half of the 500 kg of waste produced by every person in Sweden annually (2012) [1]. This material is usually incinerated in waste-to-energy plants for energy recovery. Sweden's geographical location means that its winters are long and cold, making heat from incineration useful for district heating. District heating by MSW incineration is very efficient (98 %), and certainly much more so than electricity production. District heating accounted for 30 % of the heating of private homes and public buildings in Sweden during 2011 [2]. In Umeå, that figure stands at 80 %.

WASTE AS FUEL

The composition of MSW changes over the course of a year [3] and over time in general [4]. This presents a unique challenge during incineration because the waste's composition affects both its heating value and moisture content. The MSW combustion gases can contain acids and may leave deposits of corrosive salts that are highly destructive to boilers, superheaters and flue gas cleaning systems [5]. Because of these harsh conditions, MSW incinerators usually have yearly production standstills for surveying and repair. Furthermore, MSW is sometimes co-combusted with other combustible waste fractions such as industrial waste (IW), which consists of construction and demolition waste from building sites and so on. This increases the complexity of the fuel.

COMBUSTION

Combustion is an exothermic reaction between a fuel and an oxidizing agent. A simple example is the combustion of hydrogen gas to produce water and heat (R1):

$$2H_{2(g)} + O_{2(g)} \rightarrow 2\,H_2O_{(g)} + 242\ kJ \cdot mol^{-1} \qquad \text{(R1)}$$

Complete combustion of a simple hydrocarbon yields only water and carbon dioxide (CO_2) (R2). However, as the complexity of the fuel increases, so does that of the reaction mechanisms involved in its combustion.

$$CH_{4(g)} + 2O_{2(g)} \rightarrow CO_{2(g)} + 2H_2O_{(g)} + 890kJ \cdot mol^{-1} \qquad \text{(R2)}$$

Because combustion primarily involves radical reactions, it is virtually impossible to establish a complete mechanism for a given combustion process. In addition, virtually all fuels contain elements other than carbon and hydrogen, such as oxygen, nitrogen, sulphur, chlorine, phosphorus, silicon, and various alkali and transition metals [6, 7]. During the complete combustion of a complex fuel, these elements form combustion gases such as sulphur oxides (SO_x), nitrogen oxides (NO_x), and hydrogen chloride (HCl), in addition to the release of water and CO_2. The chemically bound oxygen is consumed during the combustion process and the metals either volatilize or end up in the ash, depending on their properties. Complete combustion requires an adequate oxygen supply as well as sufficiently high temperatures, residence times, and levels of turbulence. If these conditions are not satisfied, incomplete combustion will occur, resulting in the formation of carbon monoxide (CO), soot, and products of incomplete combustion (PICs) such as chlorinated hydrocarbons. In reality, complete combustion is never achieved so at least some CO is always produced, albeit at trace levels. CO can thus be used as an indicator of combustion efficiency: low levels of CO indicate good combustion.

INCINERATION TECHNIQUES

Most MSW incineration in Sweden is done in grate-fired mass burn combustors (Figure 1). In a mass burn combustor the fuel is fed onto a grate, which conveys the fuel though the combustion zone and then allows the bottom ash to fall off at the end. Such combustors allow the maintenance of a stable process and tolerate large variances in fuel composition. The other major incineration technique relies on fluidized bed combustors where the fuel is fed into an air fluidized sand bed, which ensures good mixing of fuel and air.

This allows complete combustion to take place at a lower temperature than in a mass burn combustor (850 °C vs. 1050 °C), reducing the emissions of gases that cause acidifying air pollution. However, the fluidized bed combustor is more sensitive to changes in fuel composition. Unfavourable fuels can cause the sand bed to agglomerate by encasing the sand grains in adhesive alkali metal salts. This causes the grains to stick together, disrupting fluidization. The relative production of bottom ash (heavy ash that stays in the bed of the incinerator) and fly ash (light weight ash particles that follows the flue gas stream) also differs between combustors. In a mass burner combustor, most (around 80 %) of the ash produced is bottom ash. The opposite is true for fluidized bed.

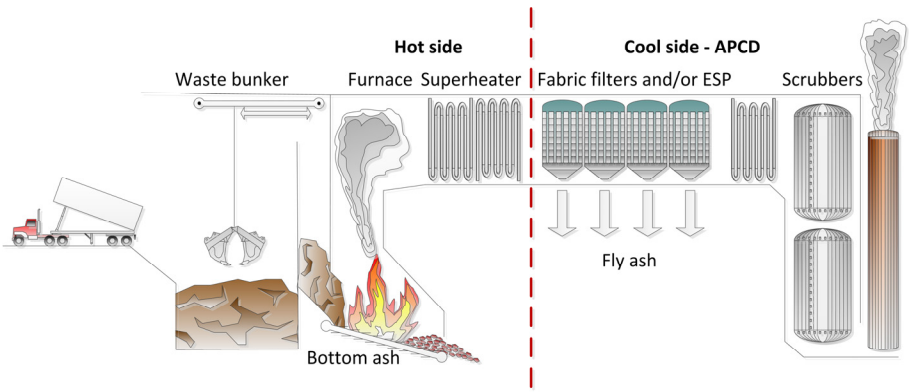

Figure 1. Schematic overview of a grate-fired mass burner for MSW incineration, showing its key components: the furnace, energy recovery, APCD, economizer, scrubbers and stack.

FLUE GAS CLEANING

The current strategy for minimizing emissions from MSW incineration involves both preventive measures (e.g. the injection of ammonia into the combustion zone to minimize NOx emissions [8]) and end-of-pipe solutions based on air pollution cleaning devices (APCDs) that remove both inorganic and organic emissions. The APCD traps emissions via a multi-step process that first removes fly-ash particles and then removes metals and acid gases using scrubbers [9]. Fly ash and soot can be removed from the flue gases using electrostatic precipitators (ESPs) and fabric filters. ESPs work by applying a voltage over the flue gas stream, causing the statically charged flue gas particles to fall out. Fabric filters trap particulate matter while allowing gases to pass through unimpeded. Active carbon and lime are often injected into the gas stream before passage through a fabric filter in order to increase the surface area of particles present within the stream and facilitate PIC capture. Both ESPs and fabric filters can be

used separately but are often used together. The composition and PIC content of the fly ash collected in the filters of the APCD vary greatly depending on fuel composition and the furnace and process conditions.

ENVIRONMENTAL IMPACT OF MSW INCINERATION

MSW incineration presents several advantages: in addition to enabling energy recovery, it sterilizes the waste and reduces its volume and weight. However, there is an ongoing debate about its disadvantages. MSW incineration has had a bad reputation for contributing to acidifying air pollution, spreading mercury through the flue gases, and forming and distributing persistent organic pollutants (POPs) in the environment. The most infamous POPs are the dioxins, which have been discussed extensively in the media.

"Dioxins" is a generic term that refers the toxic congeners of polychlorinated dibenzo-*p*-dioxins (PCDD), polychlorinated dibenzofurans (PCDF), and sometimes also the dioxin-like congeners of polychlorinated biphenyls (PCB). PCDD and PCDF were found to form during MSW incineration in the 1970's [10, 11] and they were subsequently discovered to be widely distributed in most environmental compartments [12]. Since then, many studies have been conducted to determine the mechanisms by which these POPS are formed and how their emissions can be prevented.

PCDD and PCDF have never been intentionally produced and their presence in the environment is largely due to anthropogenic factors [13]. Energy producers have been forced to install APCD at their incineration and combustion plants in order to reduce POPs emissions. This process has been driven by the Stockholm Convention, which was framed in 2001 to protect human health and the environment from persistent organic pollutants [14], and legislative pressure from the environmental protection agencies of both Sweden and the European Union. In Sweden and several other countries, the legal limit for dioxin emissions is 0.1 ng toxic equivalences per normalized cubic meter (Nm^3) of flue gas (the toxic equivalence concept is explained in the next chapter). In addition to regulating POPs emissions, many countries have laws governing combustion parameters such as furnace temperature and residence time to ensure good combustion with minimal emissions of PCDD, PCDF, NO_x, SO_x, HCl and particles [15]. Today, water vapour and CO_2 account for the majority of all gaseous emissions from MSW incineration. However, MSW incineration still produces POPs that remain in the fly ash.

AIM OF THE THESIS

The aim of this thesis is to extend the knowledge about the behaviour of polychlorinated dibenzofurans, polychlorinated dibenzo-*p*-dioxins and other persistent organic pollutants during flue gas sampling, in-plant POPs removal and when thermally treating MSW incineration fly ash.

This thesis contains a case study, where PCDD form in the fabric filters in a MSW incineration plant (**Paper I**), a method development study (**Paper II**) that explores unintentional formation of PCDD and PCDF during flue gas sapling and aims to improve flue gas sampling at high temperatures, a study where MSW fly ash is thermally treated under inert atmosphere **(Paper III)** and PCDF and PCN were found to behave differently from PCDD and PCB, and a study where the thermal desorption/decomposition of MSW incineration fly as is examined **(Paper IV)**.

TARGET CONTAMINANTS

This thesis is primarily concerned with four different types of POPs: polychlorinated dibenzofurans (PCDF), polychlorinated dibenzo-*p*-dioxins (PCDD), polychlorinated biphenyls (PCB) and polychlorinated naphthalenes (PCN). Of these POPs classes, only PCN and PCB have been produced commercially.

PCN production began in the 1910s; the resulting materials were sold under trade names such as Halowax and were used in cable insulation, wood preservation, and as engine oils, among other things. PCB were sold under trade names such as Archlor and were used as transformer oils, plasticizers, and additives for electrical wire coatings. PCDD and PCDF have never been intentionally produced but are formed as by-products in industrial processes including incineration [10], iron ore processing [16], and paper and pulp production [17].

PCDD, PCDF, PCB and PCN have several common properties: they are all polycyclic aromatic compounds with one or more chlorine substituents, they are all toxic, and they can all be formed in the post-combustion zone during MSW incineration. They also bioaccumulate, biomagnify, and are persistent in the environment.

MOLECULAR STRUCTURE

The core structures of all four compound classes consist of two benzene rings. These rings may be fused or linked by carbon-carbon bonds or oxygen bridges (Figure 2). They all have between zero and eight chlorine substituents (zero to ten for PCB) are be assigned systematic names using the nomenclature of the International Union of Pure and Applied Chemistry (IUPAC). All positions on their carbon backbones are numbered, meaning that the PCDD with a chlorine substituent on the carbon labelled 1 (Figure 2A) would be named 1-monochlorodibenzo-*p*-dioxin while the PCDF (Figure 2C) with chlorines located on the carbons labelled 1, 4, 7 and 8 would be named 1,4,7,8-tetrachlorodibenzofuran. In total there are 75 PCDD, 75 PCN, 135 PCDF and 209 PCB congeners.

Most PCDD, PCDF and PCN congeners are planar but the carbon-carbon single bond in the PCB core structure allows the two benzene rings to rotate

freely with respect to one-another (although some congeners can assume a planar conformation). The entire polycyclic core structures of PCDF and PCN are aromatic. As such they are more thermodynamically stable than PCDD and PCB, which exhibit only localized aromaticity [18-21].

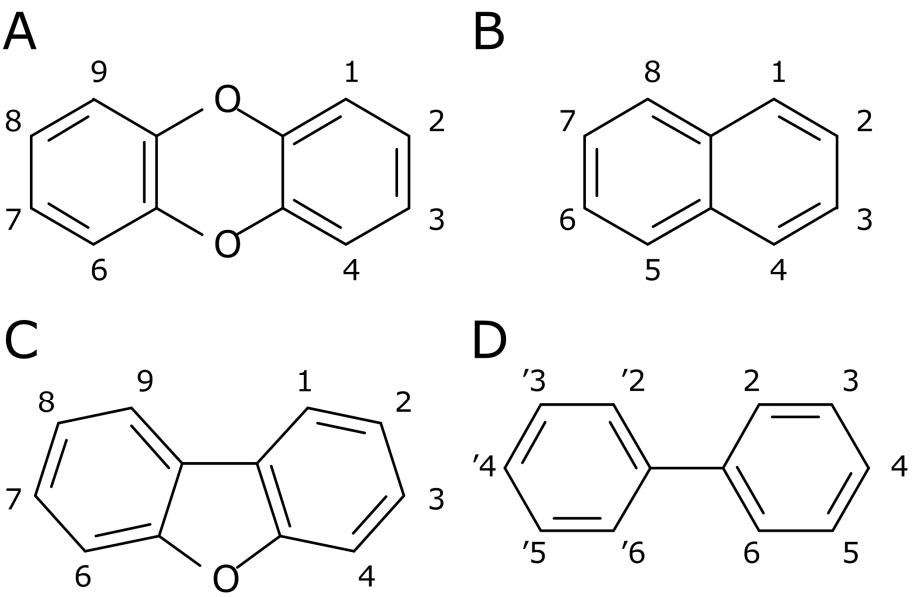

Figure 2. Core molecular structures of four POPs classes and the numbering of their potential sites of substitution. For PCDD (A) and PCDF (C), the 2, 3, 7, and 8 carbons are referred to as β-carbons. For PCN (B), the 2, 3, 6, and 7 positions are referred to as β carbons. The 2, 2', 6, and 6' positions of the PCB skeleton (D) are known as the *ortho* positions.

TOXICITY

The most toxic PCDD, PCDF, PCB, and PCN congeners are 2,3,7,8-TeCDD and 1,2,3,7,8-PeCDD [22]. While the mechanisms responsible for their toxicity have not been fully elucidated, their high affinity for the aryl hydrocarbon receptor (AhR) is believed to play a central role. The AhR is a transcription factor and its abnormal activation can disrupt cell function by altering gene transcription. The known toxic effects of 2,3,7,8-TeCDD exposure include, apart from death by direct high dose exposure, dermal effects (e.g., chloracne), suppression of the immune system due to induction of cell death in immune cells, and cancer [23]. Not all PCDD, PCDF, PCB and PCN congeners activate the AhR; their binding is governed by their pattern of chlorine

substitution and the planarity of their carbon skeletons. Toxic PCDD, PCDF and PCN congeners bear chlorine substituents in the β positions, i.e. the 2, 3, 7, and 8 positions for PCDD and PCDF, and the 2,3,6,7 positions for PCN. Toxic PCB congeners have at most one chlorine substituent in an *ortho* position, enabling them to adopt a planar configuration and thus fit into the AhR binding pocket. However, they may carry multiple chlorines in the *meta* (3, ‘3, 5 and ‘5) and *para* (4 and ‘4) positions (Figure 2D) [22].

Because PCDD, PCDF, PCN and PCB are very lipophilic, they can accumulate in the body’s fatty tissues. It has also been shown that they can be passed from mothers to their foetuses via the umbilical cord and placenta, and to infants via breast milk, causing early exposure [24].

TOXIC EQUIVALENCE FACTORS (TEQ)

Toxic dioxin congeners and dioxin like compounds have the same mode of action and their toxic effects are additive and to enable comparisons between samples, a comparative scale of toxicity is used. This toxic equivalence (TEQ) value is calculated by giving the AhR activity of the most toxic congener (2,3,7,8-TeCDD) the toxic equivalence factor (TEF) one ($TEF_{2,3,7,8\text{-TeCDD}} = 1$). The $TEF_{2,3,7,8\text{-TeCDD}}$ is then used as benchmark to evaluate the toxicity of the other AhR activating congeners, i.e., a congener that exhibits half the AhR activating ability compared to 2,3,7,8-TeCDD receives the value TEF 0.5 (Table 1) [22]. To determine the TEQ value of a sample, the TEF values are multiplied by the congener concentration (see equation 1). The resulting values are then summarized into a sample specific TEQ value.

$$TEQ = \sum_{n1}[PCDD_i \times TEF_i] + \sum_{n2}[PCDF_i \times TEF_i] + \sum_{n3}[PCB_i + TEF_i] \quad \text{(eq 1)}$$

The toxicity of samples with different congener distributions can be compared by comparing their TEQ values. The TEQ scales are re-evaluated periodically as more accurate and comprehensive toxicity measurements become available. At present, no official TEF values have been assigned to 2,3,6,7-substituted PCN congeners. One study on the AhR-activating ability of PCN suggested that 1,2,3,4,6,7-HxCN and 1,2,3,5,6,7-HxCN should have TEF values of around 0.0015-0.0072 and 0.00029-0.00067, respectively [25]. PCNs are candidates for classification as POPs under the Stockholm convention and their status is currently being reviewed [14].

Table 1. The TEF values assigned to various POPs by the WHO2005-TEQ. These values are used throughout this thesis.

PCDD and PCDF	WHO $_{2005}$TEF	PCB	WHO $_{2005}$TEF
2,3,7,8-TeCDD	1	*Planar PCB*	
1,2,3,7,8-PeCDD	1	3,4,4',5-TeCB (81*)	0.0003
1,2,3,4,7,8-HxCDD	0.1	3,3',4,4'-TeCB (77*)	0.0001
1,2,3,6,7,8-HxCDD	0.1	3,3',4,4',5-PeCB (126*)	0.1
1,2,3,7,8,9-HxCDD	0.1	3,3',4,4',5,5'-HxCB (169*)	0.03
1,2,3,4,6,7,8-HpCDD	0.01		
OCDD	0.0003	*Non- and mono- ortho PCB*	
		2,3,3',4,4'-PeCB (105*)	0.00003
2,3,7,8-TeCDF	0.1	2,3,4,4',5-PeCB (114*)	0.00003
1,2,3,7,8-PeCDF	0.03	2,3',4,4',5-PeCB (118*)	0.00003
2,3,4,7,8-PeCDF	0.3	2',3,4,4',5-PeCB (123*)	0.00003
1,2,3,4,7,8-HxCDF	0.1	2,3,3',4,4',5-HxCB (156*)	0.00003
1,2,3,6,7,8-HxCDF	0.1	2,3,3',4,4',5'-HxCB (157*)	0.00003
1,2,3,7,8,9-HxCDF	0.1	2,3',4,4',5,5'-HxCB (167*)	0.00003
2,3,4,6,7,8-HxCDF	0.1	2,3,3',4,4',5,5'-HpCB (189*)	0.00003
1,2,3,4,6,7,8-HpCDF	0.01		
1,2,3,4,7,8,9-HpCDF	0.01		
OCDF	0.0003	** numbering according to IUPAC*	

FORMATION

While MSW that is fed into incinerators may contain small quantities of POPs [26], they will normally be almost completely destroyed during incineration (which occurs at temperatures of up to 1100-1200 °C in mass burners). Unfortunately, POPs (re)formation can occur in the post-combustion zones of MSW incinerators while the flue gases are cooled in the superheaters (which typically operate at temperatures of 450-300 °C). Figure 3 shows a schematic of a typical MSW incineration plant in which the key locations for POPs formation and their typical operating temperatures are indicated.

The mechanisms that drive the thermal formation of PCDD and PCDF have been studied much more extensively than those for PCN and PCB. While complete mechanisms of formation remain to be elucidated because they involve high temperature radical reactions, our current understanding provides some key insights into POPs formation.

PCDF and PCDD can be formed by gas-phase/gas-phase processes at 500–800 °C [27, 28] but their observed concentrations under such conditions are usually low or non-detectable (**Paper II**) [29]. PCDF and PCDD

concentrations increase as the temperature drops; their overall rate of formation peaks at around 300 °C. At this temperature, they are formed by heterogeneous gas-phase/particle phase processes [30].

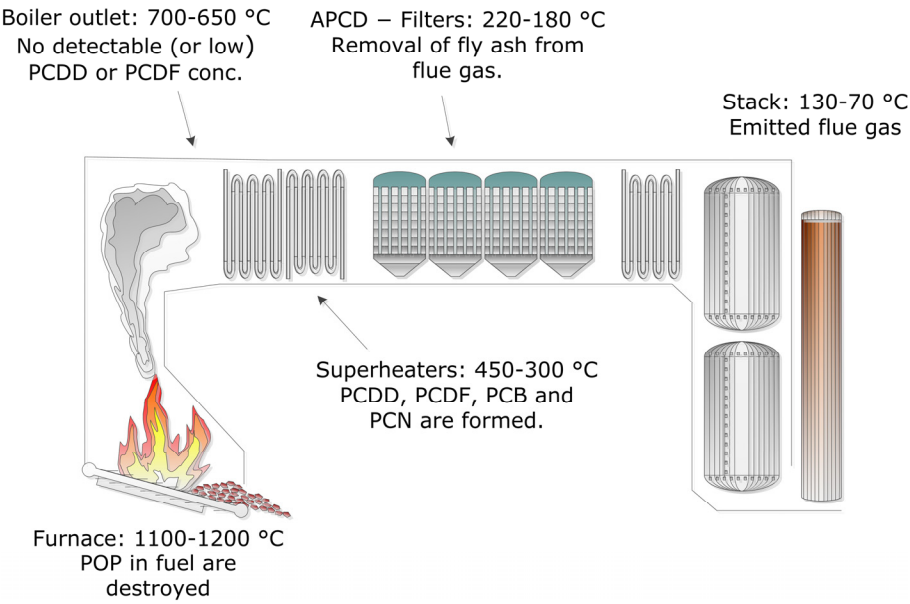

Figure 3. Important locations for POPs destruction and formation during MSW incineration and their approximate temperatures.

The heterogeneous process is often divided into two reaction pathways: formation from precursors and *de novo* formation. The final POPs concentrations, homologue profiles, and congener patterns are also significantly influenced by chlorination and dechlorination reactions that occur at the same time as the carbon skeletons are formed (either from precursors or *de novo*). All of these processes occur simultaneously and they are generally not readily differentiated. PCB and PCN are formed via similar pathways and under similar conditions.

FORMATION FROM PRECURSORS

During MSW incineration, a large variety of small organic molecules can be volatilized from the feedstock, form during combustion, or form in the combustion gases as they cool down [31, 32]. Under favourable conditions, some of these compounds act as precursors that enable the direct formation of PCDD and PCDF in the post-combustion zone. Two well-studied precursors are polychlorinated benzenes (PCBz) [e.g., 33] and polychlorinated phenols (PCPh)

[e.g., 34]. However, PCDD and PCDF can also be formed via the condensation or radical polymerization of chlorinated and un-chlorinated aliphatic hydrocarbons, which sometimes occurs at relatively low temperatures [e.g., 35]. The formation of PCDD (and PCDF to some extent) on particle surfaces is thought to occur mainly via formation from precursors, which yields very specific chlorination patterns [34, 36]. PCB are also believed to be mainly formed from precursors at temperatures above 450 °C [37, 38].

DE NOVO FORMATION

The production of unburned carbon, i.e., soot, is inevitable in MSW incineration. Soot consists of partly aromatic material that can provide both a feedstock and scaffold for the *de novo* formation of PCDF, PCDD, PCB and PCN [39-43]. *De novo* formation can also occur via the oxidation and chlorination of polycyclic aromatic hydrocarbons (PAH) [44-46]. In MSW incineration, the *de novo* pathway forms more PCDF than PCDD [47, 48], and the characteristic PCDD/PCDF ratio of < 1 in MSW incineration plants suggests that the *de novo* pathway is the predominant formation route [49].

CHLORINATION AND DECHLORINATION

Chlorination and dechlorination do not contribute to the formation of the carbon backbone but they do affect the concentrations of PCDF, PCDD, PCB and PCN homologues and their congener patterns [50-53]. While HCl accounts for the majority of the chlorine in MSW incineration flue gas, it cannot directly chlorinate aromatic structures. Instead, the chlorine must be oxidized, enabling it to react with aromatic compounds via electrophilic substitution catalysed by e.g., copper [54]. The oxidation of chlorine is suggested to take place via the copper-catalysed Deacon reaction (R3 and R4) [55]:

$$2\,CuCl_2 + O_2 \rightarrow 2\,CuO + 2\,Cl_2 \qquad \text{(R3)}$$

$$2\,CuO + 4\,HCl \rightarrow 2\,CuCl_2 + 2\,H_2O \qquad \text{(R4)}$$

The yield of the Deacon reaction peaks at around 400°C [56], meaning that chlorine formation via this process is strongest on the upper end of the temperature range that accommodates heterogeneous formation. There are other copper-catalysed reactions that can chlorinate aromatic species in the heterogeneous formation temperature window [57, 58] and other metals that can catalyse chlorination reactions (e.g., Fe), but in both cases these processes are less important than the Cu-catalysed Deacon reaction [57, 59]. Chlorination via

electrophilic aromatic substitution preferentially occurs at the β-carbons (Figure 2) for both mechanistic and steric reasons. It therefore favours the formation of toxic congeners, i.e. congeners that have been assigned TEF values [60].

The mechanisms of POPs formation are also affected by the composition of the fly ash, including the speciation and abundance of metals [42], and process parameters such as operating temperatures and start-up/shutdown conditions (yielding so called memory effects) [7, 61, 62]. During episodes of low combustion efficiency, PCDD and PCDF formation are enhanced and their homologue and congener patterns change [7]. PCN concentrations are also affected by combustion efficiency: the PCN concentration in the flue gas is higher during the start-up and shut-down of MSW incinerators than during normal operation, but the degree of chlorination shifts slightly upwards during steady-state combustion [53, 63]. Under normal combustion conditions, the PCDF, PCDD and PCB congener patterns produced during MSW incineration are relatively consistent and can be used for source identification [12, 64] and modelling [13, 17]. In addition to the overall congener fingerprint, key congeners can provide insights into the formation processes occurring in a given incinerator (**Paper I**)

IN-FILTER PCDF AND PCDD FORMATION AT LOW TEMPERATURE – **PAPER I**

This case study investigated filter performance in a 65 MW waste-to-energy plant located outside Umeå (Figure 4). The plant, capable of incinerating 20 tonnes·hour^{-1}, was originally built in 2000 and normally uses a 60:40 MSW:IW fuel mix. It was remodelled in 2005 to accommodate increased production, and a new filter (Filter 1) was added to the APCD (Figure 5). In addition, the filters' operating temperature was increased from ca 150 °C to around 200 °C in order to suppress alkaline salt caking on the filter socks. After the remodelling, increased TEQ emissions were observed in the stack. To ensure that emissions remained below legislative limits, carbon-doped tower fillers were added to the post-filter scrubbers to adsorb POPs that passed through the filters.

The purpose of this case study was to investigate the filters' performance and explain the increasing concentrations of toxic PCDF and PCDD in the flue gas.

For **Paper I**, a total of 18 samples divided into four sample sets (Figure 5) were collected using the cooled probe method specified in EN 1948:1 [65]. Sample set A (Table 2) were used as baseline samples, with 'standard' levels of carbon injection and a reference operating temperature. Sample set B (Filter 1)

was collected at an elevated operating temperature (10 °C above the reference value both pre- and post- filter); sample set C (Filter 1) was collected at baseline temperature but without carbon injection; and sample set D (Filter 2; Carbon injection: $2.5 \cdot 10^{-3}$ kg·h^{-1}·m^{-3} and baseline temperature) was collected using the old filter to compare its efficiency to the new one.

Figure 4. The Dåva MSW incineration plant. Photo: Johan Gunséus/SYNK.

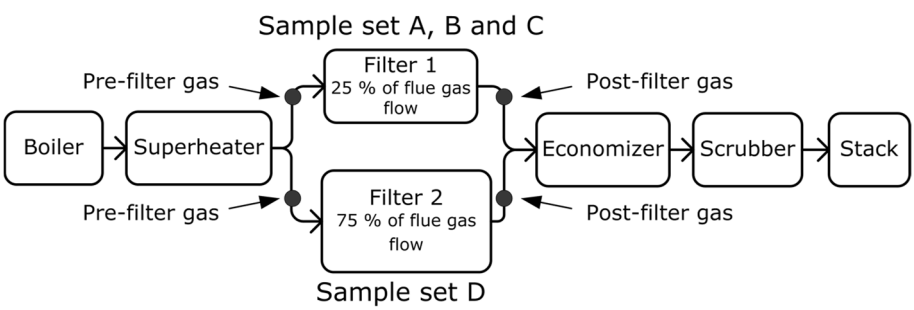

Figure 5. Schematic over the Dåva plants' incineration process and sampling locations.

The sample sets were collected simultaneously. Pre- and post- filter samples were taken at the same time (Figure 5), on separate days and in duplicate. Sampling was only conducted on days with and preceded by at least 14 days stable combustion conditions to avoid memory effects [49].

Table 2. Sample sets and information on filter operating conditions. Temperatures were obtained from plant control room readings and are shown as the mean ± standard deviation obtained from in-plant monitoring (every 15 min) during sampling. Flue-gas flows and carbon injection values reflect mean flows in the plant and are not specific to any sample set.

	Filter 1		Filter 2	
	Pre-filter gas no. of samples (flue-gas temp)	Post-filter gas no. of samples (flue-gas temp[c])	Pre-filter gas no. of samples (flue-gas temp)	Post-filter gas no. of samples (flue-gas temp[c])
A	2 (213 ± 1.0 °C)	2 (201 ± 0.4 °C)		
B	2 (221 ± 0.4 °C)	2 (206 ± 0.6 °C)		
C[a]	2 (210 ± 1.3 °C)	2 (203 ± 0.8 °C)		
D			4 (210 ± 1.7 °C)	2 (204 ± 1.1 °C)
Flue-gas flow	30000 $m^3 \cdot h^{-1}$		90000 $m^3 \cdot h^{-1}$	
Filter surface	1280 m^2		3750 m^2	
Carbon injection	5.3 $kg \cdot h^{-1}$		9.4 $kg \cdot h^{-1}$	
Carbon load	$4.1 \cdot 10^{-3}$ $kg \cdot h^{-1} \cdot m^{-3}$		$2.5 \cdot 10^{-3}$ $kg \cdot h^{-1} \cdot m^{-3}$	
Ash removal method[b]	Empties one filter tube at the time according to a programmed cycle.		Empties when back pressure in filter tubes rises to a predefined value.	
Time for entire filter to empty	460 sec		n/a (depends on particle load)	

[a] No active carbon/lime injection, turned off 1 h prior to and during sampling. [b] Ash is removed by blowing pressurised air through the filter tube. [c] Post-filter temperatures were recorded for both filters at the same location.

Both Filter 1 and Filter 2 removed most PCDF from the flue gas in all sample sets (A: -85 %; B: -70 %; C: 94 % and D: -97 %), but the removal efficiency decreased when the temperature was increased (sample set B). The reduced removal efficiency was more pronounced for toxic PCDF congeners: the TEQ_{PCDF} of the filtered gas was only halved after filtration in sample set B (-52 %) but was reduced much more strongly in sample sets A (-76 %) and C (-92 %).

PCDD removal after the filter was only observed in sample set D (-41 %). The total PCDD concentration actually *increased* in all Filter 1 sample sets

(sample sets A, B and C). This increase was most pronounced for sample set B, where the concentration in the post-filter gas was more than twice (+133%) that pre-filter. Toxic PCDD concentrations declined after filtration for all sample sets (A: -76 %; B: -56 %, C: -74 %; and D: -91 %), indicating that their formation were not promoted in Filter 1. However, the total decline in toxic PCDD and PCDF concentrations was not sufficient by itself to bring the plant below the 0.1 $ng \cdot Nm^{-3}$ TEQ limit required by law.

The observed changes in PCDF and PCDD concentrations suggested that the filter temperature had a greater effect on POPs formation than the carbon load (Table 2). The 10 °C increase in filter temperature tested in sample set B doubled the PCDD concentration in the filtered gas.

The PCDF homologue profiles (Figure 6A) for the four sample sets showed that filtration increased the relative abundance of more highly chlorinated homologues. In particular, the relative abundance of HpCDF increased sharply after filtration in sample sets A and B (i.e. samples collected during experiments using Filter 1 with carbon injection). The major HpCDF congener in the post-filter gases from these sample sets was 1,2,3,4,6,7,8-HpCDF.

The PCDD homologue profiles revealed a uniform shift to higher levels of chlorination after filtration, as shown in Figure 6B. This suggests that the increase was driven by the same process independently of the temperature, level of carbon injection, or filter used. To better determine what was happening inside the filters, the PCDD congeners were separated and quantified individually where possible (some congeners co-eluted and were therefore quantified together). The differences between pre- and post- filter congener concentrations revealed that congeners that are primarily formed by PCPh condensation [34, 66] were significantly more abundant in the post-filter gas than in the pre-filter gas (results for TeCDD-OCDD are shown in Figure 7). While congeners formed by PCPh condensation became more abundant, the most toxic PCDD congeners became less so: filtration reduced the concentration of toxic PCDD.

In summary, **Paper I** found that the increase in TEQ emissions observed after the plant's remodelling was probably due to enhanced PCDF and PCDD formation within the filters. The newly formed PCDF and PCDD, together with the PCDF and PCDD formed in the post-combustion zone probably overloaded the filters' removal capacity. Because only TEQ concentrations are monitored to ensure regulatory compliance, the total PCDF and PCDD concentrations and their changes in the aftermath of the remodelling process had not been determined. While the increased levels of PCDD in the filtered gas were primarily due to non-toxic congeners or congeners with relatively low toxicity, there was a sufficiently large increase in the abundance of low-toxicity congeners

to raise the overall toxicity of the emissions above the legal threshold. The bulk of the increase was probably due to PCDD formation via PCPh condensation. PCDD formation via condensation became more pronounced at higher filter temperatures, even though the tested temperatures were well below the peak formation temperatures. The study also showed that useful information can be gathered by quantifying compounds other than the 17 toxic congeners and that such data can be vital when attempting to resolve issues encountered in full-scale plants.

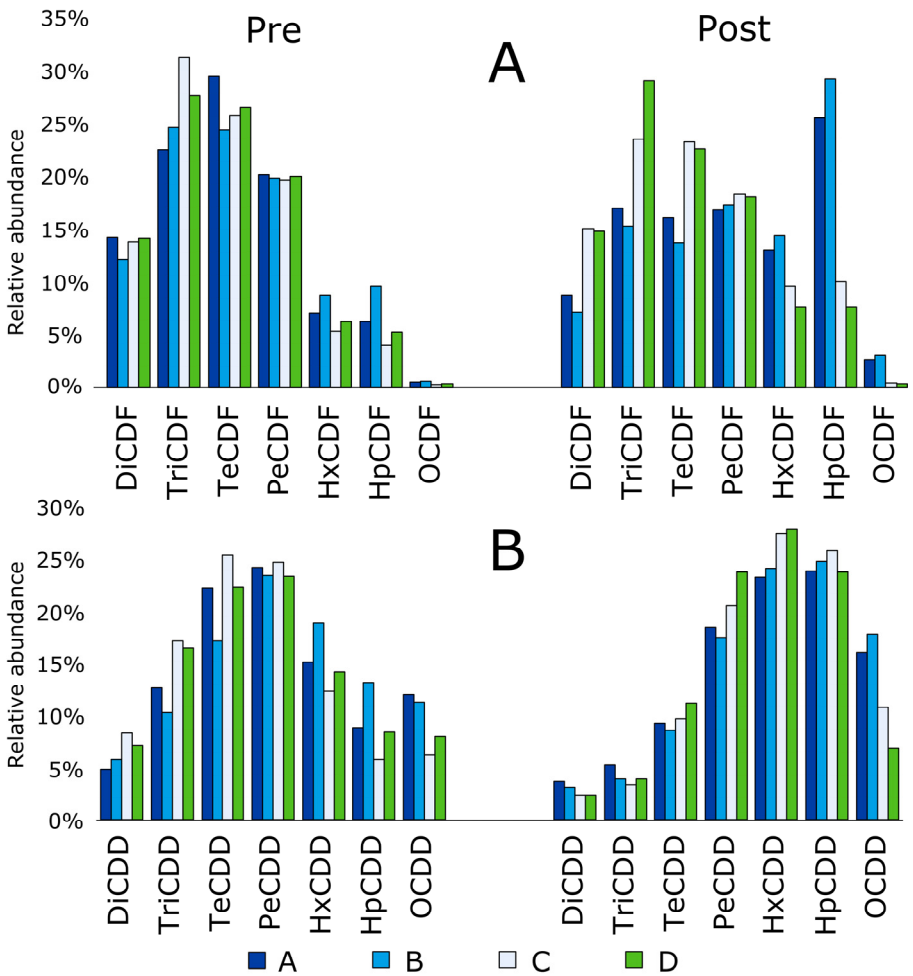

Figure 6. PCDF (A) and PCDD (B) homologue distributions in the pre- and post-filtration gas for sample sets A, B, C, and D.

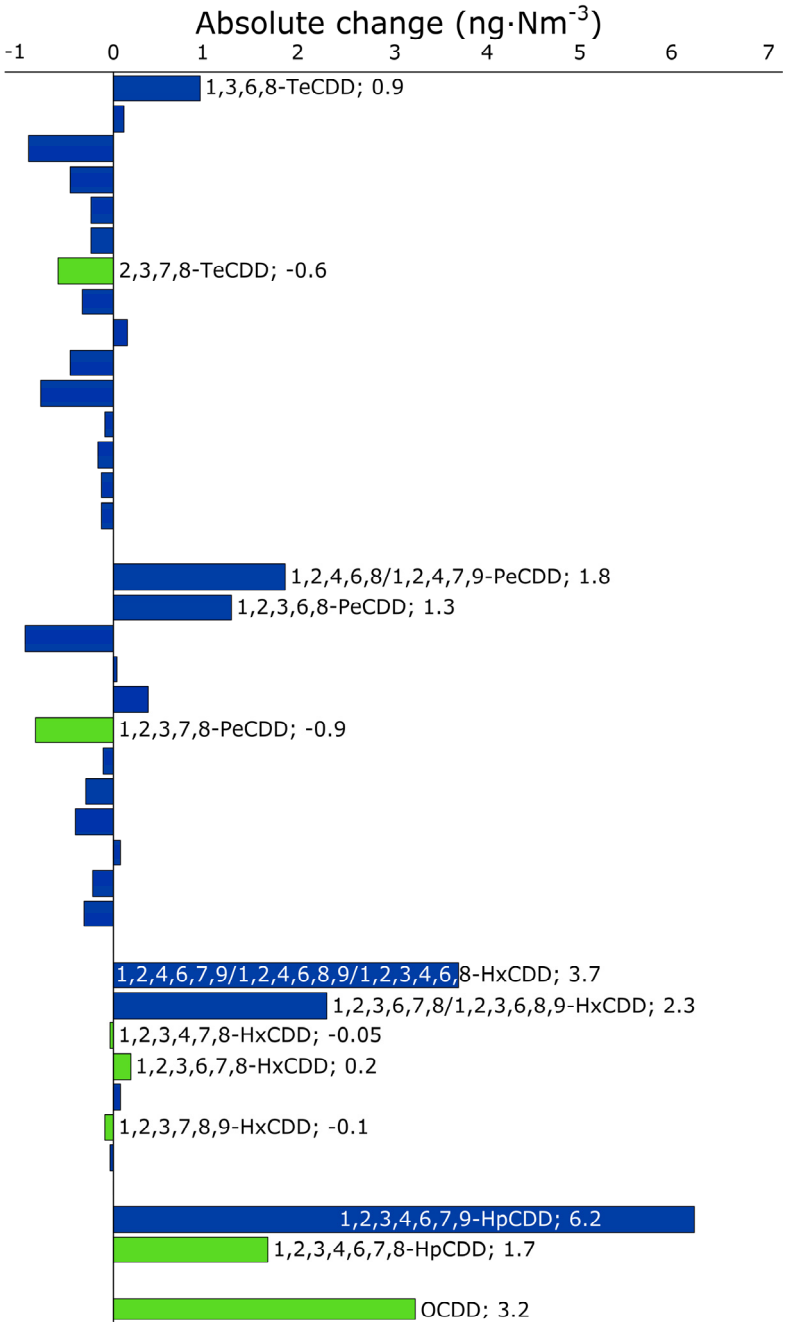

Figure 7. Differences between pre- and post-filter concentrations of specific PCDD congeners. Values quoted in the figures are based on average values for all of the tested filters.

SAMPLING AND POPS ANALYSIS

Sampling waste incineration ash is straightforward: one need only gather enough material to obtain a representative sample. The hard part is determining what constitutes a representative sample. To accurately reflect the ash produced by an individual plant, one should ideally collect material on several sampling occasions, preferably spread over a year or two, as long as there are no major changes in fuel composition during that period. The other option is to use grab samples and regard the ash as a snapshot representation, since ash composition can change from season to season and with fuel composition.

Flue gas sampling poses another type of challenge. It must be done accurately and precisely to capture the composition and distribution of flue gas particles as well as the concentrations of vaporized target substances, which may be as low as a few pmol·Nm^{-3}. Because PCDD, PCDF, PCB and PCN form rapidly in waste incineration flue gases and the speciation of the contaminants depends on both the combustion process and fuel composition, sampling procedures must be carefully designed and sampling must be conducted when incineration is proceeding under stable conditions. If the combustion conditions are unstable due to poor combustion or start-up/shutdown conditions, the previously mentioned memory effects may yield unrepresentative samples [7, 49].

FLUE GAS SAMPLING

There are several sampling standards (US-EPA 0023A, JIS K 01331:2005, EN 1948:1)) but only the cooled probe method described in the European standard committees' method for flue gas sampling (EN 1948:1) [65] was used in this thesis work. To capture the particle composition and distribution of the flue gas, a vacuum pump is used to withdraw flue gases and fly ash isokinetically (Figure 8) from the flue gas duct through a water-cooled probe that is fitted with a glass liner. Water-cooling the probe ensures that the flue gas temperature is rapidly reduced to less than 20 °C. This prevents *sampling artefacts* arising from the uncontrolled formation of target analytes during sampling. Because such artefacts increase the total POPs concentrations in the sample, they lead to overestimations of analyte concentrations. After the water-cooled probe, the sample is passed through impinger bottles containing water and then ethylene glycol to capture water and particles. Finally, the flue gases pass through two

polyurethane foam plugs (PUFP) and a 0.45 µm filter that traps organic pollutants and aerosols (Figure 9).

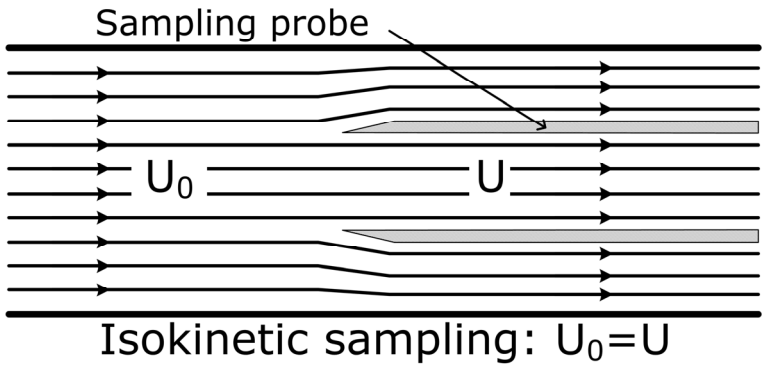

Figure 8. Isokinetic sampling: the gas velocity of the pump is matched to that of the flue gas stream. When the gas velocities match, the distribution of particles in the sampled air is similar to that in the flue gas duct as a whole. If the sampled gas velocity is too high or low, light particles will be over- or under-represented in the sample, respectively.

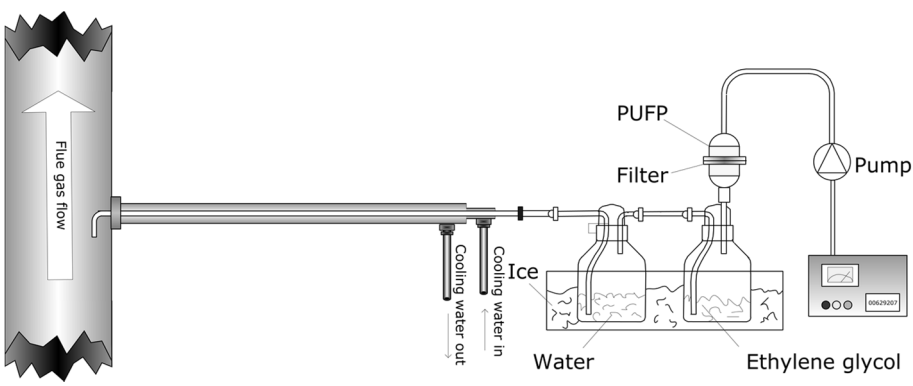

Figure 9. Schematic of the sampling train used for flue gas sampling.

SAMPLE CLEAN-UP

Different methods were used to extract PCDD, PCDF, PCB, and PCN from different sample types (e.g. ash or flue gas), but the sample clean-up process was the same in all cases (Figure 10)

For complete flue-gas samples (**Paper I** and **II**), internal standard was added directly to the water bottle. Water and ethylene glycol from the impinger bottles were combined and filtered through a 1 µm glass fibre filter followed by a 0.45 µm polyamide filter. The water/glycol mix was then diluted 10 times,

acidified (pH < 3; to protonate PCPh) and extracted using a solid phase extraction (SPE) disk. The filters, SPE discs and PUFPs used for each sample were placed together in a Soxhlet extractor equipped with a Dean-Stark separator and refluxed in toluene for 24 h. In cases where only the PUFPs were analysed (**Paper IV**), an internal standard was added directly to the Soxhlet extractor and the PUFPs were refluxed in toluene for 24 h. Ash samples (**Paper IV**) were weighed and mixed with sand (approx.1:4 w:w), before adding the internal standard. The ash was then soaked in acetic acid (99%) to break down and neutralize its matrix. All sample processing methods have been validated and are thoroughly described elsewhere. [67, 68]

The resulting toluene phase was concentrated by evaporation and divided into three aliquots (2:1:1). The largest aliquot was used for PCDD, PCDF, PCN and PCB determination, while the other two were retained for further analysis. The samples for POPs determination were cleaned up on a multi-silica column followed by an alkaline alumina column. They were then fractionated using an active carbon/celite column to yield two fractions, one containing PCDD, PCDF, PCN and planar PCB, and the other containing the remaining PCB [67]

For the flue gas samples (**Paper I** and **II**) an additional miniature multi-silica column was used prior to the addition of recovery standard and evaporation into tetradecane. (Figure 10).

ANALYSIS

All analyses were performed using a Waters AutoSpec Ultima NT 2000D GC-HRMS (Waters Corporation, Milford, MA) The mass spectrometer was operated in electron impact ionization/selected ion monitoring mode and the analytes were quantified using isotope dilution. Peaks were identified using internal standards and elution order was established according to Ryan *et .al.* [69] for DB5 column, Bacher *et. al.* [70] for SP 2331 and Nakano and Weber [71] for DB5-ms.

For **Paper I** quantification of Mo- to HpCDF and Mo-HpCDD were done using a SP 2331 column (Supelco, 60 m, 0.25 mm i.d., 0.2 µm film thickness) while a DB 5 column (Supelco, 60 m, 0.25 mm i.d., 0.25 µm film thickness) was used to quantify OCDF and OCDD.

For **Paper II**, the GC-HRMS was equipped with a DB 5 (J&W Scientific; 60 m × 0.25 mm i.d., 0.25 µm film thickness) column.

For **Paper III** and **IV**, a DB 5-ms (Supelco 60 m × 0.25 mm i.d., 0.25 µm film thickness) column was used for quantification and separation of PCDF, PCDD, PCB and PCN congeners.

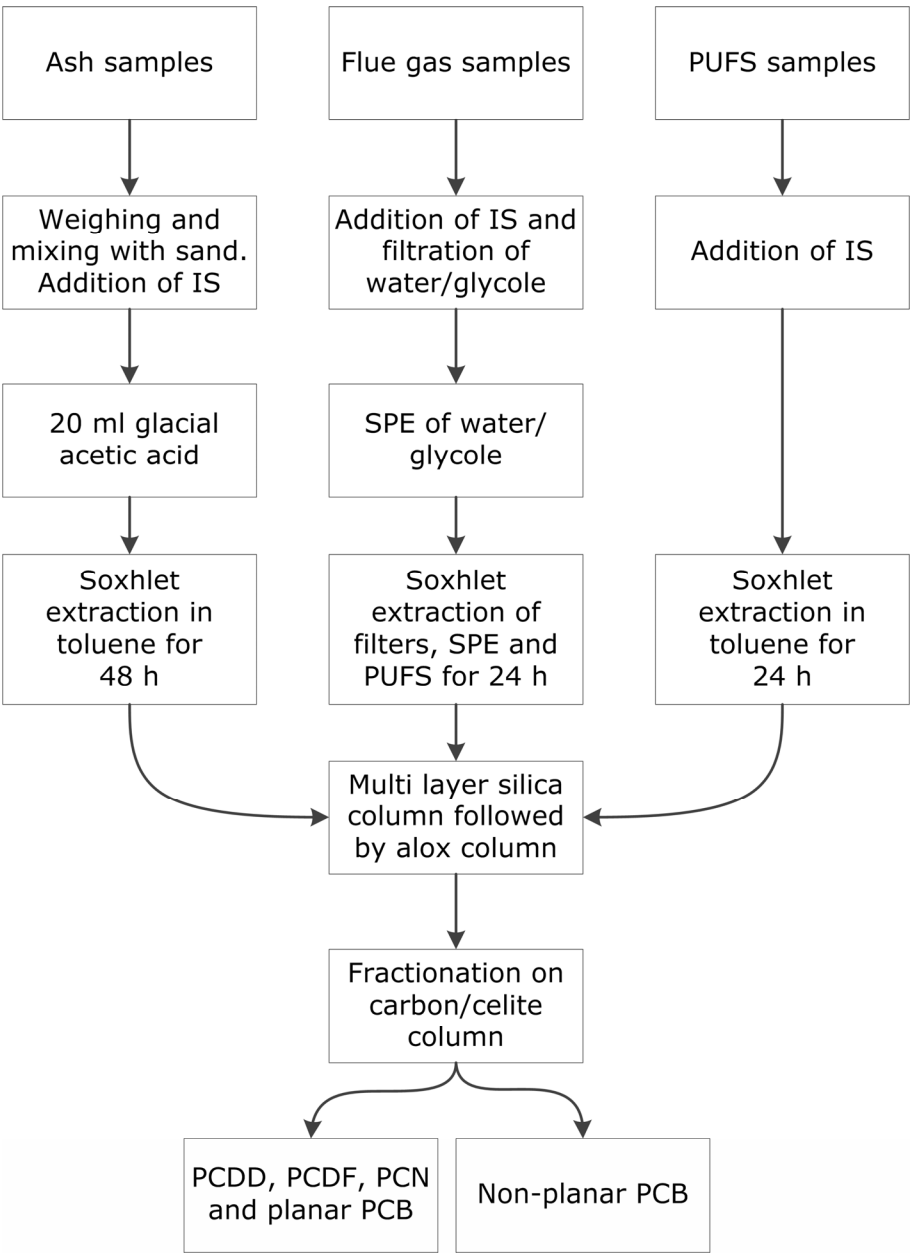

Figure 10. Flow chart for the extraction and clean-up of ash, PUF and flue gas samples.

For the sake of quality assurance, blank samples and field blank (where applicable) samples were processed together with the actual samples. Where blank concentrations were found to be greater than 10 % of corresponding sample concentrations, they were reported and their relevance discussed. In **Paper II**, blank subtractions were performed for MoCDD and DiCDD homologue groups. In **Paper I, III** and **IV**, MoCDD was excluded due to low recoveries.

THE SUB-ZERO PROBE – PAPER II

Current emissions laws only require stack gas sampling in MSW incineration plants. Stack temperatures are usually around 70-130 °C, i.e. well below the 450-250 °C range at which PCDF and PCDD formation occurs. This means that the concentration and composition of these compounds does not change in the stack – their concentrations in the stack are equal to those that are emitted. On the other hand, for research purposes it is sometimes necessary to collect samples from locations with higher temperatures (e.g. superheaters or boiler outlets). To ensure adequate cooling when sampling at high temperatures, Dr Johanna Aurell (PhD in Environmental Chemistry at Umeå University) designed a modified version of the water-cooled probe described in EN 1948:1 [29]. The modification consists of an extra outer casing filled with a salt and ice mixture, further enhancing the probe's cooling capacity (Figure 11). To withstand the high temperatures of the flue gases, the original glass probe liner was replaced by a custom-made titanium probe liner. **Paper II** describes the validation of the sub-zero cooling probe and illustrates and defines its cooling efficiency. The study also illustrates the risk of artefact formation during high temperature sampling.

The study reported in **Paper II** had two parts: the first dealt with determining temperature profiles in the original and modified sampling probes while the second aimed to show the importance of adequate cooling during high temperature sampling. All measurements and sampling were performed in a 5 kW laboratory scaled fluidized bed reactor [7, 72]. The original probe was used in two setups, a horizontal configuration similar to that used in full-scale plants and a vertical configuration like that normally used with laboratory-scale fluidized-bed reactors.

The difference in cooling efficiency between the original probe and the sub-zero probe was significant: flue gases with an original temperature of 700 °C were cooled to less than 200 °C within the first 5 cm of the sub-zero probe but did not reach these temperatures until they had travelled 35 cm along the original

cooling probe (Figure 12). For initial gas temperatures of 400 °C, the gas temperature was below 200 °C even before it entered the sub-zero probe whereas it had to travel 20 cm along the original probe before reaching this temperature. The greater cooling distances required with the standard probe meant that the sampled gas remained in the temperature window for POPs formation for extended periods of time. The POPs concentrations measured with the original probe when sampling gases at 700 °C varied greatly (Table 3): the highest total PCDF concentrations were almost 20 times higher (120 ng·Nm^{-3}) than the lowest (4.3 ng·Nm^{-3}), even though the probe was in the horizontal configuration on both occasions.

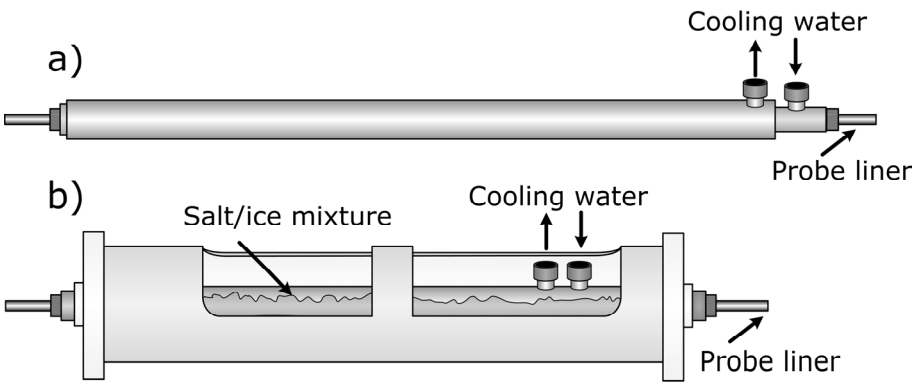

Figure 11. a) The original 1948:1 water cooled probe and b) the modified sub-zero probe.

Even the lowest summed PCDF concentration measured using the original probe was twice as high as the highest value observed with the sub-zero probe (17 ng·Nm^{-3} vs. 9.7 ng·Nm^{-3}). The same trend was seen for the summed PCDD concentrations: the results obtained with the original probe varied substantially (9.3-510 ng·Nm^{-3}) and even the lowest measurement acquired with the original (9.3 ng·Nm^{-3}) was much greater than the highest value determined using the sub-zero probe (2.6 ng·Nm^{-3}). For the samples taken at a lower temperature (400 °C) the original probe provided sufficient cooling – there were no discernible differences between the two cooling probes despite the longer cooling distance in the original probe.

In summary, the study confirmed the importance of rapid cooling during high temperature (> 450 °C) flue gas sampling. Moreover, it showed that the cooling capacity of the sub-zero probe was sufficient to prevent artefact formation and demonstrated that PCDD and PCDF formation in the 200-500 °C temperature window is so rapid that PCDD concentrations can increase by a factor of 50 in

the time it takes for a gas sample to travel a few centimetres along a glass tube. The aim of the study was not to discredit the EN1948:1 method for stack gas sampling but rather to encourage caution when preforming high temperature flue gas sampling to avoid overestimating PCDF and PCDD concentrations.

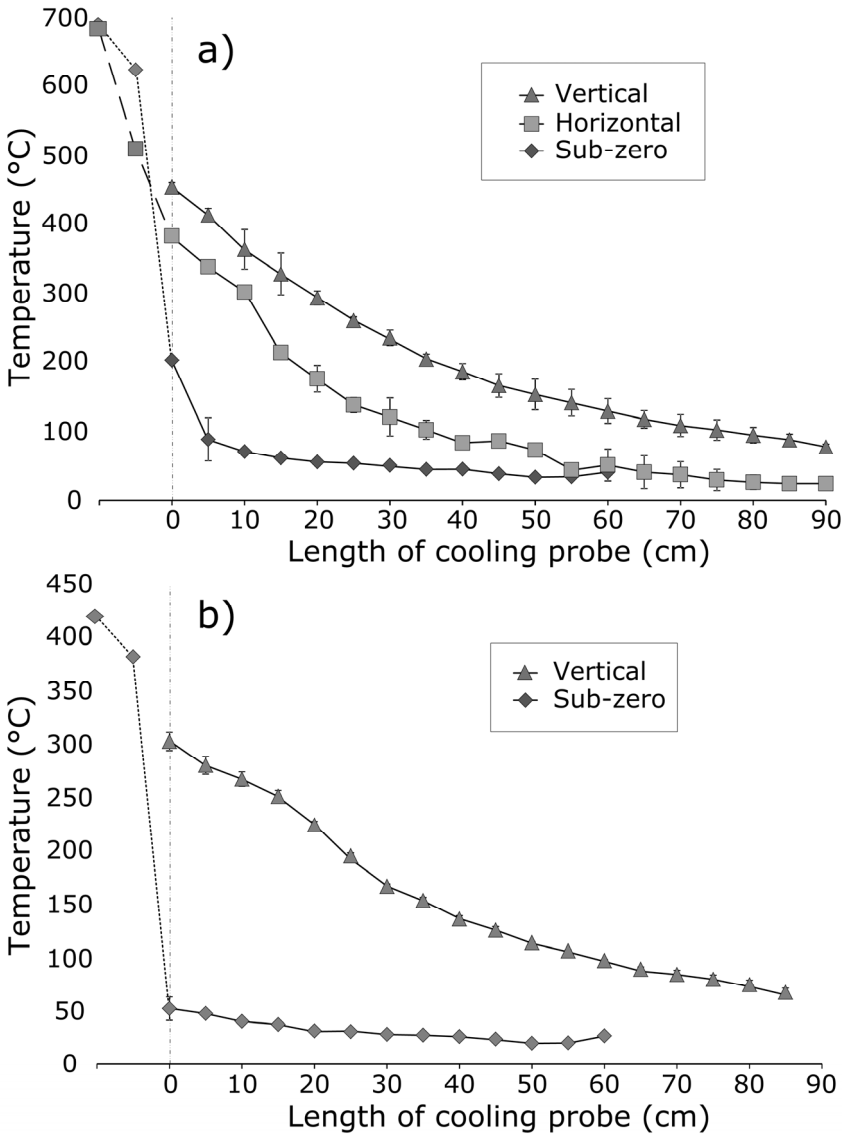

Figure 12. Temperature profiles of the sub-zero probe and different configurations of the original probe when sampling flue gases at initial temperatures of 700 °C (a) and 400 °C (b). The error bars correspond to ±1 standard deviation.

Table 3. Concentrations of PCDF and PCDD (ng·Nm^{-3}) in flue gas samples taken at 700 °C using the sub-zero probe and the original probe in its vertical and horizontal configuration.

	Horizontal			**Vertical**		**Sub-zero**	**Sub-zero** (Aurell et al. (2009)[29])		
MoCDF	35	120	4.3	n/a[d]	n/a[d]	3.2	3.0	2.6	4.9
DiCDF	13	72	3.1	6.9	21	0.88–2.9[a]	0.62	0.59	0.80
TriCDF	12	32	1.0–3.4[a]	5.5	16	0.72–2.4[a]	0.36	0.27	0.41
TeCDF	12	11	1.1	2.5	8.7	0.38	0.09–0.3	0.08–0.3	0.09–0.3
PeCDF	9.9	8.3	1.3	2.3	7.3	<0.27[b]	0.05–0.20	0.04–0.14	0.05–0.20
HxCDF	6.5	5.4	1.6	2.2	6.2	<0.25[b]	<0.09	<0.08	<0.09
HpCDF	1.7	1.6	1.1	1.4	3.1	<0.18[b]	0.06–0.2	<0.05	<0.05
OCDF	0.43	0.72	0.70	0.73	1.3	<0.07[b]	0.2	0.03	0.04
Σ PCDF	90	250	17[e]	22[f]	64[f]	9.7[e]	5.0[e]	4.1[e]	6.8[e]
MoCDD[c]	1.5	23	0.2[b]	n/a[d]	n/a[d]	<0.14[b]	0.03	0.03	0.04
DiCDD[c]	1.8	24	0.5[b]	0.40	1.0	<0.27[b]	<0.04	<0.03	<0.03
TriCDD	8.2	62	0.67–2.2[a]	0.94	3.5	<0.48[b]	0.02–0.05	<0.01	<0.02
TeCDD	19	72	1.2	0.25	0.54	0.16	0.02–0.08	<0.01	0.01–0.03
PeCDD	54	120	1.8	2.5	6.2	0.14–0.48[a]	<0.04	<0.04	<0.03
HxCDD	100	140	3.7	4.1	6.8	0.14–0.48[a]	<0.1	<0.08	<0.08
HpCDD	52	58	1.8	1.1	3.3	0.15–0.18[a]	n/a[d]	n/a[d]	0.02–0.07
OCDD	7.5	7.3	0.80	0.85	1.7	<0.07[b]	n/a[d]	n/a[d]	0.11
Σ PCDD	240	510	12[e]	9.3[f]	23[f]	2.6[e]	0.34[f]	0.20[f]	0.41[e]

[a] Values below limit of quantification (LOQ) but above limit of detection (LOD). LOD and LOQ were calculated for each individual sample. Interval denotes LOD–LOQ. [b] Value below LOD, LOD value shown. [c] Blank values were subtracted from measured homologue concentrations. [d] Omitted due to analytical errors. [e] Sum calculated using LOD or LOQ values, respectively. [f] Sum calculated without MoCDD/F values.

WASTE INCINERATION ASHES

Waste incineration creates two main types of solid residues: bottom ash and APCD residues - also known as fly ash. The ratio of these two ash fractions depends on the boiler type: grate-fired mass burn combustors tend to generate more bottom ash than fluidized bed combustors. Around 80 percent by weight of the ash generated by grate-fired mass burn combustors is bottom ash, compared to only around 20 percent of that produced by fluidized bed combustors.

As a fuel, MSW resembles biomass more than coal. In particular, biomass and MSW have very similar relative contents of C, H, N, O, S and Cl. However, MSW has higher moisture and ash contents than biofuel, as well as a lower heating value and energy density [73]. Figure 13 shows a general outline of the ash-forming mechanisms that occur during biofuel combustion. Given the similar properties of MSW and biofuel, ash formation during MSW combustion presumably occurs via similar mechanisms.

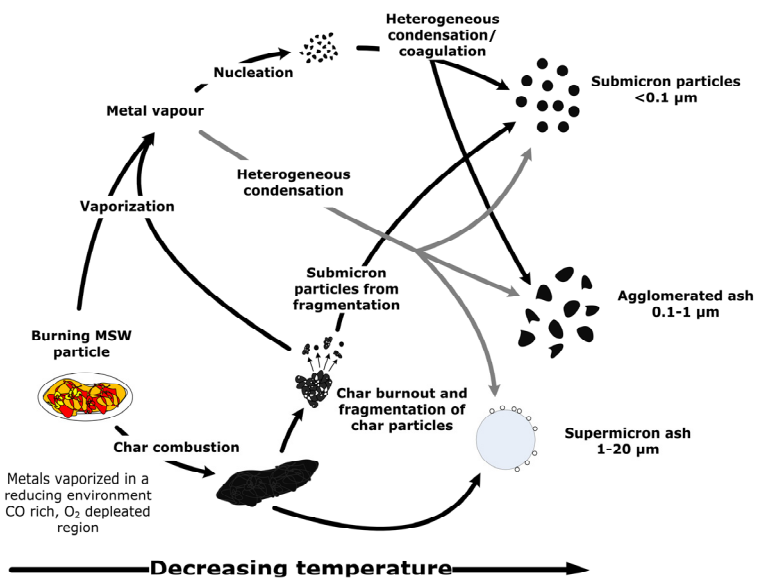

Figure 13. An outline of ash formation and transformation pathways from Lightly *et al* (2000) [74].

Biofuel ash is formed via several pathways: nucleation, condensation and coalescence form both ultrafine soot (20-100 nm i.d.) and inorganic particles while agglomeration, fragmentation and residual unburnt material form larger ash particles. [74]. Heavier particles tend to stay in the bottom ash while lighter particles will be carried by the combustion gases as fly-ash.

Because most PCDD, PCDF, PCN, and PCB formation occurs during flue gas cooling in the post-combustion zone, their concentrations are generally lower in the bottom ash than in the fly ash [75, 76]. They also preferentially associate with smaller particles having higher surface areas in both bottom [77] and fly ash [78]. This attribute is exploited to clean the flue gases, as injecting active carbon and/or lime into the flue gas stream provide a supply of high surface area particles for POPs capture.

The distribution of metals and other elements between bottom ash and fly ash depends on their volatility. Non-volatile elements stay in the bottom ash while more volatile species become enriched in the fly ash or volatilize fully and are emitted with the flue gases [79]. Figure 14 provides a general overview of the distribution of metals in MSW incineration ash. However, the groupings shown in this figure are not absolute: both mercury (which 'should' volatilize completely) and manganese (which 'should' stay in the bottom ash) can be found in fly ash, indicating that the distribution of elements is not governed by volatility alone. For example, thermodynamic modelling has shown that the presence of chlorine can increase the volatilization of copper and zinc while sulphur can reduce the volatility of copper [80, 81].

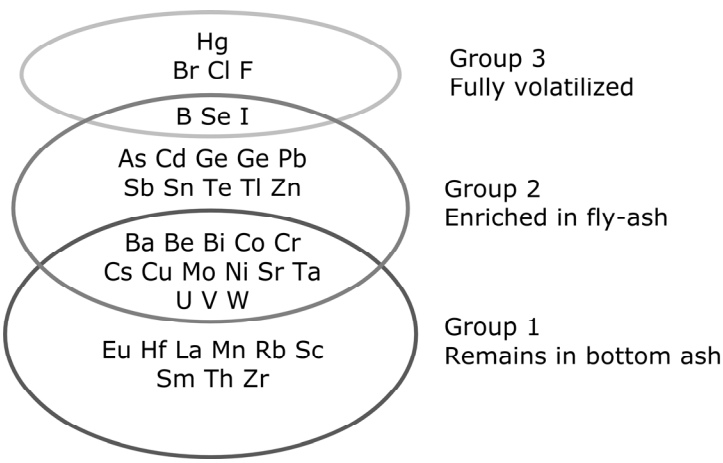

Figure 14. The distribution and volatilization of selected metallic and non-metallic elements in MSW combustion products. Image adapted from the doctoral thesis of Karin Lundholm (2007) [79].

STUDIED ASHES

Papers III and **IV** examined three MSW incineration fly ashes. Ash samples were collected from three MSW plants in Sweden, one in the north of the country and two in its central region. All three plants incinerated MSW mixed with IW, but in different ratios. At each plant, the ashes were collected as grab samples directly before the ash bunkers, on a single sampling occasion.

PLANT A

A 65 MW grate-fired mass burn combustor that primarily uses a 50:50 (wt %) MSW and IW fuel mix. The plant's APCD consisted of fabric filters with active carbon/lime injection before the scrubbers. The scrubbers contained carbon doped tower fillers to ensure adequate POPs removal.

PLANT B

A 61 MW grate-fired mass burn combustor incinerating MSW and IW in a 60:40 ratio. The APCD was similar to that of plant A with fabric filters followed by scrubbers, but the active carbon/lime was added in a NID (Novel Integrated De-acidification) reactor that was situated before of the fabric filters and used to remove sulphuric compounds, hydrogen chloride, mercury and POPs from the flue gas.

PLANT C

Has two 10 MW fluidized bed boilers incinerating 25 % MSW and 75 % IW. Both boilers have APCDs featuring cyclones followed by fabric filters with active carbon/lime injection and subsequent scrubbing. The ashes from plant C were pooled because they were collected from the joint ash bunker feed.

The studied ashes are referred to as ashes A, B and C based on the plants they originated from. Table 4 provides a brief overview of the ashes' origins and carbon speciation.

BULK AND SURFACE COMPOSITION ANALYSIS

Various techniques were used to investigate the ashes' bulk and surface composition. Their bulk carbon concentration and speciation were determined by combustion analysis and their bulk elemental composition was determined by acid dissolution. Their surfaces were characterized by determining their crystalline mineral content using X-ray diffraction (XRD) and the elemental composition of the topmost 2-10 nm ash surface layer by X-ray photoelectron spectroscopy (XPS). In addition, scanning electron microscopy (SEM) was used

to characterize the surface morphology and size of the ash particles, and energy-dispersive X-ray analysis (EDX) was used to determine the elemental composition of the topmost 2 nm of the ash particles.

EDX and XPS were performed in-house but XRD and the analyses of bulk elemental composition and carbon speciation were performed by a commercial laboratory accredited by the Swedish Board for Accreditation and Conformity Assessment (SWEDAC).

BULK CARBON CONCENTRATION AND SPECIATION

The ashes were analysed by an accredited laboratory using combustion analysis (LECO RC412; LECO Corporation, MI, USA) (Table 4). Ashes A and B had higher total carbon concentrations than ash C but each ash exhibited different carbon speciation. Organic carbon and carbonates were predominant in ash A, ash B contained mostly graphite, and ash C had a low carbon content with a fairly even distribution of the analysed carbon species. These differences in carbon speciation were probably due to transient differences in fuel composition and incineration conditions at the sampled plants, as well as the active carbon used in their filters.

Table 4. Ash origins and carbon speciation ($mg \cdot g^{-1}$) of ash A, B and C.

	Ash A	Ash B	Ash C
Boiler type	Grate fired	Grate fired	Fluidized bed
MSW:IW	50:50	40:60	25:75
Plant effect	65 MW	61 MW	2×10 MW
Total Carbon	35	48	11
Organic C	17	9.0	2.0
Amorphous C	0.5	4.5	2.1
Graphite	1.0	20	3.0
Carbonates	14	5.1	<1.0
Carbide	2.1	6.4	2.6

X-RAY DIFFRACTION

XRD experiments were performed at a commercial laboratory (Table 5). The analyses were done by finely grinding the material and examining it between 5-65° 2θ using a Philips X-ray diffractometer equipped with a Cu K_α X-ray tube

The XRD results clearly show that the ashes differed in their crystalline mineral content and its composition. Ash A was rich in calcium-containing

minerals such as anhydrite and calcite, as well as alkali chlorides such as halite and sylvite. The lime added to the filters for flue gas cleaning was only present as a trace constituent and had probably converted into calcite by reacting with carbon dioxide. Calcite was a major constituent of ash B, which also contained lesser quantities of halite, anhydrite and sylvite. CaClOH can be formed by the reaction of portlandite with alkali chlorides [82]. Ash C was the only ash to feature crystalline phases containing non-alkali metals: several of its minor constituent minerals contained aluminium. The dominant mineral in ash C was quartz; the difference between its composition and that of ashes A and B was probably due to its production in a fluidized bed incineration process. This is reflected in its content of minerals typically found in sand, such as quartz, muscovite and albite.

Table 5. XRD data: the ashes' mineral contents were determined on a qualitative and semi-quantitative basis, and are reported as follows: xxx - major constituent, xx - abundant constituent, x - minor constituent, (x) - trace constituent

Mineral (formula)[a]	Ash A	Ash B	Ash C
Quartz (SiO_2)	x	(x)	xxx
Anhydrite ($CaSO_4$)	xx	x	x - xx
Bassanite ($CaSO_4 \cdot 0.5H_2O$)	x		
Calcite ($CaCO_3$)	xx	xxx	(x)
Halite (NaCl)	xx	x - xx	(x)
Sylvite (KCl)	xx	x	(x)
Lime (CaO)	(x)	(x)	(x)
CaClOH		(x)	
Portlandite ($Ca(OH)_2$)		(x)	
Gypsum ($CaSO_4 \cdot 2\ H_2O$)		x	
Muscovite ($KAl_2[AlSi_3O_{10}](OH, F)_2$)			x
Albite ($NaAlSi_3O_8$)			x
Microcline ($KAlSi_3O_8$)			x
Gehlenite ($Ca_2Al[AlSiO_7]$)			x

[a] LOD was ca. 2 % by weight, given that the composition was known.

BULK COMPOSITION

The ashes' bulk contents of copper, sulphur and zinc were determined by acidic digestion according to ASTM D3683 followed by ICP-AES analysis using

a modification of EPA method 200.7. The other elements were analysed by ICP-SFMS using a modification of EPA method 200.8 after fusion with $LiBO_2$ and subsequent digestion (ASTM D3682). Chlorine was analysed using XRF or an ion-selective electrode depending on the sample.

The ashes had different chemical compositions (Figure 14) but the main elements found in each ash were aluminium, calcium, chlorine and silica. Ash C had higher content of copper than ashes A and B, ash A had higher sulphur content than the other two, and ash B had the highest chlorine content based on the bulk composition analyses. The dominance of calcium and chlorine observed in the bulk composition analyses of ashes A and B is in good agreement with their mineral composition as determined by XRD. However, the bulk composition analyses of these ashes also indicate the presence of aluminium and iron, which were not detected in the XRD analyses.

SCANNING ELECTRON MICROSCOPY AND ENERGY DISPERSIVE X-RAY ANALYSIS

Surface particle size and morphology was determined using a Cambridge 360ixp scanning electron microscope equipped with a LaB6 electron emitter (Leica Cambridge Ltd. Cambridge, UK). The equipment was operated at 20 kV with a 375 pA probe current and a tilt angle of 0°. The obtained SEM images (at 250 times magnification) show that the surface morphologies of the three ashes differed as much as their elemental compositions (Figure 15-17)

The surface of ash A (Figure 15) featured small, irregular structures, suggesting that its particles were formed by agglomeration. Conversely, the surfaces of ash B particles (Figure 16) were smoother and seemed to be composed of small agglomerates placed on top of larger structures. Ash C (Figure 17) seemed to be coarser than ashes A and B, which may be due to its relatively high content of sand. The ash particles' surface areas were determined using the Brunauer-Emmett-Teller (BET) N_2 sorption/desorption method (Micrometrics Tristar, Norcross, GA, USA) [83]. Ashes A and B had similar surface areas of 4.8 and 4.1 $m^2 \cdot g^{-1}$ but the surface area of ash C was comparatively low (1.5 $m^2 \cdot g^{-1}$). The BET methodology can also be used to determine pore diameters; while each ash had a different cumulative pore diameter, they were all rich in pores with diameters of around 4 nm.

EDX was used to qualitatively and quantitatively determine the composition of the uppermost ~2 μm of the ashes' surfaces. The results of these analyses are shown in Figure 14. The samples were not coated to avoid biasing the analyses; unfortunately, this reduced the quality of the images.

The elemental compositions determined by EDX were generally in good agreement with those determined by bulk analysis. However, the silicon contents

measured in the bulk content analyses were somewhat higher than those obtained by EDX. In addition, the ashes' carbon contents could not be quantified by EDX because the samples were fixed using carbon-based sticky tape. The EDX images (Figure 18) show that aside from some clustering of metals (e.g. Fe on ash A and Al on ash B), the ashes' surface constituents were evenly distributed across their surfaces.

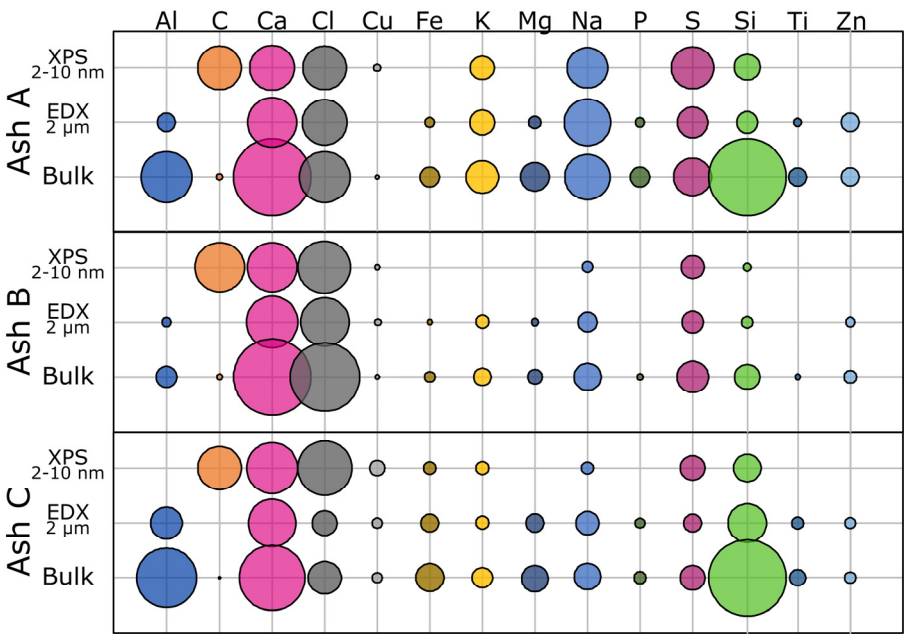

Figure 14. Bulk elemental compositions of the ashes and their surface compositions as determined by EDX and XPS. Circle radius reflects relative atomic %.

X-RAY PHOTOELECTRON SPECTROSCOPY

X-ray photoelectron spectroscopy (XPS) was used to determine the elemental composition of the topmost 2-10 nm of the ashes (Figure 14). These analyses were performed using a Kratos Axis Ultra electron spectrometer (Manchester, U.K.) equipped with a monochromatic Al K_α source operated at 150 W. A 160 eV pass energy (with a 1 eV step size) was used for survey scans. The binding energy (BE) scale was referenced to the C 1s peak at 285.0 eV (corresponding to adventitious carbon) and charge neutralizing equipment was used to compensate for surface charge build-up. To identify elements present on the carbon surface, the experimentally determined BE values were compared to values from the NIST XPS database.[84]

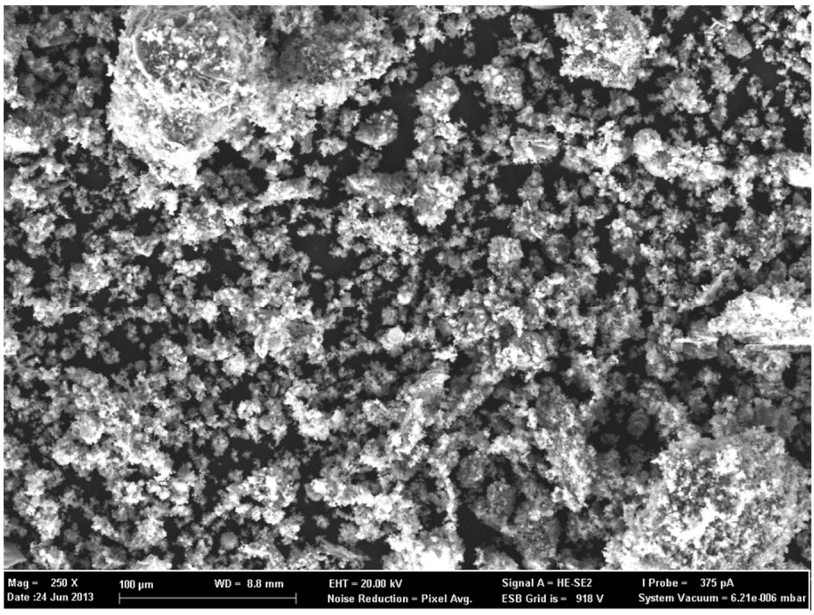

Figure 15. Ash A surface visualized by SEM at 250 times magnification

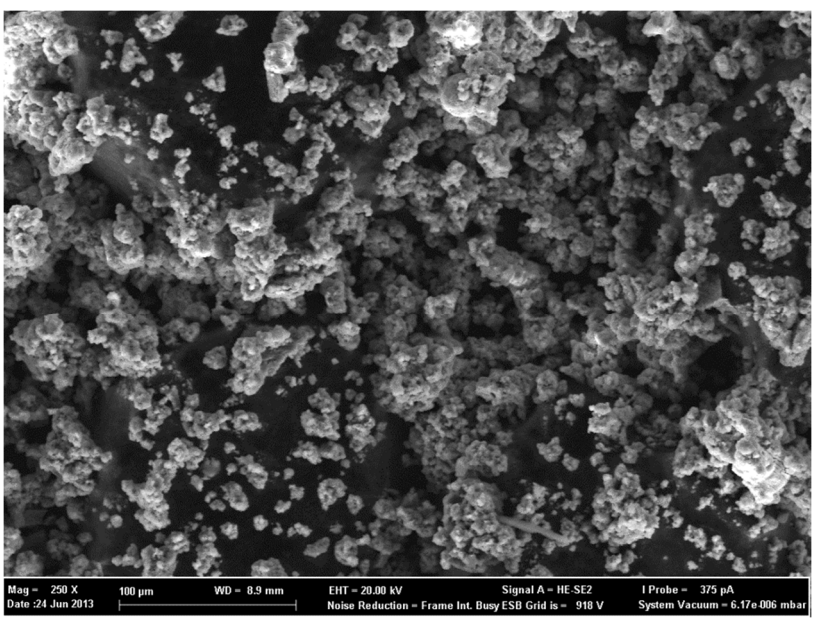

Figure 16. Ash B surface visualized by SEM at 250 times magnification.

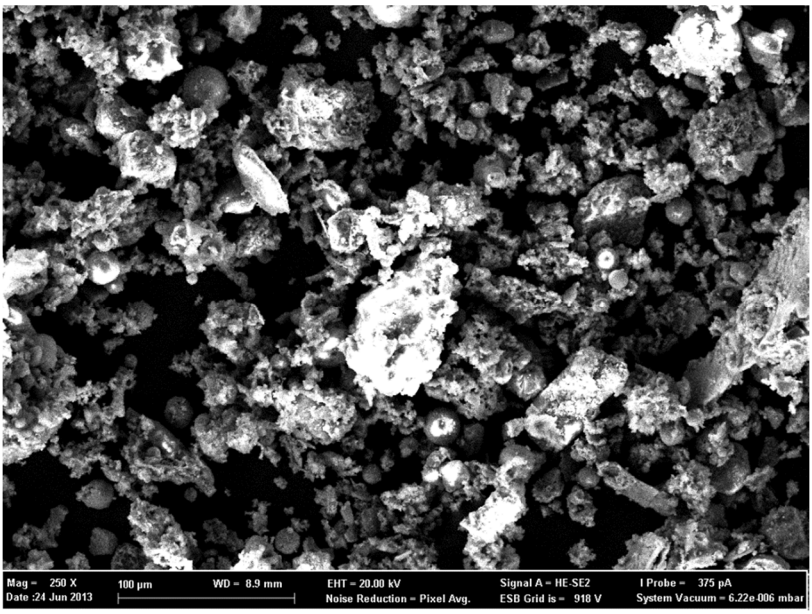

Figure 17. Ash C surface visualized by SEM at 250 times magnification

The XPS analysis detected fewer elements than the EDX and bulk composition analyses, indicating that the ashes' surface compositions may have been less diverse than their bulk compositions. This is consistent with the findings of previous studies [85] and may occur because most of the elements present in the bulk material but not on the surface originated from the incineration bed and were incorporated into the ash during the primary formation stage. The elements detectable on the surface then congeal or agglomerate onto these 'core' particles during a secondary process that occurs at lower temperatures and forms a coating on the particle surface. The surface coating would thus be dominated by substances that remain in gaseous form for relatively long periods of time. Considering only the elements detected in the XPS analyses, the XPS compositions of the ashes' topmost surface layers correlated well with their bulk and EDX compositions. The greatest discrepancy was observed for carbon, whose abundance on the surface was greater than the values determined for the bulk material and in the carbon speciation combustion analysis. Its high abundance on the ash surface could be due to the injection of active carbon in the studied combustion plants' APCDs. Active carbon is injected after most of the bulk ash has formed and would thus form part of the surface layer. However, some of the surface carbon may also derive from atmospheric contaminants.

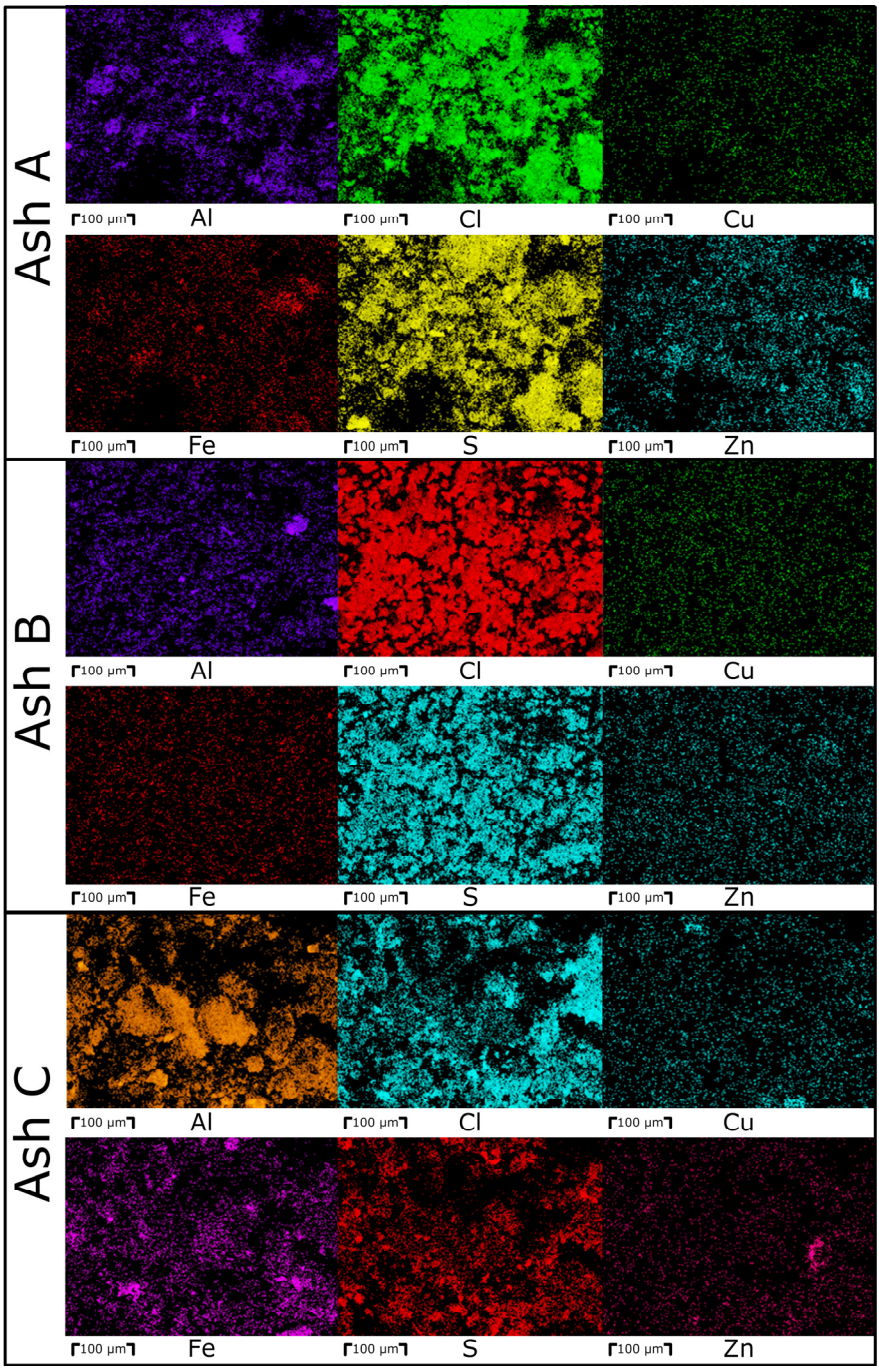

Figure 18 Distributions of Al, Cl, Cu, Fe, S and Zn in ashes A, B and C as determined by EDX.

ASH TREATMENT

Fly ash is environmentally problematic because of its high chlorine and heavy metal contents as well as the potential presence of toxic POPs. Different countries have different fly ash handling strategies. Due to the affinity of POPs for surfaces, their mobility in water and air is limited [86]. However, these contaminants can adsorb onto particulate matter and be spread as dust; this must be accounted for during their treatment and storage. Sweden treats fly ash as hazardous waste and only permits its landfilling in special cases. Most Swedish MSW incineration plants export their fly ash to Norway, where it is stabilized with sulphuric acid and landfilled at a special repository on the island of Langøya in the Oslo fjord. [1] Other countries allow fly ash to be used in asphalt or concrete production [87], usually after pre-treatment or stabilization. However, the erosion of these materials over time may eventually re-mobilize the dust. It would therefore be preferable to simply destroy the POPs.

High temperature (around 1500 °C) processes have been developed that turn fly ash into slag, immobilizing the heavy metal content and destroys the POPs [88, 89]. However, slagging consumes a lot of energy and is therefore expensive and environmentally unfriendly.

LOW TEMPERATURE THERMAL TREATMENT

Low temperature fly ash detoxification could be an attractive alternative to slagging and vitrification due to its potentially lower energy consumption. However, there are some key challenges that must be overcome to make such processes practical. PCDD and PCDF in fly ash can be degraded at low temperatures (<500 °C) [68, 90-93], but the extent of decomposition depends strongly on the ash composition and treatment conditions. Under an inert atmosphere, the PCDD and PCDF in certain ashes can be decomposed at low temperatures (300 °C) [68, 91, 92] but they may reform in the absence of appropriate cooling.

THERMAL TREATMENT OF FLY ASH - **PAPER III**

A series of experiments was performed to determine how ashes with different compositions behaved during thermal treatment. Ashes A, B and C were subjected to thermal treatment in both an in-house built rotary kiln (Figure 18) and in sealed 25 cm^3 glass ampoules. In the kiln experiments, triplicate samples

of each ash were heated at 400 °C for 120 min, collecting off-gas during the entire treatment period and ash samples after treatment. Ampoule experiments were performed in duplicate for each ash and involved heating samples at 400 °C for 60 min. The untreated, kiln and ampoule ashes were analysed for PCDF, PCDD, and PCB, as were the corresponding off-gases.

The kiln gas temperatures were lower than the set temperature (400 °C) and varied between ashes. The kiln gas temperatures for gases A, B, and C were 386 °C, 352 °C and 366 °C, respectively. The discrepancies between the set temperature and the gas temperatures was probably due to the ashes' different heat transfer capacities. The thermocouples controlling the temperature were situated on the outside of the kiln, while gas temperature was measured using a thermocouple inserted into the oven (Figure 18). Ash B tended to stick to the kiln wall whereas the coarser ashes A and C were more prone to tumbling. Stable gas temperatures were achieved after approximately 40 min of the 120 min treatment time.

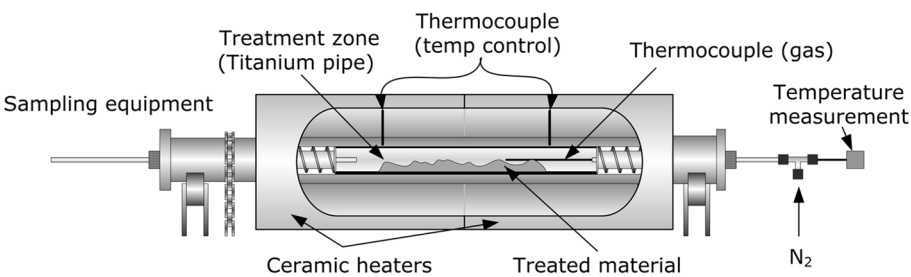

Figure 18. Schematic of the rotary kiln used in the thermal treatment experiments. The total length of the treatment zone is 900 mm and its inner diameter is 80 mm.

The concentration analyses revealed that PCDF, PCDD, PCB and PCN responded differently to thermal treatment in the kiln (Figures 19 and 20). The concentration of PCN increased strongly (Figure 20), by between 248 % in ash C and 236 % in ash B, while PCDF concentrations increased by between 122 % in ash C and 39 % in ash B (Figure 19). However, PCDD levels declined by between 86 % and 68 % (Figure 19). The PCB contents of ashes A and C fell by 89 % and 92 %, respectively. However, that of ash B increased slightly from 6.5 pmol·g^{-1} to 11 pmol·g^{-1} (Figure 20).

Kiln treatment reduced the concentrations of toxic PCDFs by 32 %, 14 %, and 28 % in ashes A, B, and C, respectively. Similarly, the ashes' toxic PCDF concentrations declined by 70 %, 78 %, and 62 %, respectively.

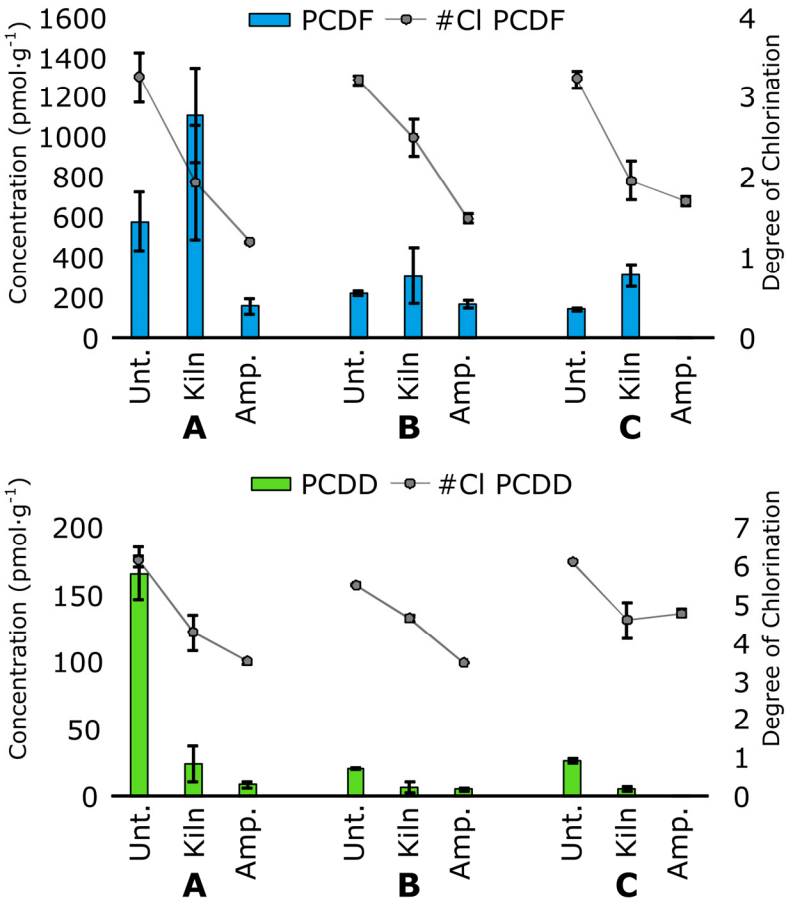

Figure 19. Total concentrations and degrees of chlorination for PCDF (top) and PCDD (bottom) before and after thermal treatment in the kiln and ampoules. The left-hand scale shows concentrations (pmol · g^{-1}) while the right-hand side scale shows the degree of chlorination, i.e. the average number of chlorine substituents on the carbon backbone of the POPs, calculated as Σ ((Homologue sum/Total sum) × No. of Cl). Monochlorinated PCDD were omitted due to low recoveries.

Thermal treatment in the ampoules reduced the POPs concentrations of all three ashes. The POPs in the kiln- and ampoule-treated ashes had similar degrees of chlorination in all cases, and both thermal treatments yielded residual POPs with a lower degree of chlorination than that in the untreated ash. The only exception was ash C, for which thermal treatment had no significant effect on the degree of chlorination of PCB.

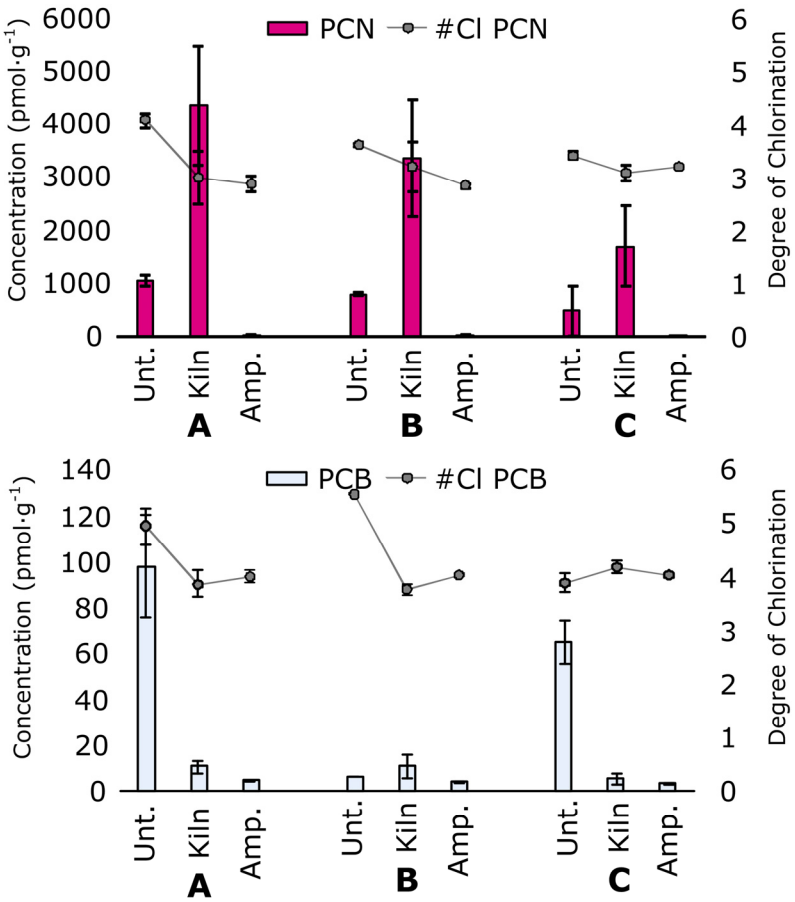

Figure 20. Total concentrations and degrees of chlorination for PCN (top) and PCB (bottom) before and after thermal treatment in the kiln and ampoules. The left-hand scale shows concentrations (pmol · g^{-1}) while the right-hand side scale shows the degree of chlorination, i.e. the average number of chlorine substituents on the carbon backbone of the POPs, calculated as Σ ((Homologue sum/Total sum) × No. of Cl). Monochlorinated PCN homologues as well as mono- and di-chlorinated PCB were omitted because they eluted at the solvent front.

The kiln gas concentrations of all studied POPs were substantially lower than those in the untreated ashes. In addition, the kiln gas PCDF concentrations produced by ashes A and B varied widely between replicates, suggesting that the gases contained both newly formed PCDF and volatilized material that had been present in the untreated ashes (Table 6). If the PCDF content of the kiln gas was due to vaporization alone, it would depend only on the gas temperature.

However, while ashes A and B had very different in-kiln temperatures, the POPs concentrations of their kiln gases spanned similar ranges and varied greatly between replicates. In contrast, the kiln gas concentrations for ash C did not differ appreciably between replicates.

The increase in the PCDF and PCN contents of the ashes during kiln treatment may have occurred because the kiln was not airtight and therefore admitted oxygen. In a method development test, 700 g samples of ash A were heated in the kiln at 400 °C for 60 min under an inert atmosphere and in ambient air. The inert atmosphere treatment reduced the PCDD and PCDF contents of the ash (Figure 21). Conversely, heating in air increased its PCDF content but left its PCDD content unchanged. This was not inconsistent with the leaky kiln hypothesis. However, analyses of the PCDD and PCDF homologue distributions in each case (Figure 22) revealed that the inert atmosphere treatment reduced the ashes' degree of PCDF chlorination relative to that for the air treatment. This implied that if the kiln were leaking, thermal treatment of ash A in the kiln would increase both its PCDF concentration and its degree of PCDF chlorination. This was not consistent with the results of the other kiln experiments (Figure 19) and thus suggests that the kiln was not leaking.

Table 6 PCDF, PCN, PCDD and PCB concentrations (pmol · g^{-1} treated ash) for ashes A, B, and C, as well as the corresponding kiln gases.

		Ash A[e]		Ash B			Ash C		
	Rep	1	3	1	2	3	1	2	3
PCDF	Untr.	581 ± 146		222 ± 8.8			142 ± 6.2		
	Total	3.4	0.02	2.8	0.02	0.02	0.4	0.4	0.5
	# Cl[a]	1.6	1.5	1.8	2.1	1.8	1.5	1.3	1.4
PCN	Untr.	1047 ± 96		789 ± 31			489 ± 465		
	Total[b]	114	1.2	390	2.4	5.0	14	16	14
	#Cl[a]	3.2	2.1	4.1	2.3	2.2	2.2	2.2	2.2
PCDD	Untr	166 ± 19		21 ± 0 .6			26 ± 2.0		
	Total[c]	0.04	9.8×10^{-4}	0.02	0.002	0.002	0.03	0.02	0.02
	# Cl[a]	3.8	3.7	3.4	4.8	5.2	3.3	3.2	3.2
PCB	Untr.	98 ± 23		6.2 + 0.03			65 ± 9.6		
	Total[d]	0.1	0.01	0.1	0.02	0.01	0.04	0.04	0.1
	# Cl[a]	3.5	4.3	3.3	4.5	4.4	3.9	3.8	3.7

[a] #Cl: Degree of chlorination, i.e. average number of chlorine substituents on carbon backbone calculated as Σ ((Homologue sum/Total sum) × No. of Cl) [b] MoCN not analysed, elutes with solvent front on DB5-ms column. [c] MoCDD omitted due to low recovery [d] Mo and DiCB not analysed as they eluted with the solvent front on the DB5-ms column. [e] Replicate 2 omitted due to sampling pump malfunction.

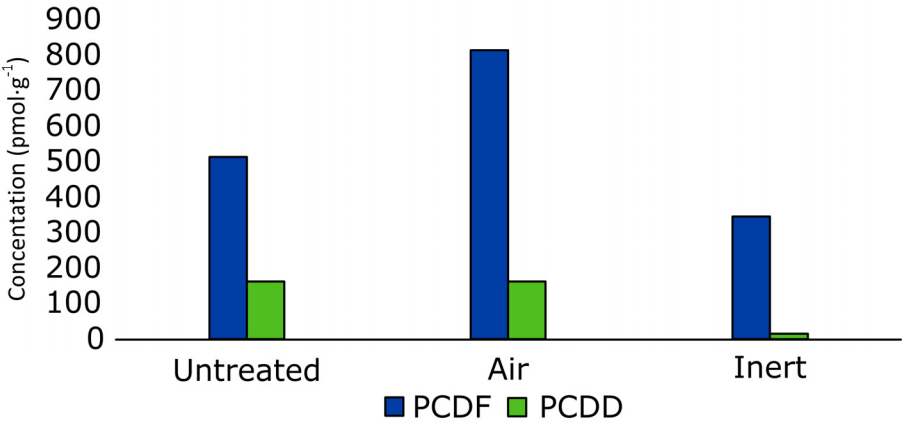

Figure 21. Total concentrations of PCDD and PCDF in untreated ash A samples and samples heated in the kiln at 400 °C for 60 min under an inert atmosphere or in ambient air.

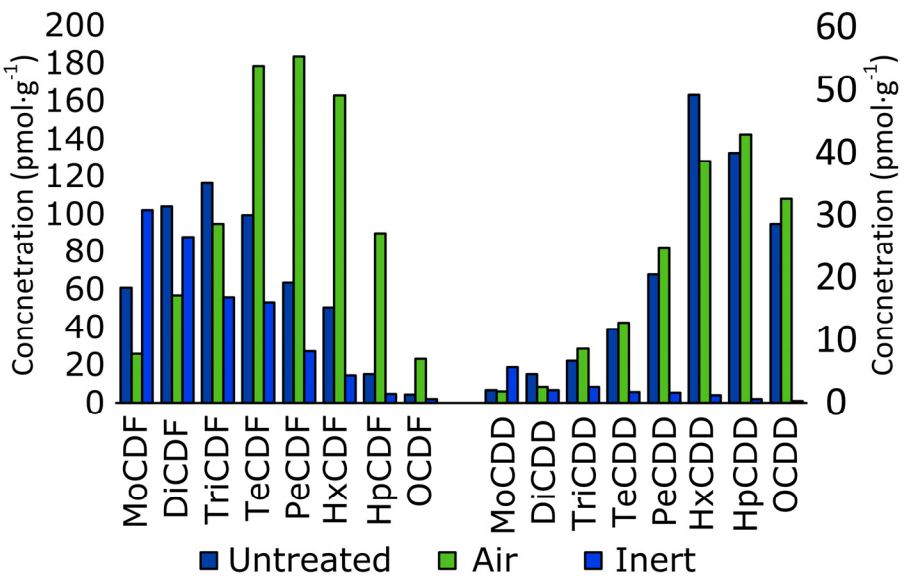

Figure 22. PCDD and PCDF homologue profiles for untreated ash A, an ash A sample heated in the kiln under an inert atmosphere, and an ash A sample heated in the kiln under ambient air.

The thermal degradation of PCDD but not PCDF has previously been observed during the pyrolysis of sediments [94] and automotive residues [95]. However, the thermal treatment of fly ash has only ever been reported to degrade PCDF and PCDD at comparable rates [68, 96-98].

To determine whether the formation of PCDF and PCN in the kiln-treated ashes was due to in-kiln processes or occurred outside the kiln while the treated ash was cooling down, homologue-specific congener profiles for mono- to hepta-chlorinated PCDF and di- to hepta-chlorinated PCN were constructed by dividing the peak areas of individual congeners by the summed areas for all congeners of the corresponding homologues (i.e. the 1-MoCDF peak area would be divided by the sum of the peak areas for 1- to 4-MoCDF, etc.) for untreated ash, kiln ash, ampoule ash and kiln gas samples generated during the thermal treatment of ash in the rotary kiln.

Principal component analysis (PCA) [99] was used to graphically visualize the relationships between the ash and gas samples and the corresponding homologue-specific PCDF and PCN congener patterns. Because the two compound groups exhibited different behaviours, separate PCA models were constructed for PCDF and PCN. The score plots showed how the untreated ash, kiln ash, ampoule ash and kiln gas samples (observations) related to each other (Figure 23 and 24). The variables were centre scaled (because the peak size was part of the congener pattern) and logarithmically transformed when needed. To ensure that the models did not model noise, only components with eigenvalues higher than 2 were included. The models' predictive capacity was tested by 7-fold cross validation [100]. All PCA modelling was done using Simca 13.0 [101] (Umetrics, Umeå, Sweden).

The PCDF model had a predictive capacity (Q^2) of 55 % and explained 74 % of the observed variance in total (R^2), using three components: t1 (47 %), t2 (18 %) and t3 (12 %). Figure 21 shows a score plot for the first two components of the PCDF model. The PCDF congener profiles of the kiln ash samples generally occurred on the right-hand side of the plot (at positive t1 values) whereas the ampoule samples were further to the left, regardless of ash composition. This suggests that different reactions occurred in the kiln and the ampoules. The ampoule ash, untreated ash and kiln gas congener profiles were quite similar with respect to the first component but differed with respect to the second, revealing similarities between the congener profiles of the kiln ash and the corresponding off-gas. This suggests that at least some of the PCDF formation observed in the kiln-treated ash samples occurred inside the kiln. Analyses of the third component were not informative.

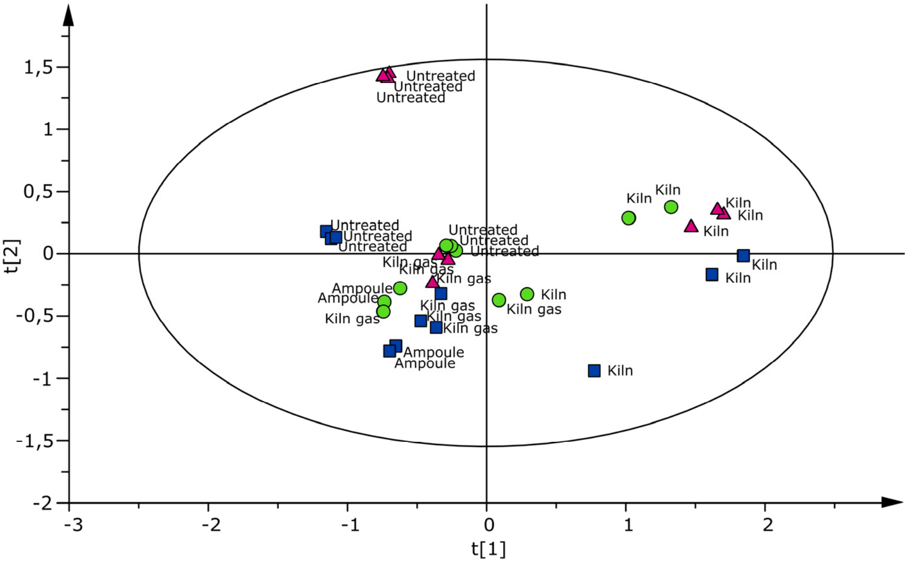

Figure 23. Scores plot for the first two components of the PCDF PCA model. Green circles denote ash A, blue squares denote ash B and red triangles denote ash C. Ash C ampoule profiles were not included because only mono- to tetra-chlorinated homologues could be individually integrated due to the low concentrations of individual congeners of other homologues.

The PCN model had a predictive capacity (Q^2) of 57 % and explained 82 % of the observed variance (R^2) using three components: t1 (51 %), t2 (18 %) and t3 (13 %). The first component separated ashes A, B, and C regardless of their treatment and may thus reflect ash composition. The second component (not shown) did not provide any useful information, but the third separated the kiln ash samples from the untreated ash, ampoule ash, and kiln gas, so a score plot was constructed for components t1 and t3 (Figure 24). Ash C samples were generally located on the right-hand side of the score plot (at positive values of t1) while those of ashes A and B were generally located further to the left. The kiln gas samples were located in the lower half of the plot (at negative t3 values). However, the differences between samples with respect to t3 were less pronounced than those with respect to t2 in the PCDF model, suggesting that the PCN congener profiles were more dependent on the original composition of the ash than was the case for PCDF.

To illustrate the behavioural differences between PCDF and PCDD, a third PCA model was constructed using PCDD congener profiles. This model had a predictive capacity (Q^2) of 54 % and explained 82 % of the total variance (R^2) using three components: t1 (50 %), t2 (20 %) and t3 (12 %) (Figure 25). The kiln and ampoule ash samples were not separated with respect to the first component, indicating that they had similar congener profiles. Moreover, the kiln gas congener profiles were not well separated from the untreated ash profiles with respect to the first component, suggesting that the PCDD content of the kiln gas was largely due to the vaporization of pre-existing PCDD in the untreated ash rather than being formed by in-kiln processes. The second component separated the ampoule ashes from the untreated and kiln ash, suggesting that more comprehensive PCDD degradation occurred in the ampoules. The third component (not shown) reinforced the conclusions drawn by considering the first two components.

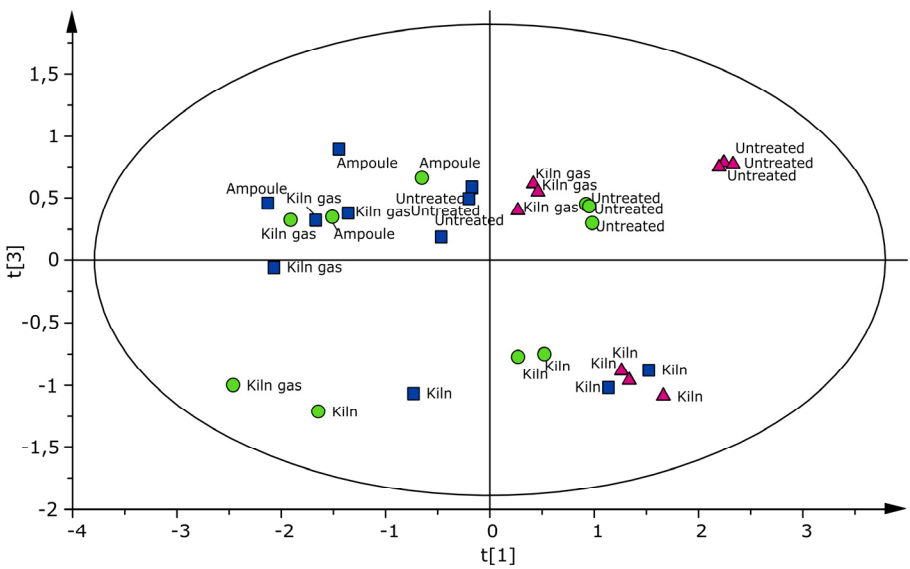

Figure 24. Scores plot for the first and third components of the PCN PCA model. Green circles denote ash A, blue squares denote ash B and red triangles denote ash C. Ash C ampoule profiles were not included because only di- to tetra-chlorinated homologues could be integrated individually; the concentrations of individual congeners of the other homologues were too low to be determined.

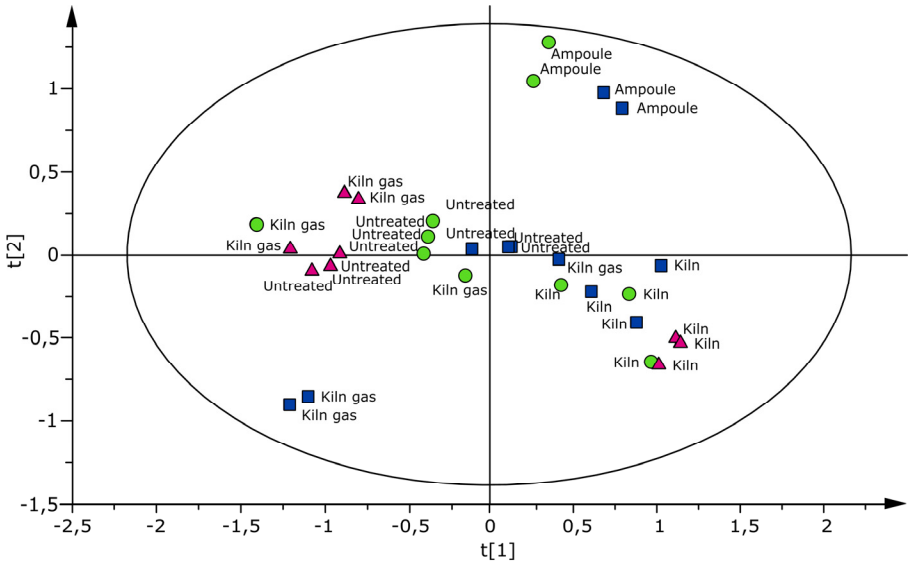

Figure 25. Scores plot for the first and second components of the PCDD PCA model. Green circles denote ash A, blue squares denote ash B and red triangles denote ash C. Ash C ampoule profiles were not included because only mono- to tetra-chlorinated homologues could be integrated individually; the concentrations of individual congeners of the other homologues were too low to be determined.

As suggested by the PCDF PCA model, the ampoule ash and kiln gas derived from ash A had the same dominant Mo-TeCDF congeners (Table 7). In addition, the congener distributions for the kiln gas resemble those for the kiln ash, as demonstrated by their similar relative abundances of species such as 1,2- and 2,6/4,6-DiCDF. This is consistent with the suggestion that the same degradation processes occurred in the ampoules and the kiln, but that there were additional reformation processes that either occurred in the kiln or after thermal treatment in the cooling kiln-treated ashes. For ashes A and B, the dominant congeners of each homologue appeared to have a common substitution pattern involving chlorination at the 2-, 4-, and 6-positions: the most abundant di-, tri-, and tetra-chlorinated dibenzofurans were the 2,6/4,6-, 2,3,6/2,3,4/3,4,6-, and 2,3,6,7/3,4,6,7-susbstituted species, respectively. These could be formed by either dechlorination of 2,3,6,7 or 3,4,6,7, or chlorination of 2,6 or 4,6, or both dechlorination and chlorination taking place at the same time. The gas phase congener profile for ash A closely resembled the ampoule ash profile and was very different to the kiln ash profile. However, the gas phase profile for ash B was more like an intermediate between the ampoule and kiln ash profiles. The ash A

mono-to tri- chlorinated furans gas phase congener profiles had similarities to those for both the kiln and ampoule treatments whereas the gas phase profile for the tetrachlorinated congeners most closely resembled that for the ampoule ash. The profiles for kiln ash B resemble those for kiln ash A, suggesting that similar in-kiln processes occurred in both cases despite the differences in untreated ash composition.

Table 7. Relative abundances of mono- to tetra-chlorinated dibenzofurans in the untreated ashes, kiln gases, and ashes after kiln- or ampoule treatment. The values represent the average peak area for the indicated congener divided by the summarized peak areas for all congeners of the corresponding homologue, expressed as a percentage. The most abundant congeners in each case is indicated with a grey background.

		Ash A				Ash B				Ash C				Flue gas
		Untr.	Kiln	Gas	Amp	Untr.	Kiln	Gas	Amp	Untr.	Kiln	Gas	Amp	
MoCDF	1	30	35	34	37	40	43	33	36	33	47	26	31	17
	3	29	27	27	28	25	21	26	30	28	22	44	23	32
	2	23	20	26	27	20	19	20	22	26	18	16	22	29
	4	18	17	13	8	15	17	21	12	14	14	13	24	22
DiCDF	17	16	8	21	20	15	7	17	23	8	4	18	18	6
	24	9	5	7	6	5	7	10	4	19	7	15	8	35
	37	10	5	17	17	11	4	16	15	4	1	15	15	5
	12	29	24	19	7	29	18	15	6	19	15	17	8	14
	36/28/23	4	2	5	19	6	2	3	17	4	1	6	18	3
	26/46	21	30	18	7	24	33	23	4	25	31	18	6	22
	34	7	22	6	16	7	26	9	19	19	35	8	19	10
TriCDF	137	9	3	9	8	10	1	7	7	3	1	6	5	2
	138	8	3	8	9	8	1	6	7	3	0	7	6	3
	168/134	4	3	4	5	3	2	4	5	2	2	4	6	3
	124	2	4	3	1	2	3	4	2	6	6	6	1	7
	147/146	7	8	11	10	6	5	13	12	8	5	12	9	8
	148/246	5	4	6	8	5	2	6	8	6	5	7	9	3
	248/247	4	2	4	4	4	4	4	3	3	1	5	3	7
	178	7	4	5	7	7	1	5	8	2	1	3	5	4
	123	7	10	7	6	6	2	6	7	10	9	8	6	10
	139/126/128	7	7	8	8	7	2	7	9	4	5	5	8	5
	237	8	5	5	6	8	6	4	5	4	2	3	5	3
	236/234/346	9	26	9	4	6	51	13	5	31	48	17	13	25
	149/267/347	9	11	7	8	13	7	8	8	8	9	4	8	7

Continues on next page.

Table 7. Continued.

	Ash A				Ash B				Ash C				Flue gas
	Untr.	Kiln	Gas	Amp	Untr.	Kiln	Gas	Amp	Untr.	Kiln	Gas	Amp	
TeCDF													
1368	5	2	5	6	6	1	6	6	2	0	7	6	4
2468	2	1	2	2	1	1	2	1	2	1	4	5	8
1246/1347/1378	18	10	15	18	19	6	16	17	8	3	12	14	8
1247/1348	4	2	3	3	3	1	3	3	2	1	2	10	7
1367/1248/1379	8	5	8	9	9	3	8	9	4	2	6	0	4
1478	5	2	5	6	5	2	4	7	2	2	3	4	10
1364/1237	6	5	7	6	7	6	7	5	10	6	8	5	5
2467/2368	3	4	3	4	3	1	3	2	23	1	4	3	16
1469/1238/1234/1678/1236	11	5	11	8	8	13	11	8	3	17	17	9	3
1278	5	13	5	7	6	4	3	6	2	3	3	5	1
1349	3	5	3	3	3	3	3	4	8	3	2	3	2
1267	3	3	4	2	2	11	4	2	6	14	5	4	6
2378	3	4	2	3	8	0	2	2	10	1	1	2	2
2367/3467	7	19	10	5	1	27	9	6	1	30	7	9	6

The occurrence of similar in-kiln processes with different ashes was also supported by the congener profile of kiln ash C, which had similar dominant kiln ash congeners to ashes A and B. The congener profiles of five flue gas samples sampled at 600 °C in the post-combustion zone of a laboratory-scale fluidized bed incinerator (from **Paper II**) [102] in which uncontrolled PCDF formation had occurred due to inadequate cooling during sampling were compared to those obtained for the kiln ash samples to determine whether the same PCDF-forming processes occurred in the two cases. The congener profiles were very different, indicating that the PCDF-forming processes that occur on the ash surface are not the same as those that occur in the flue gas.

Overall, these results indicate that kiln treatment decomposed PCDD and PCB without permitting their reformation, whereas PCDF and PCN were decomposed but subsequently reformed. PCDF formation occurred on the surface of the cooling ashes after kiln treatment but also occurred during the treatment as a result of in-kiln processes. However, PCN formation probably occurs exclusively after removal from the kiln. The tendency for PCDF and PCN (re)formation differed between the ashes and may depend on the speciation of the carbon in each case. This may explain why ash C, whose carbon content was only a quarter of that for ashes A and B, had such a low tendency to reform PCDF

and PCN. Differences in carbon speciation may also explain the different levels of PCDF and PCN formation seen for ashes A and B: ash A was comparatively enriched in organic and amorphous carbon whereas B was enriched in graphite. The former should be quite amenable to rapid PCDF formation but the latter may be much less so. None of the ashes' kiln ash PCDF congener profiles matched those generated by uncontrolled PCDF formation in insufficiently cooled flue gases (**Paper II**). Instead, the PCDF (and PCDD) congener profiles of the post-kiln ashes generally resembled one-another, suggesting that PCDF formation occurred by the same processes in each case, regardless of ash composition.

MECHANOCHEMICAL TREATMENT

Mechanochemical treatment, i.e., ball milling, has shown promise as non-thermal alternative for MSW fly ash detoxification. The advantage of using a non-thermal treatment is that it could conceivably be done using mobile apparatus that could be moved between sites as required. In addition, non-thermal treatment reduces the risk of POPs reformation during cool down. Large-scale ball mills have a horizontal axis of rotation such that the milling balls fall down on to the treated material. Planetary ball mills (Figure 26) are often used on smaller scales because they have higher rotating speeds and can produce ultrafine powders.

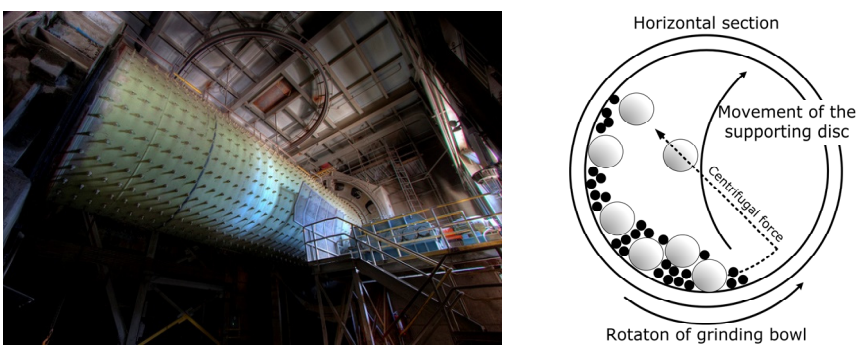

Figure 26. Left: an industrial sized ball mill that rotates about a horizontal axis. Right: a schematic of a planetary ball mill in which the milling containers are placed on a disc that rotates in the opposite direction so that the milling balls move around inside the container. The left image is used under Creative Commons licence, photograph by Jonathan Haeber. (www.flikr.com)

The impact of the balls with the treated material breaks it up into progressively smaller fragments. In addition some of the kinetic energy of each impact is

presumably converted into thermal energy at the collision site, as demonstrated by the heating of the treated material during high speed ball milling.

The destruction of chlorinated POPs by mechanochemical treatment was first discussed by Rowlands *et al.* [103] and Birke *et al* (2004) [104], suggested that the dominant mechanism involved was dechlorination. The dechlorination reactions are facilitated by the presence of an alkali metal and a hydrogen source, and resulted in the reduction of the carbon backbone to a less toxic or harmless organic molecule.

This suggestion was supported by several studies, which showed that the presence of calcium oxide enhanced dechlorination [105-107]. It has also been suggested that ball milling breaks the carbon backbone down and causes it to re-polymerize into larger carbon-based structures or graphite [105, 107]. Mechanochemical treatment has been applied successfully to substrates such as pure PCB [106], DDT [108], PCN [109], PCPh [107] and PCDD/PCDF [105]. Mechanochemical treatment could potentially be useful for removing POPs from MSW fly ash because calcium oxide, which seems to facilitate POPs decomposition, is often added in the APCD, and the ash itself often contains alkali metals. Mechanochemical treatment has previously been applied successfully to two ashes generated by incinerating medical waste, and was reported to reduce their degree of POPs chlorination [110].

As a preliminary experiment to assess the utility of mechanochemical approaches to the treatment of MSW fly ash without additives, 5 g of ashes A and C were treated in a planetary ball mill (Pulverisette series 7 model 680, Fritsch GmbH, Germany) for 90 and 240 min at 400 rpm. Before treatment, the ashes were dried at 120 °C for 3 hours and then stored in a desiccator before use. The grinding bowls were 45 cm^3 stainless steel cups containing five 15 mm stainless steel balls that were washed and rinsed with toluene before and after each experiment to prevent cross contamination. All experiments were performed in triplicate and approximately 3 grams of each ash sample was extracted and analysed to determine its PCDF and PCDD content. Data for MoCDD and one ash A replicate that had been milled for 240 min were excluded due to low recoveries.

Milling did not greatly change the PCDF or PCDD content of ash A (Figure 27, left). The total PCDF and PCDD concentrations of the ash increased slightly (by 19 and 52 %, respectively) after 90 min of milling but fell back to original levels after 240 min. The degrees of PCDF and PCDD chlorination remained practically unchanged for both treatment times.

For ash C the total PCDF and PCDD concentration was unchanged after 90 min and decreased by 42 % and 56 % after 240 min (Figure 27, right). However, the degree of chlorination increased for both PCDF and PCDD at both treatment times. Toxic PCDF and PCDD concentrations (TEQ) of both ash A and C behaved similarly to the total concentrations of ash A, i.e. increased after 90 min and reduced again after 240 min, but the changes were slight.

The total PCDF and PCDD concentrations of ash C were unchanged after 90 min of ball milling but decreased by 42 % and 56 % respectively after 240 min (Figure 25, right). However, the degree of chlorination increased for both PCDF and PCDD at both treatment times. The toxic PCDF and PCDD concentrations (TEQ) of both ashes behaved similarly to the total concentrations for ash A, i.e. they increased slightly after 90 min and then declined to their original levels after 240 min.

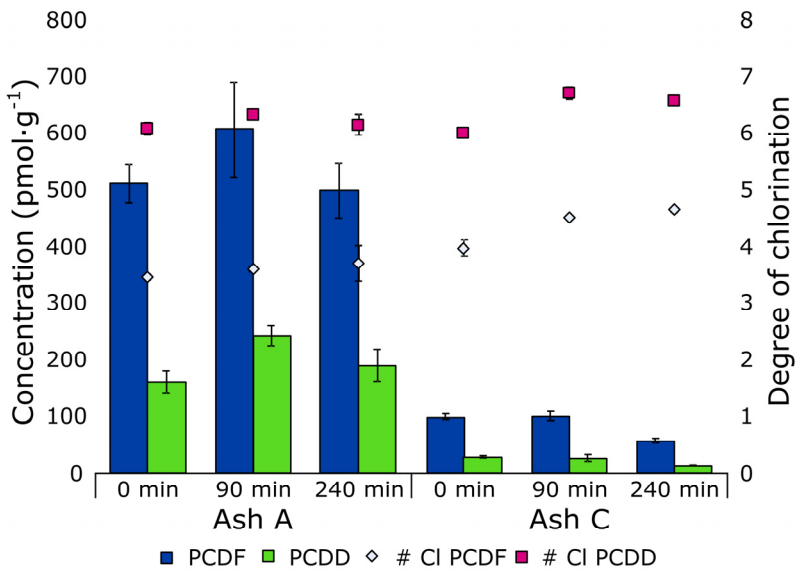

Figure 27. Average total PCDF and PCDD in pmol/g and degrees of chlorination in ball-milled samples. Bars denote ± standard deviation for all cases except that for ash A at 240 min, where they represent the average of the highest and lowest value.

The ash A PCDF homologue profiles (Figure 28) revealed that the less chlorinated species (Mo-TriCDF) became less abundant than they were in the untreated ash after 240 min of milling, but the levels of TeCDF increased after both 90 and 240 min. The PCDD profiles indicated that Hx-OCDD became more abundant after 90 min compared to the untreated ash but fell back to its original level after 240 min, albeit with a more variable concentration.

The decline in the abundance of less chlorinated PCDD congeners and the corresponding increase in more highly chlorinated congeners resembles the homologue patterns reported in **Paper I** (Figure 6), which described PCDD formation inside fabric filters. The use of ball milling in organic synthesis [111] suggests that it may initially polymerize precursor molecules (represented by the 90 min treatment) and that dechlorination occurs later on, at extended treatment times.

The 90 min homologue profile for ash C shows a similar trend to that seen for ash A at the same time point: more highly chlorinated homologues are more abundant than in the untreated ash (Figure 29). After 240 min, the profile resembles that at 90 min but with lower overall concentrations. That is to say, PCDF and PCDD congeners of all chlorination levels seem to have been degraded at approximately the same rate. This behaviour seems to be unique to mechanochemical treatment and has not been observed in thermal experiments such as the ampoule studies discussed above (**Paper III**).

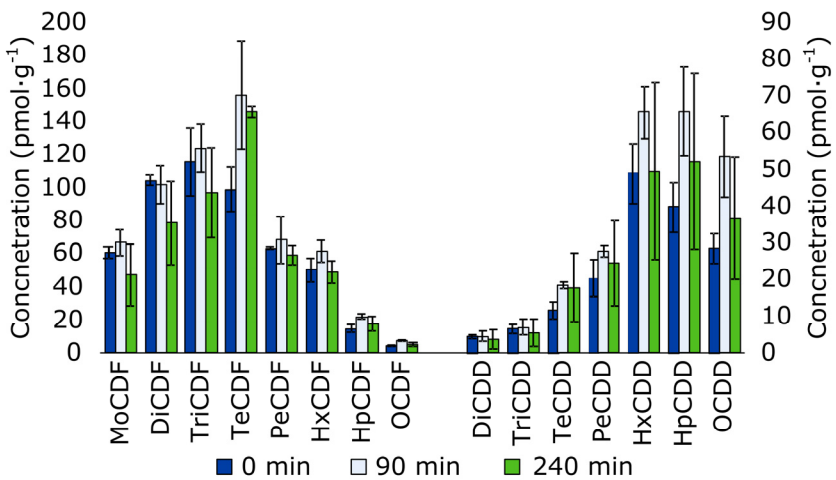

Figure 28. Ash A homologue profiles. MoCDD and one 240 min replicate were excluded due to low recoveries of the corresponding internal standard.

The homologue profiles for ashes A and C indicate that the behaviours of PCDF and PCDD during mechanochemical treatment depend on the initial composition of the ash. The available data cannot be used to determine which ash constituents are responsible for the observed differences; both ashes had similar calcium contents, but XRD analysis revealed that CaO was less abundant than other calcium-containing species such as $CaSO_4$. It may be that ash A would have started to behave like ash C and seen more extensive PCDF and PCDD

degradation if its treatment time had been extended. It would therefore be interesting to study the behaviours of these ashes under prolonged milling, both to unravel the mechanisms driving POPs degradation during milling and to properly assess the method's potential for MSW degradation. However, such studies were beyond the scope of this preliminary investigation.

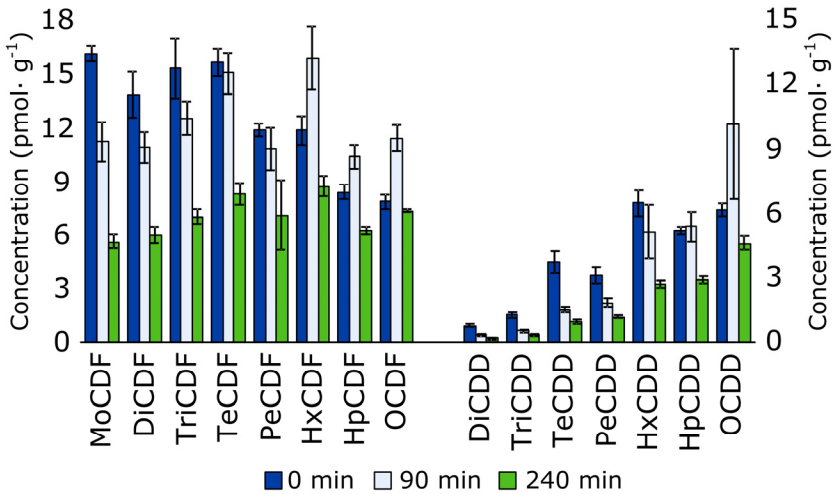

Figure 29. Ash C homologue profiles.

THERMAL DESORPTION AND DEGRADATION OF MSW FLY ASH - **PAPER IV**

Because the reactions that form and degrade organic pollutants in MSW ashes largely occur on the surfaces of ash particles, data on the composition and properties of ash surfaces can provide key insights into these processes. While there have been some studies on the properties and leaching behaviour of fly ash particles' surfaces [85, 112, 113], few studies have examined the relationship between ash particles' surface chemistry and POPs formation [e.g., 114]. The formation and degradation of PCDF and PCDD on fly ash have been studied extensively [68, 96, 115, 116], and it is known that the ashes' composition [42] and metal content have profound effects on reactions that form and degrade PCDF and PCDD [116].

To characterize the surfaces of the studied fly ash particles and their effects on the ashes' responses to thermal treatment, ashes A, B and C were gradually heated under vacuum while monitoring their surfaces using Fourier transform infrared spectroscopy (FTIR) in a series of temperature programmed desorption/

degradation (TPD) experiments. The gases emitted during this process were characterized by low-resolution mass spectroscopy.

For the TPD experiments, ash samples were pressed onto a fine tungsten mesh (0.002'' mesh diameter; Unique wire weaving, Hillside, NJ, USA) and placed into a copper sample holder (Figure 30). The sample holder was then wedged into a copper heating probe, placing the sample directly in the optical path of a FTIR (Bruker Vertex 70/V). The copper probe was subsequently heated from 30 to 900 °C in an IR chamber (AABSPEC #2000-A) with KBr windows at a pressure of less than 0.0025 torr (the limit of detection of the pressure sensor used in the apparatus). The gases released from the sample during this process (H_2O, CO, CO_2, NO and SO_2) were detected using a low resolution mass spectrometer (PrismaPlus, Pfeiffer Vacuum, Asslar, Germany).

FTIR spectra of the ash surface in the 600-4500 cm^{-1} range were acquired continuously throughout every TPD experiment. Each spectrum was obtained by averaging 50 co-added scans collected over a 43 sec period. Ashes A and C were ball milled for 10 min at 400 rpm before being used in the experiments because they were too coarse to be pressed onto the tungsten mesh without prior treatment. Ashes A and B were analysed in triplicate but only duplicate experiments were performed for ash C.

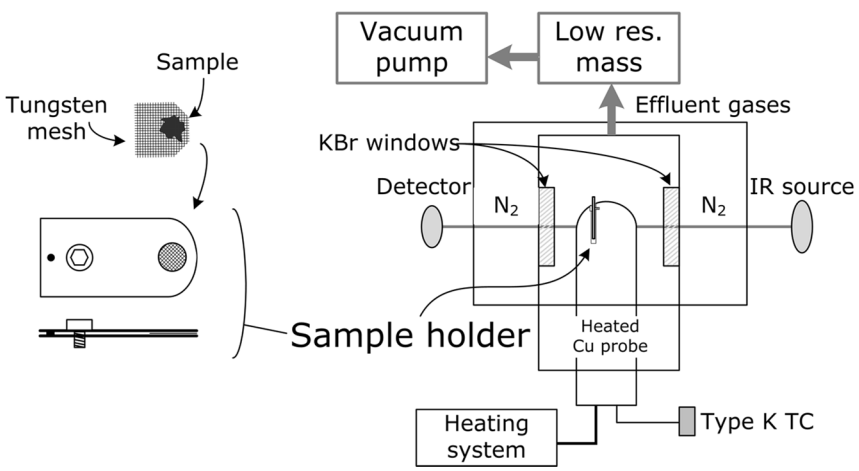

Figure 30. Schematic image of the sample holder (left) and TPD-FTIR setup (right) used in the temperature programmed desorption/degradation experiments.

The TPD effluent gases of each ash were comparable in each replicate. For Ash A, CO_2 emissions increased slightly at 150 °C (Figure 31) and then again at 450 °C. At 720 °C there was a further increase in CO_2 emissions accompanied

by an increase in CO emissions, presumably because the ash began to decompose (Figure 32). Water also started being released from the matrix at this temperature, and sulphur dioxide formation began at 770 °C (Figure 33).

CO and water emissions from ash B rose sharply at 100 °C, accompanied by more modest increases in CO_2 (Figure 31) and NO emissions (Figure 33). The second release of CO_2 took place at a higher temperature (550 °C) in ash B than in ash A (Figure 32) and was accompanied by a release of SO_2 (Figure 33). At 720 °C a third release of CO_2 began (Figure 32), together with water and more NO (Figure 33). The release of SO_2 subsided slightly at 790 °C and increased again at 810 °C (Figure 33).

The release of CO_2 from ash C started at 120 °C, increased again at 340 °C (Figure 31), and peaked at 650 °C (Figure 32). Water emissions first increased at 120 °C and rose again at 660 °C, while SO_2 release began at 780 °C (Figure 33). The emissions of CO from this ash were consistently higher than those of CO_2 but the curves for the two gases were very similar in shape at most temperatures other than those around 120 °C, where CO emissions increased sharply but CO_2 increased more modestly.

The TPD curves indicate that there were three major stages of CO_2 release in all three ashes, one at 100-120 °C, again at 340-550 °C and another at higher temperatures. The latter corresponds to the breakdown of the ash matrix. The CO_2 release at 720 °C observed for ashes A and B corresponds to the breakdown of calcite [117], which was one of the dominant mineral species in both ashes (Table 5). The CO_2 release from ash C that began at 650 °C could not be explained by its mineral composition because no carbonate species were found in this ash. In addition, the release of SO_2 from ash B at the low temperature of 550 °C is not readily explained by its mineral composition. The only sulphur-containing mineral that was present in B but not A and C was gypsum (Table 5). However, gypsum dehydrates to bassanite and/or anhydrite when heated (which were present in ash A), suggesting that the release of SO_2 from B was not due to mineral breakdown. Ash B also had the lowest sulphur content of the three ashes and its surface layers contained no sulphur (Figure 14).

The FTIR spectrum of ash A at 30 °C featured a broad peak between 1250 and 1470 cm^{-1} due to organic and carbonate moieties. These features were completely absent at 500 °C and were replaced by double peaks at 2800-3000 cm^{-1} reflecting the formation of C-H bonds and a minor peak around 1700 cm^{-1} that may be due to C=O bonds. These new peaks first appeared shortly after the increase in CO_2 emissions at 450 °C.

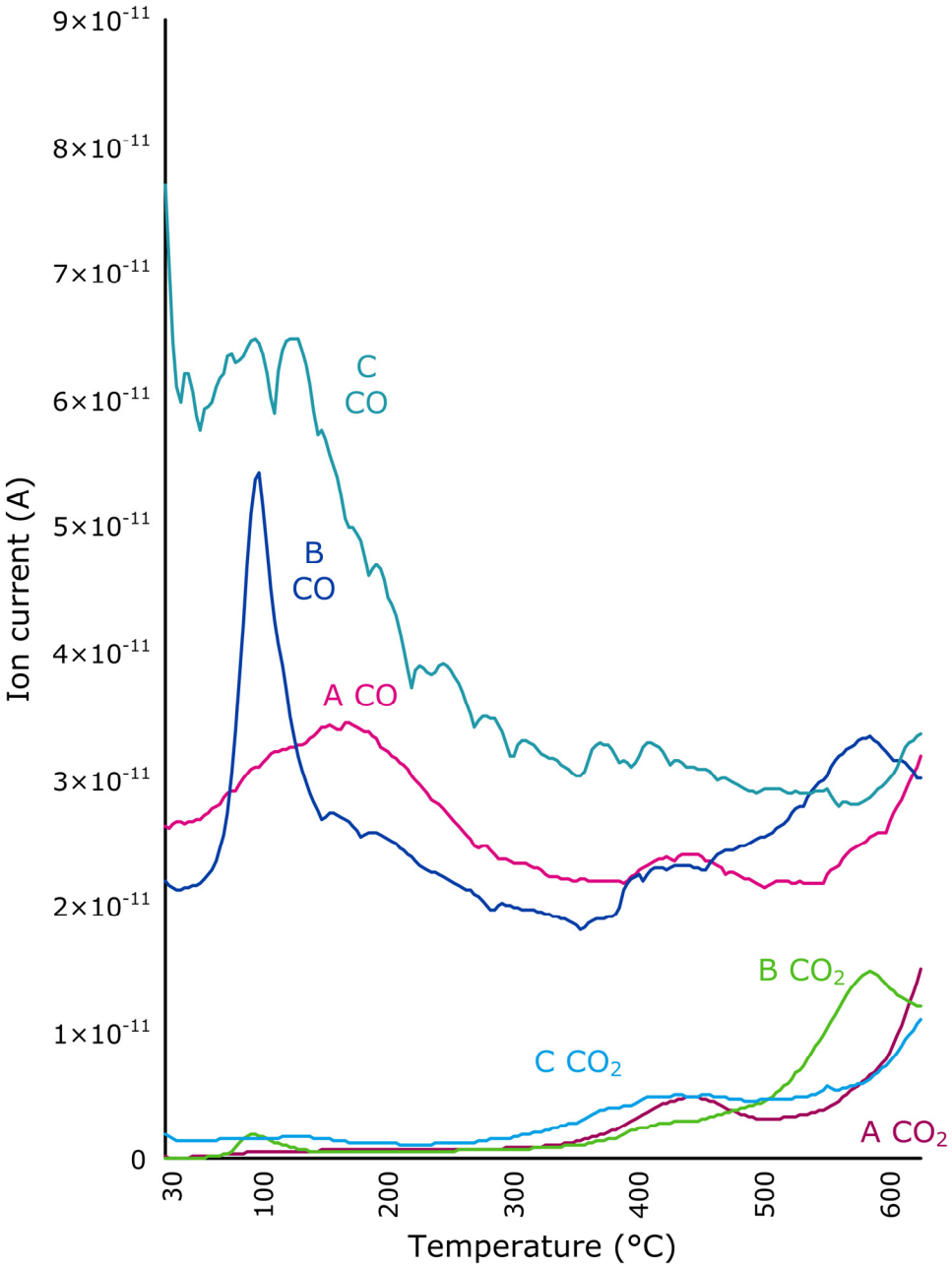

Figure 31. CO and CO^2 emissions from ashes A, B and C between 30 °C and 620 °C as determined by mass spectrometry.

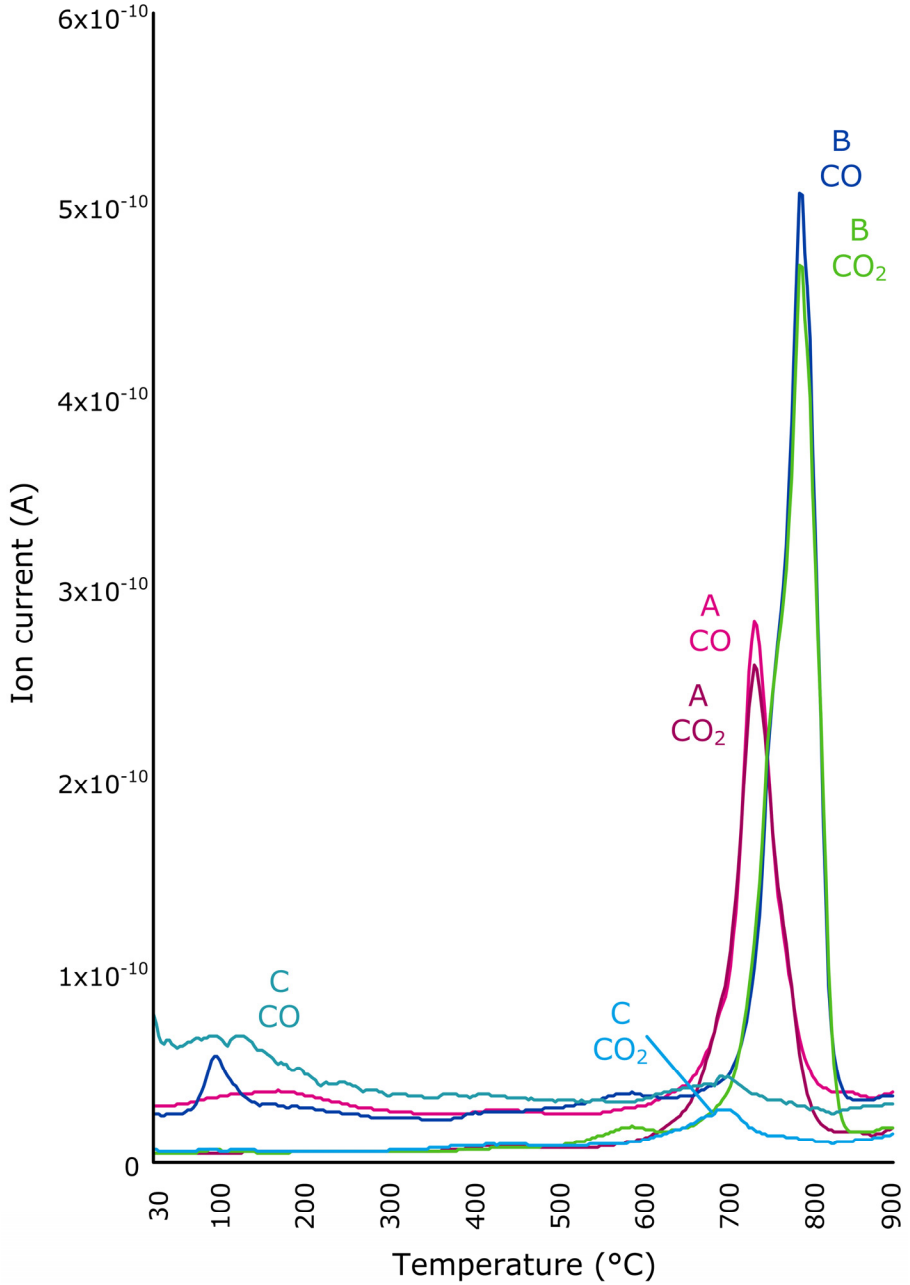

Figure 32. CO and CO_2 emissions from ashes A, B and C between 30 °C and 900 °C as determined by mass spectrometry.

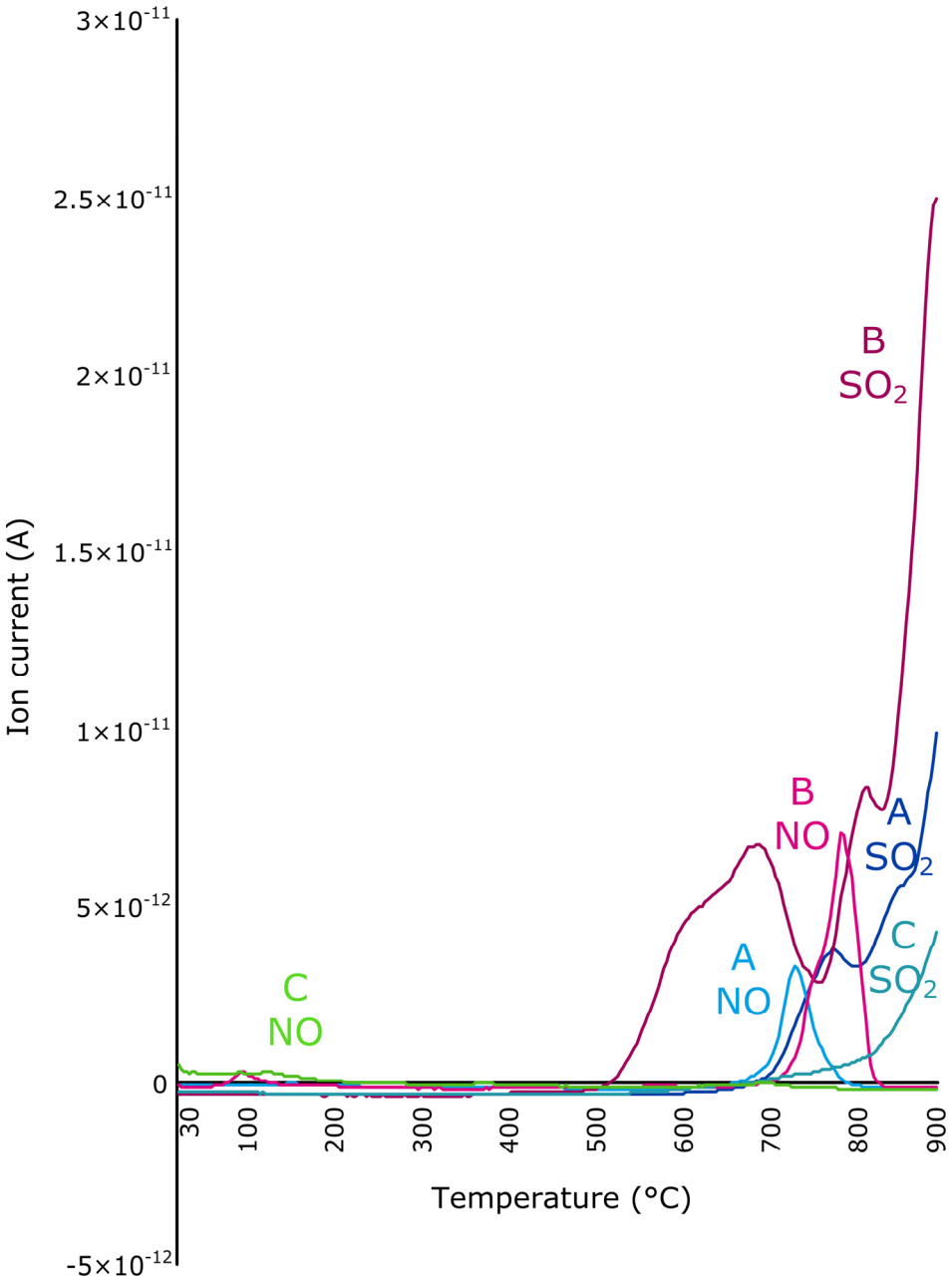

Figure 33. SO_2 and NO emissions from ashes A, B and C between 30 °C and 900 °C as determined by mass spectrometry.

The FTIR spectra of ash B exhibited similar trends but did not contain any peaks in the 1250-1470 cm^{-1} region at 30 °C. The peaks at 2800-3000 cm^{-1} and 1700 cm^{-1} became visible once the temperature reached 400 °C, along with a new peak at 1150 cm^{-1}. The TPD data did not reveal any changes in gas evolution that could explain these changes in the FTIR spectra. In the spectra of ash C, the 'new' peaks observed for ash A became apparent at 200 °C.

While the conditions in the TPD-FTIR experimental setup do not perfectly mimic those applied in thermal treatment facilities, the data gathered can be used in conjunction with the surface characterization results to better understand the mechanisms governing PCDF and PCDD degradation in MSW fly ash.

Ashes A, B and C were treated in sealed ampoules to mimic low temperature treatment under an inert atmosphere (from **Paper III** and Lundin *et al.* [68]), and analysed for PCDF and PCDD. The resulting PCDF and PCDD concentrations in the ampoule-treated ashes were compared to those in untreated ash (Figure 19). This treatment caused a modest reduction in the PCDF contents of ashes A and B, together with a much stronger reduction in their PCDD contents (Figure 34). The reductions in the levels of both PCDF and PCDD in ash B following treatment were much less pronounced than in ashes A or C. Ash C was the only one for which this treatment caused the near-complete decomposition of both PCDF and PCDD. Because the treatment conditions were identical for all three ashes, the different responses of their PCDF and PCDD contents must be due to differences in the ashes' composition. For example, the extent of decomposition may be governed by the ashes' contents of elements such as copper, which catalyses POPs degradation [116]. The strong reduction in PCDD and PCDF levels observed for ash C could be due to its high copper content (Figure 14) and availability (Figure 18). On the other hand, ashes A and B had comparable contents of copper but exhibited drastically different behaviour, indicating that other factors also were involved.

The TPD curves show that the CO and CO_2 emissions from ashes A and B behaved quite differently: Ash B had relatively sharp early CO and CO_2 peaks at around 100 °C whereas the CO and CO_2 emissions from ash A initially increased more gently, peaking at around 200 °C. This was presumably due to differences in the carbon speciation on the ashes' surfaces (Table 4) and may have influenced the degradation of POPs in the heated ashes. For example, the sharp increase in CO and CO_2 emissions from ash B could have created an environment inside the ampoule that adversely affected the degradation process. This would not have happened to the same extent at such low temperatures in ash A due to its different carbon speciation. However, this theory does not explain the behavioural differences between PCDF and PCDD in ashes A and B.

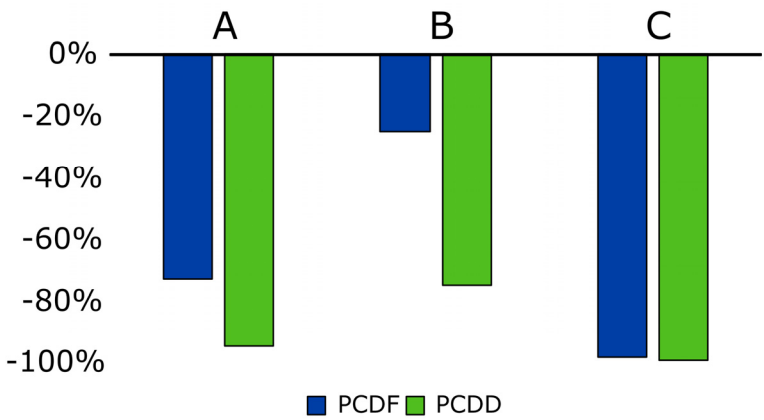

Figure 34. Changes in the abundance of PCDF and PCDD in the ampoule-treated ashes.

To investigate these behavioural differences between PCDF and PCDD, two separate subsamples of ash B were doped with ^{13}C-labeled 2,4 DiCDF and 2,3 DiCDD. At the sampled incineration plant, native PCDF and PCDD were removed from the flue gas stream by active carbon injection and subsequent filtering, meaning that they should have been adsorbed onto the surfaces of the fly ash particles. It stands to reason that native pollutants adsorbed to the ash surface would release at similar temperatures to the labelled compounds. Thus, doping with labelled PCDF and PCDD should not greatly affect the surface composition of the ash.

The TDP mass spectrometry results clearly show that the DiCDF- and DiCDD-doped ashes differed with respect to the temperature at which they started emitting $^{13}CO_2$ and ^{13}CO (Figure 35). The $^{13}CO_2$ emissions from the DiCDF-doped ashes peaked at around 110 °C while those from the ^{13}C DiCDD-labelled ashes peaked at around 90 °C. In both cases, the $^{13}CO_2$ emissions peaked slightly earlier than those of native $^{12}CO_2$. This suggests that the labelled DiCDF and DiCDD on the ash surfaces desorbed at relatively low temperatures, slightly before the ashes' native carbon species. The observation that DiCDD desorbed at a lower temperature than DiCDF was unexpected because the enthalpies of vaporization of PCDDs are generally higher than those of PCDFs [87]. Comparing the labelled $^{13}CO_2$ emissions from the DiCDF- and DiCDD-doped ashes to the CO_2 emissions from the un-doped ash (black line, Figure 35) revealed that the release of native CO_2 from the DiCDF-doped ash was delayed relative to that in the un-doped ash. This may indicate that the surface chemistry was more profoundly affected by the doping process than was originally assumed. On the other hand, no such delay was

observed for the DiCDD-doped ash even though the same doping procedure was used in its preparation.

Overall, these results demonstrated that the doping procedure was viable and that the labelled carbon could be detected using the TPD apparatus. To enable more accurate and useful determination, a higher ratio of labelled to native carbon would be required, and it would be necessary to perform more replicate experiments for quality assurance purposes. In addition, it would be desirable to investigate the behaviours of all three ashes when labelled with PCDF/PCDD in order to get a more comprehensive data set.

The three ashes were shown to have diverse chemical compositions, and their bulk compositions were found to be fairly similar to their surface compositions. The different emissions profiles produced by each ash when heated in the TDP setup could generally be explained by considering their chemical compositions and mineral morphology. The influence of the ashes' chemical compositions on POPs degradation was demonstrated by the experiments involving heating in sealed ampoules. Near-complete PCDF and PCDD degradation was observed for the copper-rich low-carbon ash C but degradation was much less extensive in ashes A and B, with the latter having a somewhat lower capacity for degradation than the former. These differences were attributed to the ashes' different chemical compositions, particularly their carbon contents. For ashes A and B, PCDF degradation was much less extensive than that of PCDD. To investigate this phenomenon, ash B was doped with ^{13}C-labelled DiCDF and DiCDD and heated gradually in the TDP setup. The resulting CO_2 emissions curves revealed slight differences between the behaviors of PCDF and PCDD. However, because only one ash was tested, the implications of these differences were unclear.

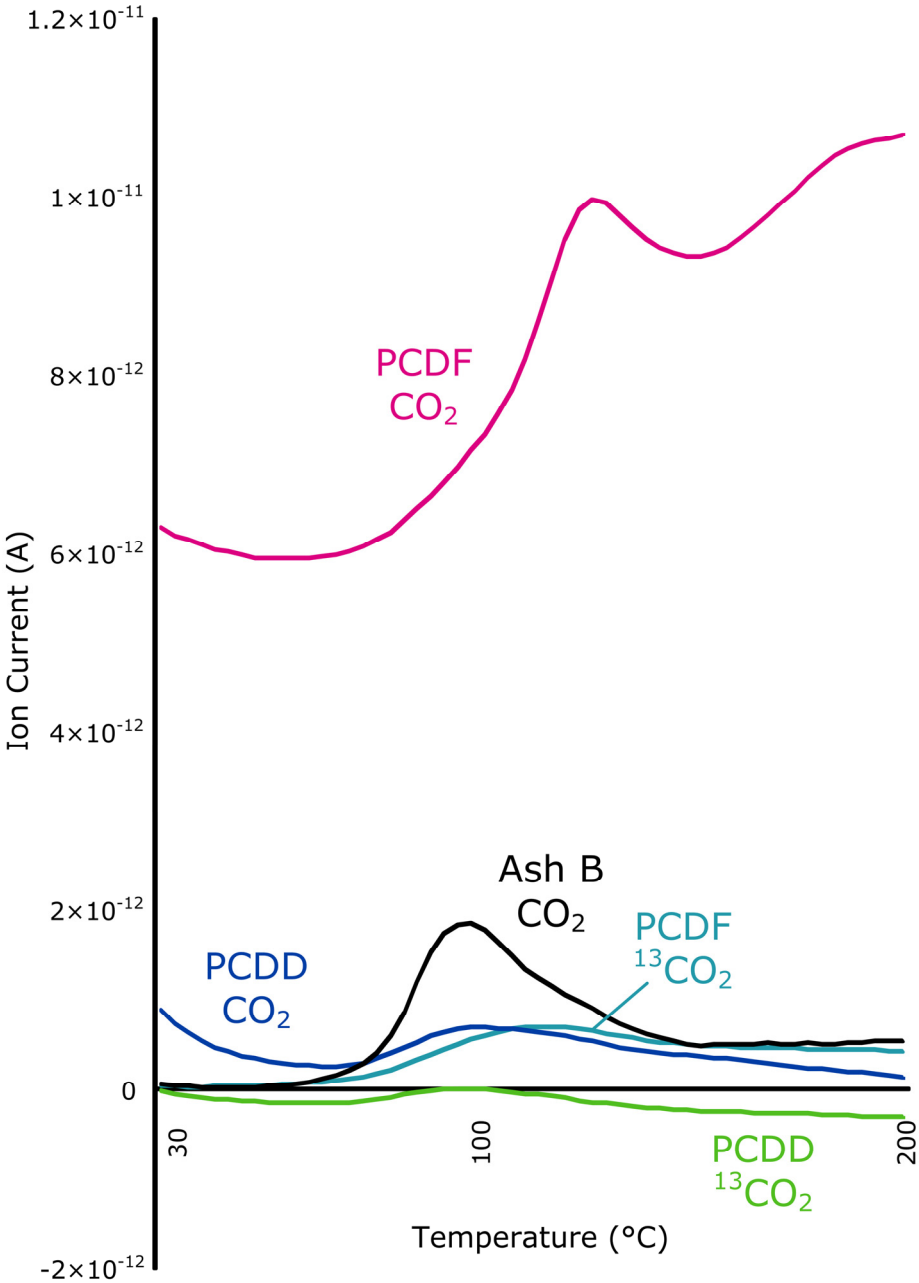

Figure 35. $^{13}CO_2$ and $^{12}CO_2$ emissions from ^{13}C-DiCDF-doped, ^{13}C-DiCDD-doped and un-doped ash B samples as determined by mass spectrometry.

CONCLUDING REMARKS

This thesis examined several problems associated with POPs formation in MSW incineration residues and describes a variety of different POPs-forming and POPs-destroying reactions. The sampling probe validation study clearly demonstrated that PCDF and PCDD formation can be very rapid under appropriate conditions. It is therefore important to use equipment and methodologies that prevent such rapid POPs formation when performing high temperature flue gas sampling in order to obtain accurate information on the sites of POPs formation and degradation in real incineration facilities. The sub-zero cooler will require further refinement before it can be used in full-scale high temperature sampling, but there is a clear need for samplers that provide extremely rapid sample cooling when studying POPs levels in hot flue gases.

The case study on the unexpected increase in toxic PCDD and PCDF levels in the filtered flue gases at an MSW incineration plant revealed that these POPs can form on filters at lower temperatures than was previously realised. They were formed via the condensation of chlorinated precursors, a process that is well characterized and not remarkable by itself. However, the results obtained clearly show how data from previous dioxin research can be used to tentatively identify the pathways responsible for POPs formation in new situations. If the study had been only considered total concentrations, homologue sums, and the concentrations of toxic congeners or TEQ values, it would have been impossible to identify the pathway responsible for the plant's increased POPs emissions.

The treatment of fly ash arguably presents the greatest environmental challenge associated with MSW incineration. It would be extremely desirable to develop low-energy methods for removing POPs from fly ash because this would greatly facilitate the handling of these materials and potentially the recovery of their metal contents. While low temperature fly ash treatment methods exist and have found practical applications in some parts of the world, the mechanisms by which they destroy POPs were largely unknown. In addition, little was known about the ash-mediated POPs reformation reactions that occur during or after low temperature treatment. In the ash treatment study, heating in the kiln yielded similar POPs congener profiles for all of the tested ashes, suggesting that the mechanisms of POPs formation and degradation were independent of the initial ash composition. However, the composition of the ashes did seem to influence

the extent of POPs degradation or reformation. In addition, PCDF and PCDD behaved differently during and after thermal treatment in the kiln. These differences in behaviour suggest that there is a temperature boundary that must be exceeded for PCDF and PCDD to break down without reforming, and that the position of this boundary depends on the ash composition.

Mechanochemical treatment represents a potential alternative to thermal treatment for removing POPs from fly ash. Preliminary investigations revealed that while it has considerable potential, it still needs further development and optimization. If its problems can be ironed out, it could conceivably be used to create mobile facilities for detoxifying old ashes on site.

Because ash-mediated reactions probably occur on surfaces, it was surprising that the influence of surface chemistry on the formation and degradation of PCDF, PCDD and other POPs had not been studied extensively. While the characterization of fly ash particle surfaces cannot by itself answer longstanding questions about POPs formation and/or degradation, it did reveal important differences between ashes and their effects on POPs-forming and -degrading reactions. Ash composition was found to influence thermal POPs desorption and decomposition. Moreover, PCDD and PCDF seemed to interact with the ash surface in different ways, which may explain their different responses to thermal treatment.

While this thesis may not provide any direct answers to unsolved questions about the formation and degradation of PCDF, PCDD and other POPs, it clearly illustrates the complexity of the reactions involved in these processes and suggests directions of study that may yield further insights.

ACKNOWLEDGEMENTS

När man tillbringat så här långt tid att arbeta på sin avhandling finns det många att tacka:

Först och främst måste jag tacka min första huvudhandledare **Stellan**, som såg potentialen och anställde mig som doktorand den där sommaren för drygt sex år sedan. Utan **Lisa,** både huvudhandledare i sluttampen och biträdande handledare från dag ett, hade det nog inte blivit någon avhandling. Jag kan inte med ord beskriva hur mycket ditt stöd betytt för mig. Tillsammans med **Stina** har du stöttat mig i vått och torrt och jag är oändligt tacksam för alla stunder av skratt, och tårar, vi delat. Min biträdande handledare **Jean-Francois**: tack för att du hoppade på projektet i ett sådant sent skede och har bidragit till att avhandlingen blivit så mycket bättre. Tack också till **Mats** för att du lyssnat, läst och engagerat dig. I also wish to extend a profound gratitude to **Dahman** for believing in me and being my friend.

Nästa stora tack går till Umeå Energi, för finansiering och till min företagsmentor **Henrik**, som gjort ett strålande jobb, genom att förmedla kontakter och komma med glada tillrop. Tack också till IDS **Petter** och **Benkt** (med k) för alla diskussioner, funderingar och kaffe.

Min tid på miljökemi hade vart mycket tristare om det inte hade vart för alla fantastiska kollegor, både nya och gamla. Tack **Maria** för att du alltid tar dig tid att svara på (dumma) frågor, och **Sture** för alla underfundiga samtal och många goda skratt. Framtida miljökemister i Umeå går miste om något.

Sarah, **Anna-Lena**, **QJ**, **Mar** och **Mirva:** det har vart ett nöje att dela rum med er alla, men jag saknar fortfarande Sarahs ryska pop och franska rap. Utöver mina rumskompisar finns det en mängd miljökemister, gamla och nya, som bidragit till att göra den här tiden väldigt trivsam.

Jag har inte heller glömt **Anders**, **Tommys** och **Ulfs** (med flera IDS-doktorander) strålande resesällskap och fantastiskt trevliga after works.

Jag har också en massa vänner och gamla studiekamrater utanför miljökemi, både på och utanför universitet som jag är djupt tacksam för deras stöd och vänskap. De som förtjänar ett extra omnämnande är **Kristina**, **Madeleine**, **Anneli**, **Anna**, **Martin,** och **Matti** för alla fikastunder, terapisamtal, studietimmar, äventyr och framförallt all vänskap, men ni är många fler.

Hade det inte vart för min pappa **Sune** hade jag nog aldrig läst kemi, men det sätter sina spår att diskutera huruvida man kan koka ägg i bensin eller inte vid middagsbordet. Min mamma **Karin** har lärt mig att följa min egen väg, även om den inte vart spikrak hela tiden. Min bror **Erik** och sambon **Jenny** som vart bollplank och stöttepelare i allt från bilköp till framtida karriärval.

Hela den här uppradningen av fantastiska människor lämnar det bästa till sist. Min lilla familj med min älskade dotter **Zelda**, som är min dansande stjärna och min man **Stephan.** Du har villkorslöst stöttat mig genom de här åren och tillsammans klarar vi allt.

Jag älskar dig.

Umeå, augusti 2014

Remember kids, the only difference between screwing around and science is writing it down.

– **Adam Savage**

REFERENCES

1. Avfall Sverige. Svensk Avfallshantering 2013 (Summary of Waste handling in Sweden, 2013) 2013
2. Energimyndigheten, ET2013:22 Energiläget 2013 (The Energy Situation 2013) 2013
3. Claesson, F.*, et al.*, *Chemical Characterization of Waste Fuel for Fluidized Bed Combistion*, in *The 20th International Conference on Fluidized Combustion*. 2009.
4. Sokka, L., R. Antikainen, and P.E. Kauppi, *Municipal solid waste production and composition in Finland—Changes in the period 1960–2002 and prospects until 2020.* Resources, Conservation and Recycling, 2007. **50**(4): p. 475-488.
5. Reichelt, J.*, et al.*, *Formation of deposits on the surfaces of superheaters and economisers of MSW incinerator plants.* Waste Management, 2013. **33** (1): p. 43-51.
6. Nordin, A., *Chemical Elemental Characteristics of Biomass Fuels.* Biomass & Bioenergy, 1994. **6**(5): p. 339-347.
7. Aurell, J., J. Fick, and S. Marklund, *Effects of Transient Combustion Conditions on the Formation of Polychlorinated Dibenzo-p-Dioxins, Dibenzofurans, and Benzenes, and Polycyclic Aromatic Hydrocarbons During Municipal Solid Waste Incineration.* Environmental Engineering Science, 2009. **26**(3): p. 509-520.
8. Zevenhoven, R.K., Pia, *Control of pollutants in flue gas cleaning*. Second edition ed. 2002: Helsinki University of Technology.
9. McKay, G., *Dioxin characterisation, formation and minimisation during municipal solid waste (MSW) incineration: review.* Chemical Engineering Journal, 2002. **86**(3): p. 343-368.
10. Olie, K., P.L. Vermulen, and O. Hutzinger, *Chlorodibenzo- p -dioxins and chlorodibenzofurans are trace components of fly ash and flue gas of some municipal incinerators in the Netherlands.* Chemosphere, 1977. **6**(8): p. 455-459.
11. Buser, H.R., H.P. Bosshardt, and C. Rappe, *Identification of polychlorinated dibenzo-p-dioxin isomers found in fly ash.* Chemosphere, 1978. **7**(2): p. 165-172.

12. Rappe, C., *Dioxins, patterns and source identification.* Fresenius' Journal of Analytical Chemistry, 1993. **348**: p. 63-75.
13. Sundqvist, K., *Sources of dioxins and other POPs to the marine environment : Identification and apportionment using pattern analysis and receptor modeling*. 2009, Department of Chemistry, Umeå University: Umeå.
14. UNEP, *Stockholm Convention on Persistent Organic Pollutants*. 2009.
15. Naturvårdsverket, *Naturvårdsverkets Författningssamling (NVF) 2004:10,* 2004.
16. Tian, B.*, et al.*, *Emission characterization of unintentionally produced persistent organic pollutants from iron ore sintering process in China.* Chemosphere, 2012. **89**(4): p. 409-415.
17. Sundqvist, K.L.*, et al.*, *Congener fingerprints of tetra- through octa-chlorinated dibenzo-p-dioxins and dibenzofurans in Baltic surface sediments and their relations to potential sources.* Chemosphere, 2009. **77**: p. 612-620.
18. Wang, Z.Y., Z.C. Zhai, and L.S. Wang, *Prediction of gas phase thermodynamic properties of polychlorinated dibenzo-furans by DFT.* Journal of Molecular Structure-Theochem, 2005. **725**(1-3): p. 55-62.
19. Wang, Z.Y.*, et al.*, *Prediction of gas phase thermodynamic function of polychlorinated dibenzo-p-dioxins using DFT.* Journal of Molecular Structure-Theochem, 2004. **672**(1-3): p. 97-104.
20. Zhai, Z. and Z. Wang, *Computational study on the relative stability and formation distribution of 76 polychlorinated naphthalene by density functional theory.* Journal of Molecular Structure: THEOCHEM, 2005. **724**(1–3): p. 221-227.
21. Zhai, Z.-C.*, et al.*, *DFT calculation on 204 polychlorinated biphenyls: their thermodynamic function and implication of Cl substitute position.* Journal of Molecular Structure: THEOCHEM, 2005. **714**(2–3): p. 123-131.
22. Van den Berg, M.*, et al.*, *The 2005 World Health Organization reevaluation of human and mammalian toxic equivalency factors for dioxins and dioxin-like compounds.* Toxicological Sciences, 2006. **93**: p. 224-241.
23. Chopra, M. and D. Schrenk, *Dioxin toxicity, aryl hydrocarbon receptor signaling, and apoptosis—Persistent pollutants affect programmed cell death.* Critical Reviews in Toxicology, 2011. **41**(4): p. 292-320.

24. Kreuzer, P.E.*, et al.*, *2,3,7,8-tetrachlorodibenzo-p-dioxin (TCDD) and congeners in infants. A toxicokinetic model of human lifetime body burden by TCDD with special emphasis on its uptake by nutrition.* Archives of Toxicology, 1997. **71**(6): p. 383-400.
25. Hooth, M.J.*, et al.*, *Repeated dose toxicity and relative potency of 1,2,3,4,6,7-hexachloronaphthalene (PCN 66) 1,2,3,5,6,7-hexachloronaphthalene (PCN 67) compared to 2,3,7,8-tetrachlorodibenzo-p-dioxin (TCDD) for induction of CYP1A1, CYP1A2 and thymic atrophy in female Harlan Sprague–Dawley rats.* Toxicology, 2012. **301**(1–3): p. 85-93.
26. Claesson, F.*, et al. Annual Variation in Elemental, Dioxin and PCB content within Swedish Waste Fuel.* in *12th International Waste Management and Landfill Symposium*. 2009. Sardinia, Italy.
27. Shaub, W.M. and W. Tsang, *Dioxin Formations in Incinerators.* Environmental Science & Technology, 1983. **17**(12): p. 721-730.
28. Procaccini, C.*, et al.*, *Formation of chlorinated aromatics by reactions of Cl, Cl-2, and HCl with benzene in the cool-down zone of a combustor.* Environmental Science & Technology, 2003. **37**(8): p. 1684-1689.
29. Aurell, J., S. Jansson, and S. Marklund, *Effects of Quench Time Profiles on PCDD/F Formation in the Postcombustion Zone during Municipal Solid Waste Incineration.* Environmental Engineering Science, 2009. **26**(3): p. 541-550.
30. Addink, R. and K. Olie, *Mechanism of Formation and Destruction of Polychlorinated Dibenzo-p-dioxins and Dibenzofurans in Heterogenous Systems.* Environmental Science & Technology, 1995. **29**(6): p. 1425-1435.
31. Jay, K. and L. Stieglitz, *Identification and quantification of volatile organic components in emissions of waste incineration plants.* Chemosphere, 1995. **30**(7): p. 1249-1260.
32. Froese, K.L. and O. Hutzinger, *Polychlorinated benzene, phenol, dibenzo-p-dioxin, and dibenzofuran in heterogeneous combustion reactions of acetylene.* Environmental Science & Technology, 1996. **30**(3): p. 998-1008.
33. Sommeling, P.M., P. Mulder, and R. Louw, *Formation of PCDFs during chlorination and oxidation of chlorobenzene in chlorine/oxygen mixtures around 340 °C.* Chemosphere, 1994. **29**(9–11): p. 2015-2018.
34. Sidhu, S.S.*, et al.*, *The homogeneous, gas-phase formation of chlorinated and brominated dibenzo-p-dioxin from 2,4,6-trichloro- and 2,4,6-tribromophenols.* Combust. Flame, 1995. **100**: p. 11-20.

35. Taylor, P.H., *et al.*, *Copper-catalyzed chlorination and condensation of acetylene and dichloroacetylene.* Chemosphere, 2000. **40**(12): p. 1297-1303.
36. Mulholland, J.A. and J.Y. Ryu, *Formation of polychlorinated dibenzo-p-dioxins by CuCl2-catalyzed condensation of 2,6 chlorinated phenols.* Combustion Science and Technology, 2001. **169**: p. 107-126.
37. Lemieux, P.M., *et al.*, *Bench-scale studies on the simultaneous formation of PCBs and PCDD/Fs from combustion systems.* Waste Management, 2001. **21**(5): p. 419-425.
38. Jansson, S., L. Lundin, and R. Grabic, *Characterisation and fingerprinting of PCBs in flue gas and ash from waste incineration and in technical mixtures.* Chemosphere, 2011. **85**(3): p. 509-515.
39. Stieglitz, L. and H. Vogg, *On Formation Conditions of PCDD PCDF in Fly-ash from Municipal Waste Incinerators.* Chemosphere, 1987. **16**(8-9): p. 1917-1922.
40. Iino, F., *et al.*, *De novo synthesis mechanism of polychlorinated dibenzofurans from polycyclic aromatic hydrocarbons and the characteristic isomers of polychlorinated naphthalenes.* Environmental Science & Technology, 1999. **33**(7): p. 1038-1043.
41. Imagawa, T. and C.W. Lee, *Correlation of polychlorinated naphthalenes with polychlorinated dibenzofurans formed from waste incineration.* Chemosphere, 2001. **44**(6): p. 1511-1520.
42. Pekarek, V., *et al.*, *Matrix effects on the de novo synthesis of polychlorinated dibenzo-p-dioxins, dibenzofurans, biphenyls and benzenes.* Chemosphere, 2007. **68**(1): p. 51-61.
43. Van Caneghem, J., C. Block, and C. Vandecasteele, *Destruction and formation of dioxin-like PCBs in dedicated full scale waste incinerators.* Chemosphere, 2014. **94**(0): p. 42-47.
44. Kakuta, Y., *et al.*, *Characterization of residual carbon influencing on de novo synthesis of PCDD/Fs in MSWI fly ash.* Chemosphere, 2007. **68**(5): p. 880-886.
45. Lasagni, M., *et al.*, *Kinetics of carbon degradation and PCDD/PCDF formation on MSWI fly ash.* Chemosphere, 2009. **74**(3): p. 377-383.
46. Weber, R., *et al.*, *Formation of PCDF, PCDD, PCB, and PCN in de novo synthesis from PAH: Mechanistic aspects and correlation to fluidized bed incinerators.* Chemosphere, 2001. **44**(6): p. 1429-1438.
47. Wikstrom, E., *et al.*, *In situ formed soot deposit as a carbon source for polychlorinated dibenzo-p-dioxins and dibenzofurans.* Environmental Science & Technology, 2004. **38**(7): p. 2097-2101.

48. Hell, K., L. Stieglitz, and E. Dinjus, *Mechanistic aspects of the de-novo synthesis of PCDD/PCDF on model mixtures and MSWI fly ashes using amorphous C-12- and C-13-labeled carbon.* Environmental Science & Technology, 2001. **35**(19): p. 3892-3898.
49. Everaert, K. and J. Baeyens, *The formation and emission of dioxins in large scale thermal processes.* Chemosphere, 2002. **46**(3): p. 439-448.
50. Ryu, J.Y.*, et al.*, *Potential role of chlorination on pathways in PCDD/F formation in a municipal waste incinerator.* Environmental Science & Technology, 2004. **38**(19): p. 5112-5119.
51. Iino, F., T. Imagawa, and B.K. Gullett, *Dechlorination controlled polychlorinated dibenzofuran isomer patterns from municipal waste incinerators.* Environmental Science & Technology, 2000. **34**(15): p. 3143-3147.
52. Ishikawa, Y.*, et al.*, *PCB decomposition and formation in thermal treatment plant equipment.* Chemosphere, 2007. **67**(7): p. 1383-1393.
53. Jansson, S., J. Fick, and S. Marklund, *Formation and chlorination of polychlorinated naphthalenes (PCNs) in the post-combustion zone during MSW combustion.* Chemosphere, 2008. **72**(8): p. 1138-1144.
54. Hatanaka, T., A. Kitajima, and M. Takeuchi, *Role of copper chloride in the formation of polychlorinated dibenzo-p-dioxins and dibenzofurans during incineration.* Chemosphere, 2004. **57**(1): p. 73-79.
55. Gullett, B.K., K.R. Bruce, and L.O. Beach, *Formation of Chlorinated Organics During Solid-Waste Combustion.* Waste Management & Research, 1990. **8**(3): p. 203-214.
56. Gullett, B.K., K.R. Bruce, and L.O. Beach, *The Effect of Metal-Catalysts on the Formation of Polychlorinated Dibenzo-Para-Dioxin and Polychlorinated Dibenzofuran Precursors.* Chemosphere, 1990. **20**(10-12): p. 1945-1952.
57. Stieglitz, L.*, et al.*, *On Formation Conditions of Organohalogen Compounds from Particulate Carbon of Fly-Ash.* Chemosphere, 1991. **23**(8-10): p. 1255-1264.
58. Nonhebel, D.C., *Copper-catalysed Single-electron Oxidations and Reductions*, in *Essays on free-radical chemistry*, D.H. Hey, W.A. Waters, and R.O.C. Norman, Editors. 1970, Chemical Society: London. p. 409-437.
59. Wikstrom, E.*, et al.*, *Importance of chlorine speciation on de Novo formation of polychlorinated dihenzo-p-dioxins and polychlorinated dibenzofurans.* Environmental Science & Technology, 2003. **37**(6): p. 1108-1113.

60. Luijk, R., *et al.*, *The Role of Bromine in the De-Novo Synthesis in A Model Fly-Ash System.* Chemosphere, 1994. **28**(7): p. 1299-1309.
61. Oh, J.E., *et al.*, *Mechanistic relationships among PCDDs/Fs, PCNs, PAHs, CIPhs, and CIBzs in municipal waste incineration.* Environmental Science & Technology, 2007. **41**(13): p. 4705-4710.
62. Aurell, J. and S. Marklund, *Effects of varying combustion conditions on PCDD/F emissions and formation during MSW incineration.* Chemosphere, 2009. **75**(5): p. 667-673.
63. Takasuga, T., *et al.*, *Formation of polychlorinated naphthalenes, dibenzo-p-dioxins, dibenzofurans, biphenyls, and organochlorine pesticides in thermal processes and their occurrence in ambient air.* Archives of Environmental Contamination and Toxicology, 2004. **46**(4): p. 419-431.
64. Kim, K.S., *et al.*, *Detailed PCB congener patterns in incinerator flue gas and commercial PCB formulations (Kanechlor).* Chemosphere, 2004. **55**(4): p. 539-553.
65. European Committee for Standardization (C.E.N), *EN 1948:1-3*, 1997.
66. Ballschmiter, K., *et al.*, *Reaction Pathways for hte Formaion of Polychloro-dibenzodioxins (PCDD) and Polychlorinated-dibenzofurans (PCDF) in Combustion Processes. 2. Chlorobenzenes and Chlorophenols as Precursors in the Formaion of Polychloro-dibenzodioxins and Polychloro-dibenzofurans in Flame Chemistry.* Chemosphere, 1988. **17**(5): p. 995-1005.
67. Liljelind, P., *et al.*, *Method for multiresidue determination of halogenated aromatics and PAHs in combustion-related samples.* Environmental Science & Technology, 2003. **37**(16): p. 3680-3686.
68. Lundin, L. and S. Marklund, *Thermal degradation of PCDD/F in municipal solid waste ashes in sealed glass ampules.* Environmental Science & Technology, 2005. **39**(10): p. 3872-3877.
69. Ryan, J.J., *et al.*, *Gas chromatographic separations of all 136 tetra- to octapolychlorinated dibenzo-p-dioxins and polychlorinated dibenzofurans on nine different stationary phases.* Journal of Chromatography A, 1991. **541**: p. 131-183.
70. Bacher, R., M. Swerev, and K. Ballschmiter, *Profile and Pattern of Monochlorodibenzodioxins Through Octachlorodibenzodioxins and Octachlorodibenzofurans in Chimney Deposits from Wood Burning.* Environmental Science & Technology, 1992. **26**(8): p. 1649-1655.
71. Nakano, T., Weber, R, *Analysis of low chlorinated PCDD/F - Isomer specific analysis of MCDF to T3CDF on DB-5ms-column and some aspects regarding air sampling*, in *Organohalogen Compounds*. 2001.

72. Wikström, E., P. Andersson, and S. Marklund, *Design of a laboratory scale fluidized bed reactor.* Review of Scientific Instruments, 1998. **69**(4): p. 1850-1859.
73. Chiang, K.Y., K.L. Chien, and C.H. Lu, *Characterization and comparison of biomass produced from various sources: Suggestions for selection of pretreatment technologies in biomass-to-energy*. Applied Energy, 2012. **100**: p. 164-171.
74. Lighty, J.S., J.M. Veranth, and A.F. Sarofim, *Combustion aerosols: Factors governing their size and composition and implications to human health.* Journal of the Air & Waste Management Association, 2000. **50**(9): p. 1565-1618.
75. Lundin, L. and S. Marklund, *Distribution of Mono to Octa-chlorinated PCDD/Fs in Fly Ash from a Municipal Solid-Waste Incinerator.* Environmental Science & Technology, 2008. **42**(4): p. 1245-1250.
76. Lin, Y.S.*, et al.*, *Polychlorinated dibenzo-p-dioxins/dibenzofurans distributions in ash from different units in a municipal solid waste incinerator.* Journal of Hazardous Materials, 2008. **154**(1-3): p. 954-962.
77. Chen, C.-K.*, et al.*, *The size distribution of polychlorinated dibenzo-p-dioxins and dibenzofurans in the bottom ash of municipal solid waste incinerators.* Chemosphere, 2006. **65**(3): p. 514-520.
78. Lu, S.-Y.*, et al.*, *Dioxins and their fingerprint in size-classified fly ash fractions from municipal solid waste incinerators in China-Mechanical grate and fluidized bed units.* Journal of the Air & Waste Management Association, 2012. **62**(6): p. 717-724.
79. Lundholm, K., *Fate of Cu, Cr, As and some other trace elements during combustion of recovered waste fuels*. 2007, Umeå : Department of Applied Physics and Electronics, Umeå University: Umeå.
80. Mkilaha, I.S.N., H. Yao, and I. Naruse, *Thermodynamic analysis of the role of chlorine and sulfur environments during combustion and incineration processes.* Journal of Material Cycles and Waste Management, 2002. **4**(2): p. 143-149.
81. Verhulst, D.*, et al.*, *Thermodynamic behavior of metal chlorides and sulfates under the conditions of incineration furnaces.* Environmental Science & Technology, 1996. **30**(1): p. 50-56.
82. Fujimori, T., Y. Fujinaga, and M. Takaoka, *Deactivation of Metal Chlorides by Alkaline Compounds Inhibits Formation of Chlorinated Aromatics.* Environmental Science & Technology, 2010. **44**(19): p. 7678-7684.

83. Brunauer, S., P.H. Emmett, and E. Teller, *Adsorption of Gases in Multimolecular Layers.* Journal of the American Chemical Society, 1938. **60**(2): p. 309-319.
84. NIST X-ray Photoelectron Spectroscopy Database*, Version 4.1*. 2012. *http://srdata.nist.gov/xps/*
85. Kida, A., Y. Noma, and T. Imada, *Chemical speciation and leaching properties of elements in municipal incinerator ashes.* Waste Management, 1996. **16**(5–6): p. 527-536.
86. Mackay, D.*, et al.*, *Handbook of Physical-Chemical Properties and Environmental Fate of Organic Chemicals: Volume II Halogenated Hydrocarbons*. Vol. Second edition. 2006: CRC Press, Taylor and Francis group.
87. Quina, M.J., J.C. Bordado, and R.M. Quinta-Ferreira, *Treatment and use of air pollution control residues from MSW incineration: An overview.* Waste Management, 2008. **28**(11): p. 2097-2121.
88. Sakai, S.-i. and M. Hiraoka, *Municipal solid waste incinerator residue recycling by thermal processes.* Waste Management, 2000. **20**(2–3): p. 249-258.
89. Park, Y.J. and J. Heo, *Vitrification of fly ash from municipal solid waste incinerator.* Journal of Hazardous Materials, 2002. **91**(1-3): p. 83-93.
90. Behnisch, P.A.*, et al.*, *Low-temperature thermal decomposition of dioxin-like compounds in fly ash: Combination of chemical analysis with in vitro bioassays (EROD and DR-CALUX).* Environmental Science & Technology, 2002. **36**(23): p. 5211-5217.
91. Hagenmaier, H.*, et al.*, *Copper-Catalyzed Dechlorination Hydrogenation of Polychlorinated Dibenzo-Para-Dioxins, Polychlorinated Dibenzofurans, and Other Chlorinated Aromatic-Compounds.* Environmental Science & Technology, 1987. **21**(11): p. 1085-1088.
92. Hagenmaier, H.*, et al.*, *Catalytic Effects of Fly-Ash from Waste Incineration Facilities on the Formation and Decomposition of Polychlorinated Dibenzo-Para-Dioxins and Polychlorinated Dibenzofurans.* Environmental Science & Technology, 1987. **21**(11): p. 1080-1084.
93. Weber, R., T. Sakurai, and H. Hagenmaier, *Formation and destruction of PCDD/PCDF during heat treatment of fly ash samples from fluidized bed incinerators.* Chemosphere, 1999. **38**(11): p. 2633-2642.
94. Zhao, L.*, et al.*, *Formation pathways of polychlorinated dibenzofurans (PCDFs) in sediments contaminated with PCBs during the thermal desorption process.* Chemosphere, 2012. **88**(11): p. 1368-1374.

95. Joung, H.-T., *et al.*, *Effects of oxygen, catalyst and PVC on the formation of PCDDs, PCDFs and dioxin-like PCBs in pyrolysis products of automobile residues.* Chemosphere, 2006. **65**(9): p. 1481-1489.
96. Weber, R., *et al.*, *Dechlorination and destruction of PCDD, PCDF and PCB on selected fly ash from municipal waste incineration.* Chemosphere, 2002. **46**(9-10): p. 1255-1262.
97. Song, G.-J., *et al.*, *Dechlorination and destruction of PCDDs/PCDFs in fly ashes from municipal solid waste incinerators by low temperature thermal treatment.* Chemosphere, 2008. **71**(2): p. 248-257.
98. Lundin, L. and S. Marklund, *Thermal degradation of PCDD/F, PCB and HCB in municipal solid waste ash.* Chemosphere, 2007. **67**(3): p. 474-481.
99. Jolliffe, I.T., *Principal Component Analysis*. 2nd ed. Springer Series in Statistics. 2002: Springer. 489.
100. Stone, M.R., J, *Cross-validatory choice and assessment of statistical predictions.* Journal of the Royal Statistical Society, 1974. **36**: p. 111-133.
101. Umetrics, *Simca 13.0*. 2012. *www.umetrics.com*
102. Phan, D.N.C., *et al.*, *Accurate sampling of PCDD/F in high temperature flue-gas using cooled sampling probes.* Chemosphere, 2012. **88**(7): p. 832-836.
103. Rowlands, S.A., *et al.*, *Destruction of toxic materials.* Nature, 1994. **367**(6460): p. 223-223.
104. Birke, V., J. Mattik, and D. Runne, *Mechanochemical reductive dehalogenation of hazardous polyhalogenated contaminants.* Journal of Materials Science, 2004. **39**(16/17): p. 5111-5116.
105. Nomura, Y., S. Nakai, and M. Hosomi, *Elucidation of degradation mechanism of dioxins during mechanochemical treatment.* Environmental Science & Technology, 2005. **39**(10): p. 3799-3804.
106. Zhang, Q.W., *et al.*, *Effects of quartz addition on the mechanochemical dechlorination of chlorobiphenyl by using CaO.* Environmental Science & Technology, 2001. **35**(24): p. 4933-4935.
107. Lu, S., *et al.*, *Ball milling 2,4,6-trichlorophenol with calcium oxide: Dechlorination experiment and mechanism considerations.* Chemical Engineering Journal, 2012. **195**: p. 62-68.
108. Hall, A.K., *et al.*, *Mechanochemical Reaction of DDT with Calcium Oxide.* Environmental Science & Technology, 1996. **30**(12): p. 3401-3407.
109. Nomura, Y., *et al.*, *Degradation of polychlorinated naphthalene by mechanochemical treatment.* Chemosphere, 2013. **93**(11): p. 2657-2661.

110. Yan, J.H.*, et al.*, *Degradation of PCDD/Fs by mechanochemical treatment of fly ash from medical waste incineration.* Journal of Hazardous Materials, 2007. **147**(1-2): p. 652-657.
111. Stolle, A.*, et al.*, *Ball milling in organic synthesis: solutions and challenges.* Chemical Society Reviews, 2011. **40**(5): p. 2317-2329.
112. Eighmy, T.T.*, et al.*, *Comprehensive Approach toward Understanding Element Speciation and Leaching Behavior in Municipal Solid Waste Incineration Electrostatic Precipitator Ash.* Environmental Science & Technology, 1995. **29**(3): p. 629-646.
113. Kirby, C.S. and J.D. Rimstidt, *Mineralogy and surface properties of municipal solid waste ash.* Environmental Science & Technology, 1993. **27**(4): p. 652-660.
114. Phan, D.N.C., S. Jansson, and J.-F. Boily, *Link between Fly Ash Properties and Polychlorinated Organic Pollutants Formed during Simulated Municipal Solid Waste Incineration.* Energy & Fuels, 2014. **28**(4): p. 2761-2769.
115. Lundin, L., J. Aurell, and S. Marklund, *The behavior of PCDD and PCDF during thermal treatment of waste incineration ash.* Chemosphere, 2011. **84**(3): p. 305-310.
116. Weber, R.*, et al.*, *Effects of selected metal oxides on the dechlorination and destruction of PCDD and PCDF.* Chemosphere, 2002. **46**(9-10): p. 1247-1253.
117. Britton, H.T.S., S.J. Gregg, and G.W. Winsor, *The calcination of dolomite. Part I.-The kinetics of the thermal decomposition of calcite and of magnesite.* Transactions of the Faraday Society, 1952. **48**: p. 63-69.